CONFORMATIONAL STATES AND TRANSITIONS IN GREEN FLUORESCENT PROTEIN CHROMOPHORE STUDIED BY SINGLE MOLECULE SERS

By

MD SHAFAYET KHURSHID

Bachelor of Science in Mechanical Engineering

Bangladesh University of Engineering & Technology

Dhaka, Bangladesh

2007

Submitted to the Faculty of the
Graduate College of the
Oklahoma State University
in partial fulfillment of
the requirements for
the Degree of
MASTER OF SCIENCE
May, 2011

CONFORMATIONAL STATES AND TRANSITIONS IN GREEN FLUORESCENT PROTEIN CHROMOPHORE STUDIED BY SINGLE MOLECULE SERS

Thesis Approved:

Dr. Ali K. Kalkan

Thesis Adviser

Dr. Raman P. Singh

Dr. Kevin D. Ausman

Dr. Mark E. Payton

Dean of the Graduate College

ACKNOWLEDGMENTS

First and foremost, I would like to express my gratitude to my adviser, Dr. Ali Kaan Kalkan. Without his support, encouragement, and warmhearted guidance, this thesis would not have been possible. I am grateful to him for inspiring me by his endless enthusiasm, and passion for science and research. I would also like to thank to the members of my thesis committee Dr. Raman Singh and Dr. Kevin Ausman for their valuable time, and feedback.

I would like to extend my sincere thanks to Dr. K. J. Hellingwerf for providing us with the GFP sample. I am really thankful to my colleague Kushagra Singhal who has been a great help when I started my research work, especially with SERS substrate preparation. I want to express my acknowledgements to Natis Zad Shafiq and Çagri Özge Topal for their help on SM-SERS studies and providing some out-of-box suggestions that were quite helpful. My sincere thanks also go to the members of the Functional Nanomaterials Laboratory for their friendship and support.

Finally, I would like to thank to my parents, my grandfather and my brother for their understanding, support, encouragement and love.

Md. Shafayet Khurshid

TABLE OF CONTENTS

LIST OF TABLES

LIST OF FIGURES

CHAPTER I

INTRODUCTION

Green fluorescent protein (GFP) found in *Aequorea victoria*, a jellyfish characteristic of Northeast Pacific, is a luminescent protein that has led to a revolution in bio-imaging [1, 12]. Comprehensive mutagenesis efforts on the wild-type green fluorescent protein (wtGFP) have succeeded in new fluorescent probes, which range in the whole visible spectrum from blue to red [2, 3]. Recently honored by Nobel Prize in chemistry to three pioneers in the field, GFP plays an indispensable role in biological imaging and analysis, as it serves as a marker for gene expression as well as proteins and allows visualization of dynamic events inside the living cell. Proving an immense impact of GFP in bio-imaging, recently neuroscientists have reported a remarkable genetic technique dubbed as “Brainbow”, which enabled them to visualize how the brain’s cell are connected to each other by using a palette of GFP mutants [4, 56, 94]. With the rapid evolution of fluorescent protein technology, the utility of GFP-like proteins for a wide spectrum of applications is now becoming fully appreciated.

GFP comprises a strongly absorbing and highly fluorescent chromophore embedded in its protein β-barrel structure (Figure I.1). Highly efficient quantum yield (0.8) of GFP has been associated with a fluorescent chromophore adopting a cis and coplanar orientation. A cis configuration is achieved by tight encapsulation of the chromophore inside the β-barrel fold and with contribution of a complex hydrogen bonding network constructed of several amino-acids

and water molecules [5, 6, 7-9, 41, 98]. Non-radiative relaxation is suppressed effectively due to the tight encapsulation of the chromophore which restrains its motion as well as chemically isolates it from the ambient, thus providing high fluorescence quantum yield. On the other hand, free GFP chromophore does not fluoresce [83-85]. GFP is known to have deprotonated-cis (B-form) and protonated-cis (A-form) forms of the chromophore and it is well accepted that conversion between these two forms take place [2, 5, 6, 8-11, 33-40, 46-48, 50, 95-97], although rare. In thermodynamic equilibrium at room temperature and pH=7, the population of A-form is twice that of B-form. The excited state dynamics of GFP's both cis forms (protonated and deprotonated) have been studied comprehensively using ultrafast fluorescence and absorption spectroscopies.

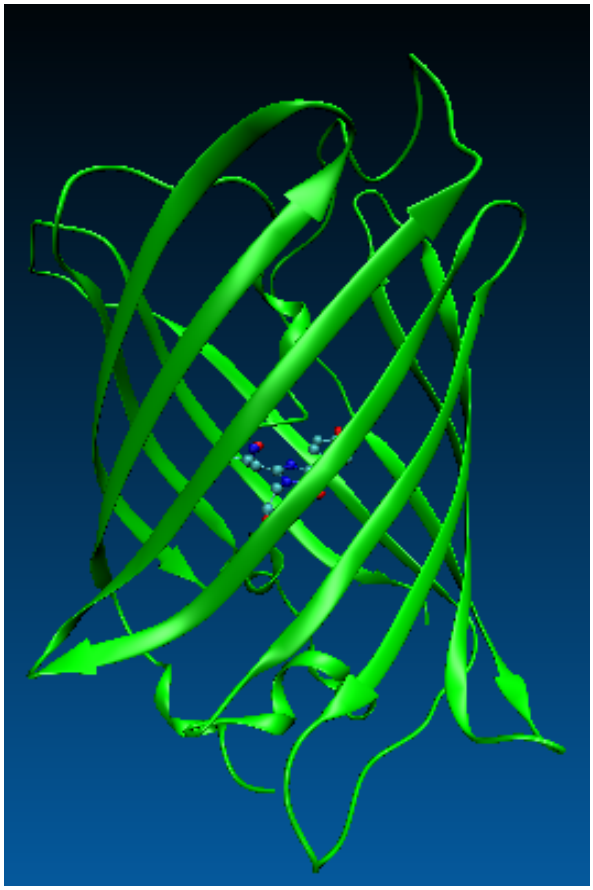

Figure I.1. Tertiary structure of wtGFP with p-HBDI chromophore inside the β-barrel.

Although GFP is a Nobel Prize winning protein, there are limited number of reports on the trans states of its chromophore (protonated/deprotonated). This situation likely arises from nonfluorescent nature of the trans state, which not only prevents access to the investigation of this state by fluorescence studies, but it also renders GFP a "useless" protein as a biomarker. On the other hand, the trans state is of significance to GFP's fluorescence intensity, if its population is a significant fraction of the population of the cis state (fluorescent state). Additionally, neither trans $\leftrightarrow$ cis nor protonated $\leftrightarrow$ deprotonated transitions of the GFP chromophore are understood well. Although these structural transitions are infrequent (i.e., less than ~1 s^{-1} per molecule), they are significant in determining the population of states. Further, a better understanding of these transitions will enable the development of photoswitching proteins.

The present thesis work reveals at least four different conformational states of GFP chromophore by single molecule surface-enhanced Raman scattering (SM-SERS). In particular, the work exploits the novel "nanometal-on-semiconductor" SERS substrates developed by Kalkan *et al* [13-15]. In addition, our work shows significant evidence of transitions between the protonated/deprotonated and cis/trans forms of the GFP chromophore at single molecule level, on the basis of Raman scattering marker peaks of the GFP chromophore reported in the literature.

Earlier, conformational changes of single protein molecules by SERS were captured in real time by only two investigations. Namely, Habuchi *et al*. and Singhal and Kalkan monitored the conformational transitions in single molecules of GFP and photoactive yellow protein (PYP), respectively [16, 17]. To the best of Author's knowledge, the present work represents the third SM-SERS protein investigation capturing conformational steps. As a substantial enhancement over the previous two milestones by Habuchi *et al*. and Singhal and Kalkan, the present work is conducted at a higher time resolution of 50 and 100 ms. Although SM-SERS work of Habuchi *et al.* also employed GFP, they only reported on the protonation/deprotonation transitions at a time resolution of 1 s [16].

SERS inherits Raman spectroscopy's capability to elucidate molecular structure [18-20]. The Raman spectrum of vibrational modes is entirely determined by molecular structure. However, SERS offers a number of advantages over Raman spectroscopy for studying the conformational states of the GFP chromophore. First, GFP is a very efficient fluorophore. Its optical excitation in the visible yields a strong fluorescence even far from the resonance, for example when the excitation is at red [5]. The strong baseline in the signal makes it very difficult to resolve the Raman peaks. On the other hand, the fluorescence is quenched in SERS due to GFP to silver nanoparticle energy transfer [18-20]. In the absence of fluorescence, the vibrational modes can be clearly resolved. Second, in the present thesis work, SERS was employed as a single molecule probe. The advantage of single molecule spectroscopy over ensemble-averaged spectroscopy (i.e., Raman spectroscopy here) is the elimination of statistical averaging [21]. Indeed, when SERS is conducted with higher concentrations, ensemble-averaged SERS yields a difficult spectrum to resolve due to overlap of signals from different state populations as well as heterogeneous broadening of the peaks. On the contrary, sharp and resolvable peaks are acquired in SM-SERS. Last but not least, the power of single molecule spectroscopy lies in the fact that transitions between states can be monitored at utmost precision, since a single molecule can be at one state at a time. On the other hand, in an ensemble, the transitions may not occur collectively (in phase) or they may occur in a distribution of time scales. In particular, this situation is valid for GFP, where the quantum efficiencies for trans/cis and protonation/deprotonation transitions are very low and these transitions cannot be triggered uniformly in time by a laser pulse. Hence, time-resolved ultrafast spectroscopy cannot be employed to study the transitions in wtGFP. Therefore, SM-SERS has a high potential to elucidate the structural origin of GFP chromophore's different states.

Finally, the significance of the present work in understanding of proteins should be mentioned. Proteins are known to be the "biological workhorses" that carry out numerous

essential functions in every living cell [22]. Of all the molecules found in living organism, proteins play the most important role. They perform their role to move muscles, sense stimuli, control metabolism and growth, digest food, defend against pathogens, transport oxygen, and many more. Therefore, single molecule (SM) studies are critically needed to resolve the conformation-function relations in proteins [21].

The present thesis is organized as follows. Chapter II follows with a review on GFP's molecular structure and photo-physics as well as fundamentals of Raman scattering and SERS. Chapter III provides a detailed presentation of the experimental protocols followed in the current study. The experimental results and their analysis as well as interpretation are reported in Chapter IV. Finally, conclusions are withdrawn in Chapter V.

CHAPTER II

LITERATURE REVIEW AND BACKGROUND

II.1. Outline

This Chapter provides a compact literature review on Green Fluorescent Protein's (GFP) molecular structure and photophysical behavior. It also presents the background on fundamentals of Surface-Enhanced Raman Scattering (SERS).

II.2. Green Fluorescent Protein

In 1955 it was first reported by Nicol *et al.* that *Aequorea victoria* (found at the west coast of North America) fluoresced in green when irradiated with ultraviolet light [23]. Shimomura *et al.* discovered green fluorescent protein from *Aequorea victoria* in 1961as a companion protein to aequorin. Both these proteins in *Aequorea* are involved in its bioluminescence. Bioluminescence involves oxidation of coelenterazine (luciferin) by an enzyme, aequorin (luciferase). While binding with three calcium ions aequorin oxidizes coelenterazine with a protein bound oxygen that results in a "Ca_3-apo-aequorin-co-elenteramide" complex that emits blue light (470 nm) in vitro [25-27, 37, 38]. Interestingly, *Aequorea* does not emit blue; instead radiationless energy transfer occurs from aequorin to GFP that excites GFP and subsequently results in its green fluorescence (509 nm) [28, 29]. No binding between aequorin and GFP is observed in the solution. Shimomura *et al.* reported energy transfer can be obtained by coadsorption of aequorin and GFP on DEAE cellulose (Diethylaminoethyl cellulose)

membranes [31]. Both of these proteins were reported as unusual proteins of no particular importance. Their value became apparent in the course of later studies, and now, fifty years after their discovery, they are well known and widely used, aequorin as a calcium probe and GFP as a bio-marker protein [2, 5, 6, 41-45, 56-59, 90, 94].

Green fluorescent protein (GFP) is a 27 kDa protein possessing 238 amino acid residues. It has a unique 11 β-sheet barrel-like structure with a diameter of about 2.4 nm and a height of 4.2 nm (Figure II.1) [5, 6, 41]. It is exceptionally stable due to its tightly packed "β- barrel" tertiary structure which is resistant to a number of biological denaturants, wide range of pH (5-12), temperature (i.e., it denatures at and above 78˚C) and chaotropic salts (i.e., it denatures at 8M urea) [5,6, 98]. The "β- sheets" form the walls of the barrel, and an α-helix runs diagonally through the barrel (Figure II.1a, b). The chromophore is in the center of the barrel and is linked by the α-helical stretch. Shimomura *et al.* deduced the structure of the chromophore of GFP in 1979 and correctly proposed that the chromophore is a p-hydroxybenzylidene- imidazolidin (p-HBDI) attached to the peptide backbone [30]. It is formed by an intramolecular autocatalytic cyclization from residues 65-67, which are Ser-Tyr-Gly in the native protein [5, 6, 41]. GFP chromophore possesses a cis conformation and is well protected in the center of the barrel (Figure II.1c). The barrel structure protects the chromophore and is presumably responsible for GFP's stability [5, 6, 98]. The "chromophore-in- capsule" design of GFP is the key to its efficient fluorescence with a quantum yield of 0.8 [5]. First, the β-barrel holds back the rotational and vibrational motion of the chromophore, thereby impeding the radiationless pathways for relaxation of the excited chromophore [5, 6, 9, 32-36]. As illustrated in Figure II.2, the most distinct feature of p-HBDI is the presence of phenol and imidazolinone rings, which are essentially frozen in in-plane and cis configuration. Out-of-plane rotation between the two rings is argued to result in non-radiative relaxation of the excited state due to collapse of π-electron conjugation over the whole molecule and subsequent nonadiabatic crossing [32, 33]. Second, the

chromophore is shielded from fluorescence quenchers, such as O_2 in the bulk solvent [5-8]. In this sense, GFP is reminiscent of a “hurricane lamp”, where a transparent glass enclosure (β-barrel) shields the glowing flame (chromophore) from wind and rain. Indeed, free p-HBDI in water does not glow [88].

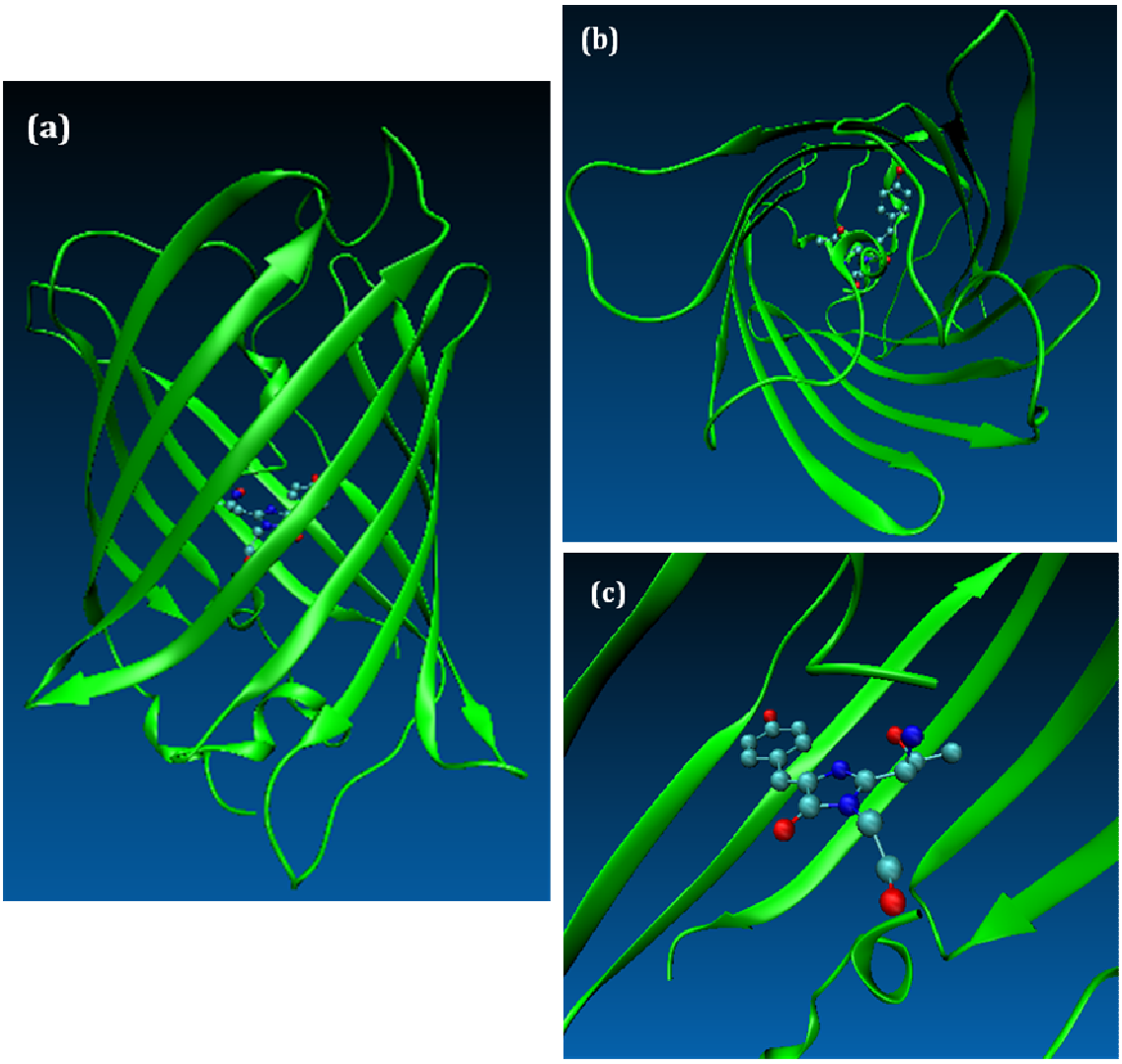

Figure II.1. Tertiary structure of wtGFP. The chromophore is located in the center of the β-barrel: **(a)** side view; **(b)** top view; and **(c)** ball-stick model of the p-HBDI chromophore (red: O; blue: N; cyan: C). Figure: courtesy of Dr. Ali Kaan Kalkan and Natis Zad Shafiq (Functional Nanomaterials Laboratory, Oklahoma State University).

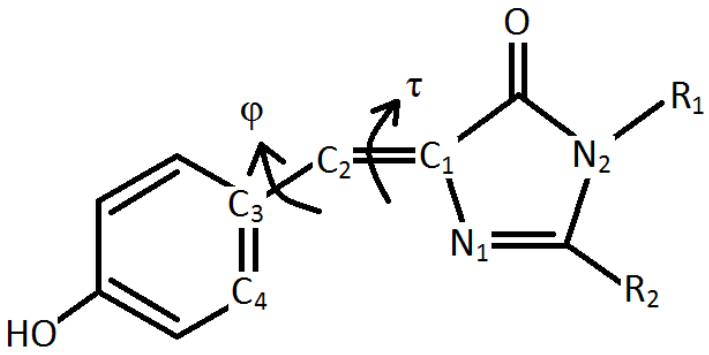

Figure II.2. The φ (C_1-C_2-C_3-C_4) and τ (N_1-C_1-C_2-C_3) dihedral angles of the GFP chromophore. In the protein R_1 is Gly67 and R_2 is Ser65.

The optical absorption spectrum of GFP has two bands at 395 nm and 475 nm, named the A and B bands, respectively (Figure II.3). Excitation at either wavelengths leads to intense green emission, either at 503 nm (475nm excitation) or 509 nm (395nm excitation) [5, 6]. The 395 nm absorption is generally attributed to a neutral/protonated form of the chromophore and the absorption at 475nm to an anionic/deprotonated form [5]. The protonated (A) and deprotonated (B) nature of these states was confirmed by X-Ray diffraction, ultrafast fluorescent spectroscopy, and studies of the effects of pH on the model chromophore (HBDI) [2, 5, 6, 8, 11, 33, 36, 37, 39, 40, 50].

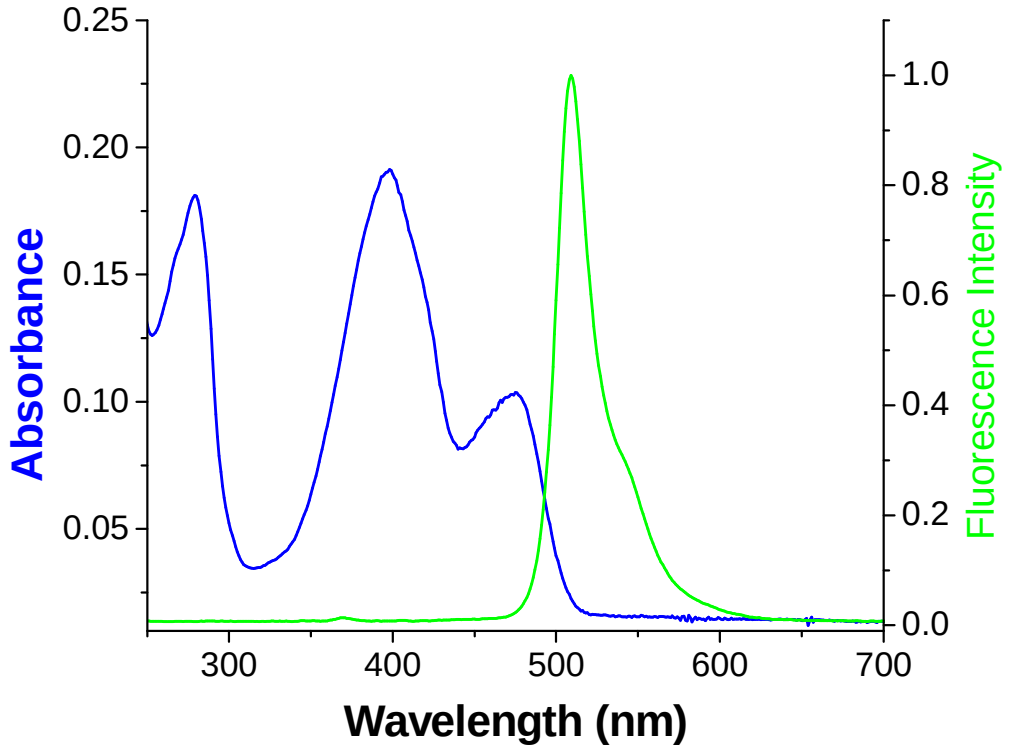

Figure II.3. Absorbance (1 cm optical path) and emission (normalized and under 365 nm excitation) spectra of 10^{-5} M wtGFP. Data: courtesy of Dr. Ali Kaan Kalkan and Natis Zad Shafiq (Functional Nanomaterials Laboratory, Oklahoma State University).

Boxer *et al.* reported the time resolved fluorescence of wild type GFP (wtGFP) by ultrafast time resolved spectroscopy [10]. The neutral (A) form of the chromophore can convert to the anionic species (B) by going through the intermediate state (I). The equilibrium between these states is controlled by the internal hydrogen- bonding network, which is assumed to facilitate excited state proton transfer (ESPT) [5, 6, 8, 9, 11, 33-40, 46-48, 50]. Irradiation at 475 nm excites the anionic chromophore (B→B*) which emits at 503nm [10, 89]. Irradiation at 395nm excites the neutral state (A→A*) which rapidly decays to the excited intermediate I* via ESPT [47-49]. ESPT occurs by transfer of the phenolic proton from Tyr 66 to Glu 222 through the "proton pipeline" shown in the Figure II.4(highlighted in orange). Further, excitation of A yields an additional weaker fluorescent peak at 460 nm, which is assigned to A*→A[11, 33-36,

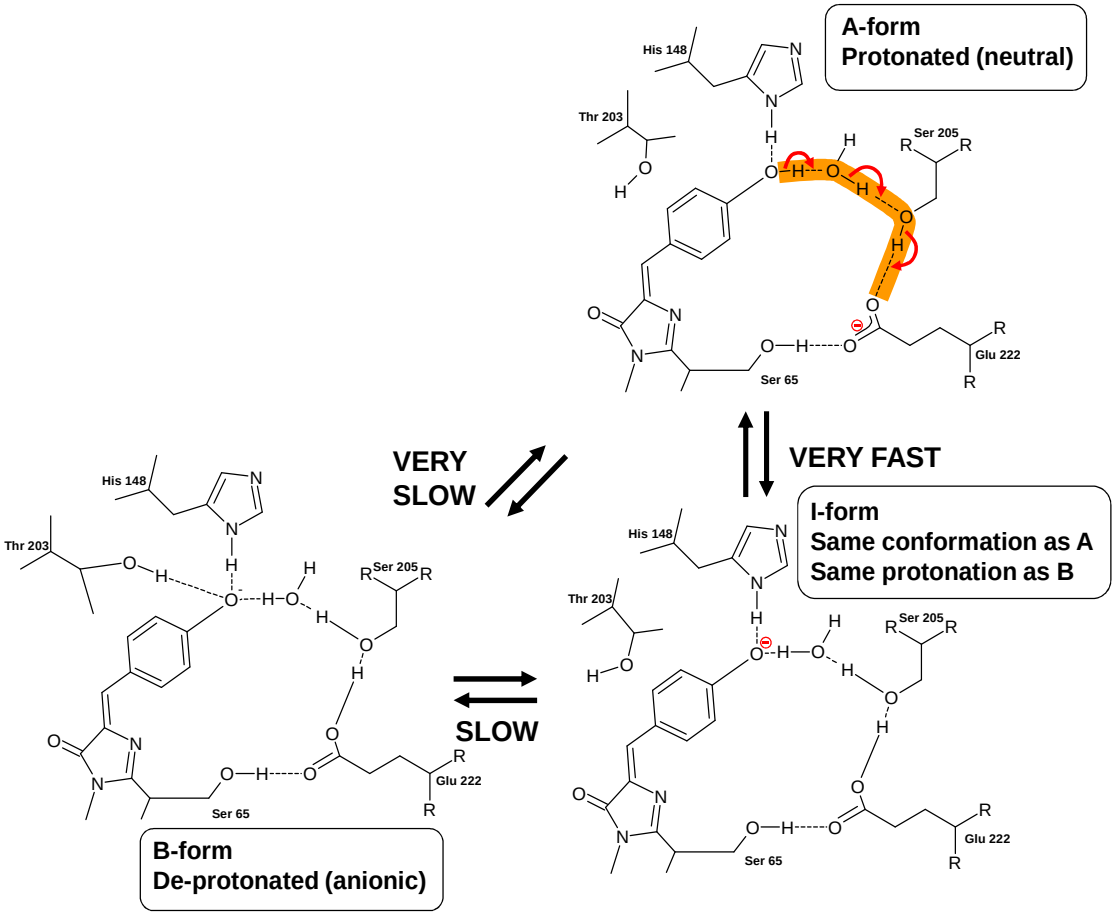

Figure II.4. Excited state proton transfer (ESPT) mechanism. The red arrows illustrate ESPT during A*→I* in terms of the proton shuttle steps along the proton wire (in orange). Figure: courtesy of Dr. Ali Kaan Kalkan and Natis Zad Shafiq (Functional Nanomaterials Laboratory, Oklahoma State University).

89]. Time-resolved fluorescence has revealed that A* (monitored at 460 nm) decays with time constants of 4 and 12 ps, while a concomitant rise of the 509 nm fluorescence occurs on the same ps timescale [11, 33-36]. These observations have suggested that A* converts to an intermediated excited form I*, which subsequently decays to I (3 ns) that produces the 509 nm emission, or more rarely, can go through the non-radiative conversion I*→B* [11, 33-36]. I re-protonates and converts to A in a time scale of 400 ps [36, 49]. The similarity in the emission maxima of I*→I (509 nm) and B*→B (503 nm) is explained by the structural similarity of I and B states and I is

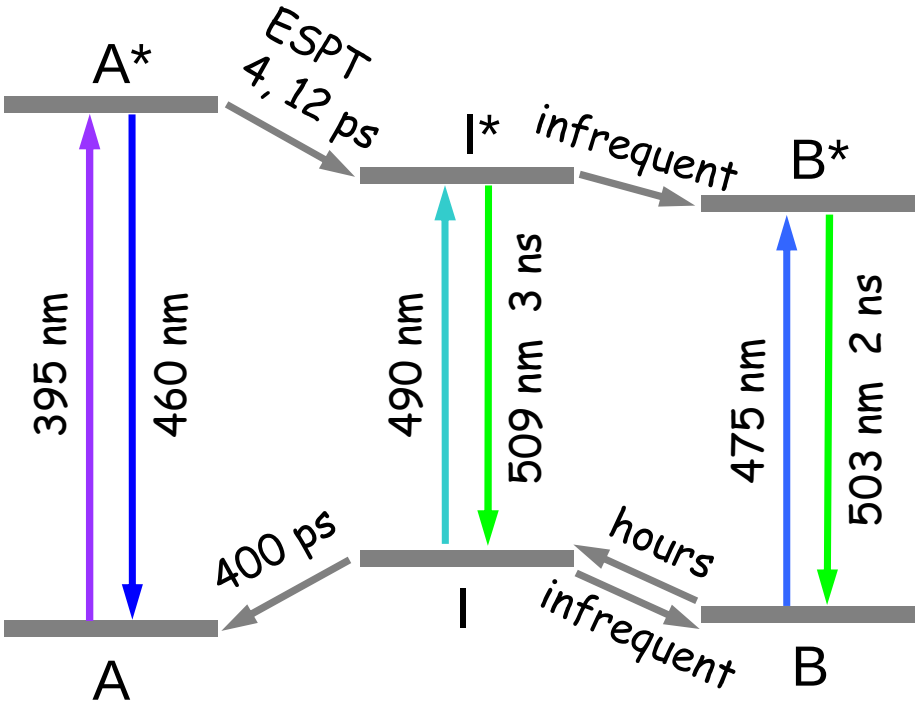

Figure II.5. Summary of the photophysics in the wtGFP chromophore. Figure: courtesy of Dr. Ali Kaan Kalkan (Functional Nanomaterials Laboratory, Oklahoma State University).

thought to be an unrelaxed from of B with a lower degree of H-bond stabilization at the phenol oxygen [5, 6, 11, 33-36]. Finally, the absorption peak corresponding to I→I* is found at 490 nm [39, 40]. So far discussed photo-physics is summarized in Figure II.5.

II.3. Surface Enhanced Raman Scattering (SERS)

C. V. Raman discovered the Raman effect in 1928 [51]. The theory behind this effect was first postulated by Smekal in 1923 [52]. The Raman effect is inelastic scattering of photons due to their interaction with the vibronic states where a vibrational quantum is excited (Stokes Raman scattering) or annihilated (Anti- Stokes Raman scattering) (Figure II.6) [51-55]. In recent years Raman spectroscopy has attracted a significant interest in the study of bio-molecules because it provides a great deal of information about molecular structure. However, Raman

spectroscopy is limited to high concentrations of analyte due to small Raman cross sections of the molecules which are on the order of 10^{-34} cm^2 [53-55]. On the other hand, fluorescent spectroscopy exploits fluorescence cross sections on the order of 10^{-17} cm^2 [53-55]. Fortunately however, in 1977, it was observed by Fleishman *et al*. that the Raman scattering could be dramatically enhanced when molecules are adsorbed on rough metallic surfaces [60]. This effect is known as surface enhanced Raman spectroscopy (SERS) and can account for 10^{14} fold enhancement of the Raman signal, enabling detection down to single molecules [18-20, 53-55, 61-68].

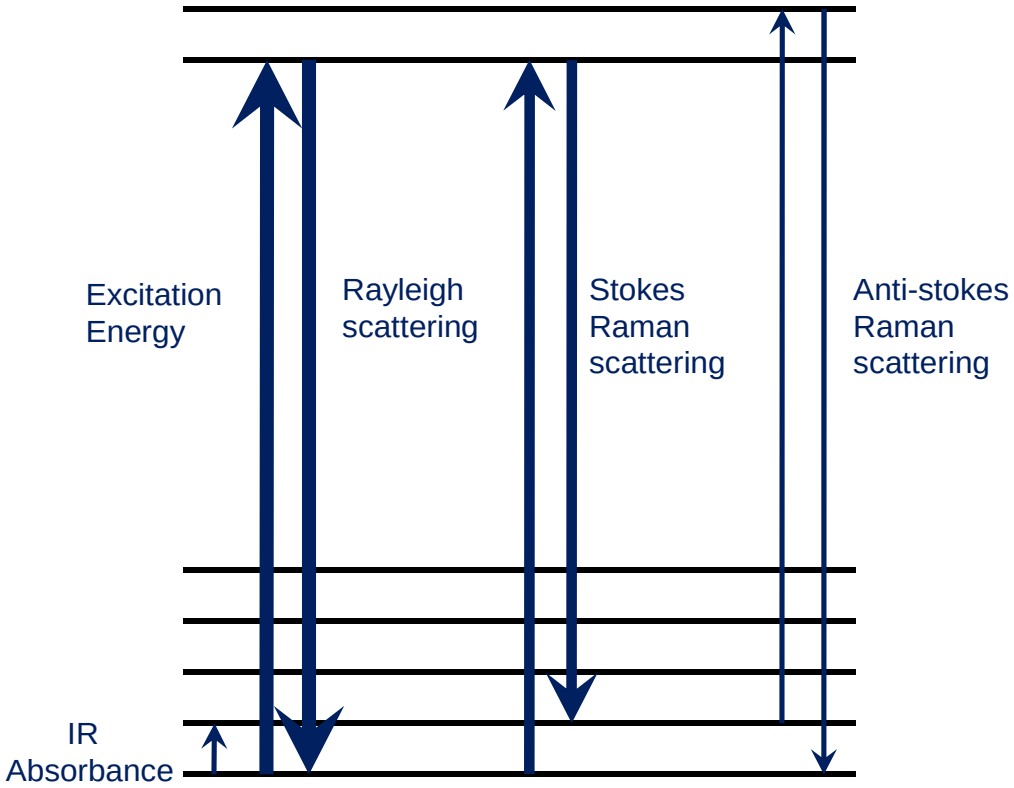

Figure II.6. Energy level diagram demonstrating Raman scattering. Thickness of lines indicates the signal strength of different mechanisms of scattering.

The origin of the SERS effect has been attributed to two mechanisms. The major contribution to SERS is known as the electromagnetic enhancement (EM) mechanism and it involves concentration of the incident and scattered field in proximity of metal nanostructures [18-20, 53-55, 62, 70]. The field concentration, in turn, is caused by excitation of oscillating dipoles in the metal nanostructures. The oscillating dipole is created by in-phase coupling of the free electron gas of the metal nanostructure to the incident field once the characteristic size of the metal is significantly smaller (i.e., 20 times or smaller) than the wavelength of the incident radiation. These collective (in-phase) oscillations of the electrons are known as *"plasmon resonances"* [18, 19, 61, 62]. Increases in the intensity of Raman signal have been regularly observed on the order of 10^4-10^6 for single particles, and can be as high as 10^8 and 10^{14} for aggregates of nanoparticles [18-20, 53-55, 61-68].

The second contributor to the SERS effect is known as chemical enhancement, or "Charge Transfer Model" (CT) [18-20, 53-55, 63, 69]. As Raman scattering is governed by the relation, $(E\alpha)^4$ (where, E = amplitude of the electric field and α = molecular polarizability), then SERS must involve an increase in either or both of the terms E and α [18-20, 52-55, 61-68]. The EM theory addresses the enhancement of the electric field (E) and proposes that observed enhancement is due to surface plasmons. On the other hand, CT model is concerned with the enhancement of the molecular polarizability (α) and is based on the principle that an adsorbed molecule can, under specific conditions, interact with a metal surface in such a way that there is a large increase in molecular polarizability. However, the existence of a CT enhancement is itself not in doubt, the level to which it contributes to SERS signal is still a matter of debate. One common feature between these two theories is that both require surface roughness for spectral enhancement to occur. SERS is observed primarily for analytes that adsorb on mintage (Au, Ag, Cu) or alkali (Li, Na, K) metal surfaces, with the excitation wavelength near or in the visible region.

In 1997, Nie *et al.* demonstrated SM-SERS for the first time from rhodamine 6G (R6G) molecules and showed that a very small number of nanoparticles exhibit unusually high enhancement efficiencies [20]. These particles emitting bright light (Stokes-shifted) towards the longer wavelengths were termed as "hot particles" by Nie *et al.* [20]. However, to screen these hot particles Nie *et al.* followed an extensive approach. They prepared Ag colloid solution by the procedure followed by Lee *et al.* [102]. Unfortunately, the citrate ions adsorbed on the Ag nanoparticles in this procedure hinder analyte adsorption. As a remedy, Nie *et al.* incubated an aliquot of the colloid with R6G molecules for an extended period of time (~ 3 hours) at room temperature. Subsequently, the analyte adsorbed Ag particles were immobilized on polylysine-coated glass surfaces prior to the SERS. Finally, this turned out to be a lengthy preparation procedure and it has to be repeated for every different analyte sample. Although this discovery by Nie *et al.* implicated the possibility of trace level detection, however, due to its extensive preparation procedure this technique has found only a limited use since its first demonstration. In this present thesis work a unique approach of SM-SERS has been adopted from the technique demonstrated by Kalkan *et al.* [14, 15] and further modified by the author. This specific technique was found to be more efficient than the approach followed by Nie *et al.* [20], as the preparation of the SERS experiment in this method was less time consuming and straightforward. Detailed discussion on the experimental protocols followed in this work is provided in Chapter III.

CHAPTER III

EXPERIMENTAL DETAILS

III.1. Outline

This Chapter provides the details of the measurement conditions and protocols that are employed in the detection of single GFP molecules. It also discloses the procedures of "nanometal-on-semiconductor" substrate fabrication.

III.2. Semiconductor Thin Film Deposition

The "nanometal-on-semiconductor" SERS substrates employed in the present thesis work consist of monolayers of Ag nanoparticles chemically reduced on thin germanium films [14, 15]. The Ge film not only immobilizes the nanoparticles, but it also serves as the reducing agent during the synthesis of nanoparticles. The reducer germanium thin films were deposited on 2" × 1" Corning 1737 code glass slides. An extensive cleaning protocol was followed during the preparation of thin films to get rid of all foreign particles as well as organic residues from the glass surface. Glass slides were immersed in a 50% IPA (isopropyl alcohol) solution (125 ml of DI water + 125 ml of 99% IPA) and a brush was used to scrub off organic residues and particles. Subsequently, ultrasonication of the glass substrate in 50% IPA solution was carried out at a temperature of 70˚ C for 10 minutes. Glass slides were then rinsed in deionized (DI) water under ultrasonication at 70˚ C for 5 minutes to remove all IPA residues. After taking the glass slides out of the ultrasonicator, they were blow dried with nitrogen/argon gas. The cleaned slides were then

put on a hot plate at a temperature of 150˚ C for 15 minutes to desorb the moisture.

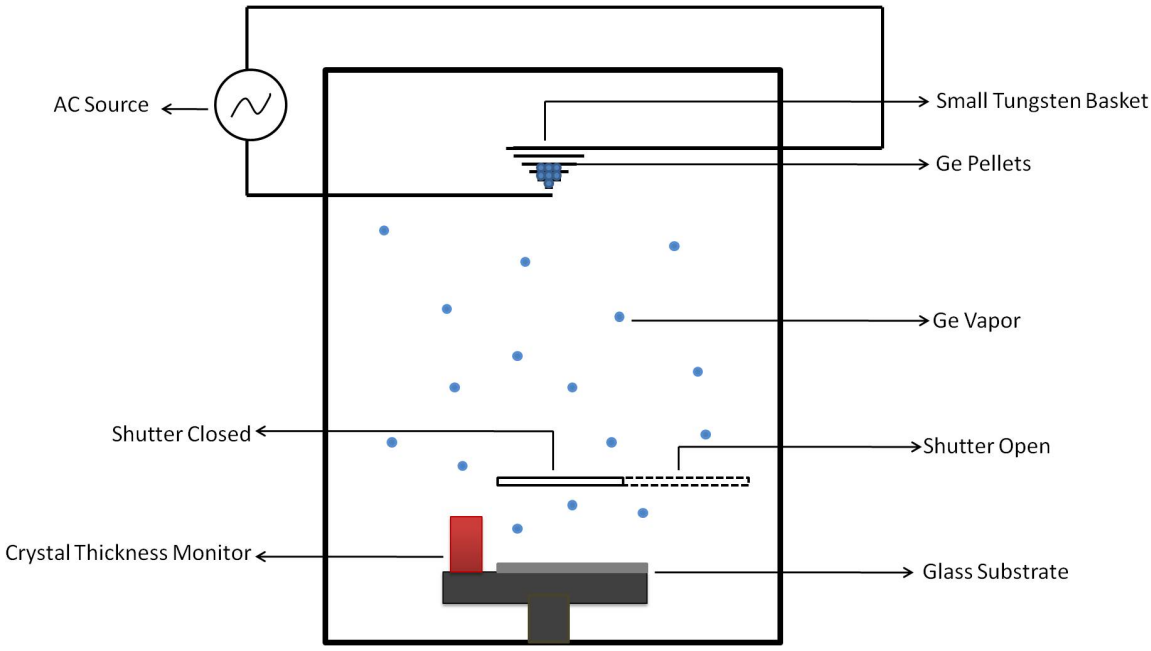

Figure III.1. Schematic of physical vapor deposition (PVD) system employed to deposit thin semiconductor films.

A Cressington 208 Physical Vapor Deposition (PVD) system was employed to deposit thin Ge films on the cleaned glass slides. Figure III.1 shows the schematics of the PVD process. As shown in the diagram, small pellets of germanium were placed inside the tungsten basket and the glass slide was positioned on the deposition stage. A turbo pump backed by a mechanical pump was used to create a vacuum with a base pressure of 4×10^{-5} mbar inside the chamber. Germanium pellets were melted by the resistance heating in the tungsten basket as the electric current adjustably increased through it. Crystal thickness monitor was set to zero before starting the deposition (shutter closed). After setting the density for Ge (5.32 g/cm^3) the rate of deposition was set to a pre-decided value of 2.5 Å/s by adjusting the current passing through the basket.

Then, the shutter was opened to start deposition of the germanium film. A thin film of 4.5 nm was thus coated in approximately 18 seconds after which the shutter was closed and current was set to zero. Subsequently, the chamber was allowed to cool down under vacuum for 15 min before it was vented and the sample was removed.

III.3. Nanoparticle Reduction

Once the 4.5 nm thick Ge film was deposited, it was immersed in 0.002 M $AgNO_3$ solution for 20 to 25 seconds to reduce Ag nanoparticles. A schematic of the reduction process employed to prepare these SERS substrates is shown in the Figure III.2.

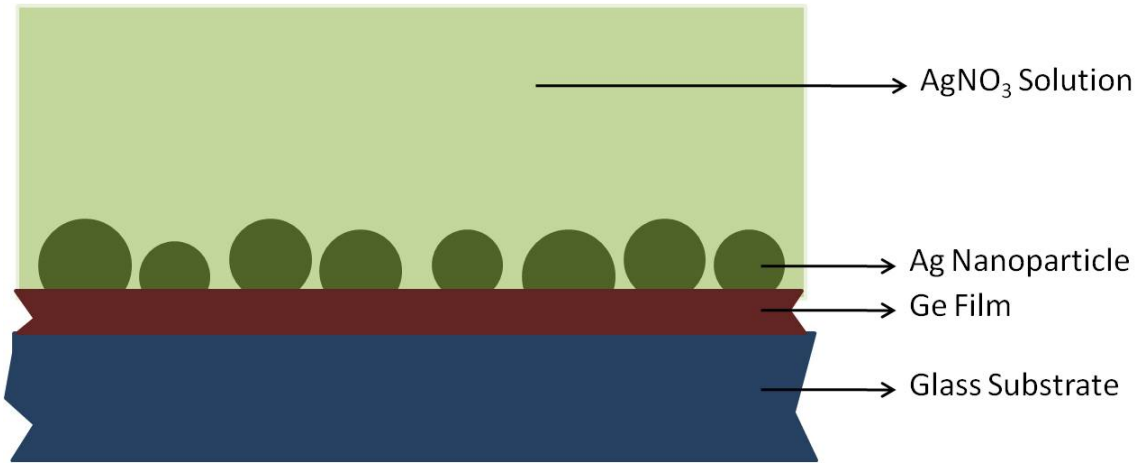

Figure III.2. Illustration of the silver nanoparticle reduction process on Ge thin films for the preparation of SERS active substrates

III.4. Acquisition of SM-SERS Spectra of wtGFP

SM-SERS measurements were performed with WITec alpha300R system. A 532 nm Nd:YAG (neodymium-doped yttrium aluminium garnet;Nd:$Y_3Al_5O_{12}$) laser was used as an excitation source. A grating of 600 g/mm was employed. In a typical SM-SERS acquisition, a 1 μL aliquot of 1×10^{-9} M wtGFP was spotted on a SERS substrate. Then the substrate was sealed

inside a spectrophotometer cell (Starna cell; 12.5×3.5×45 mm^3). Inside the cell, the aqueous aliquot reaches thermodynamic equilibrium with water vapor quickly and it does not dry.

An objective lens of 20× was employed for excitation as well as collection of the signal. It was focused at the aliquot-substrate interface (i.e., Ag nanoparticles). Laser spot size was fixed around 5 μm. Two different incident powers of 100 μW and 700 μW were employed. The signal integration time was set to 50 and 100 ms for high (700 μW) and low (100 μW) excitation power, respectively. Graphical illustration of the SERS acquisition is shown in Figure III.3.

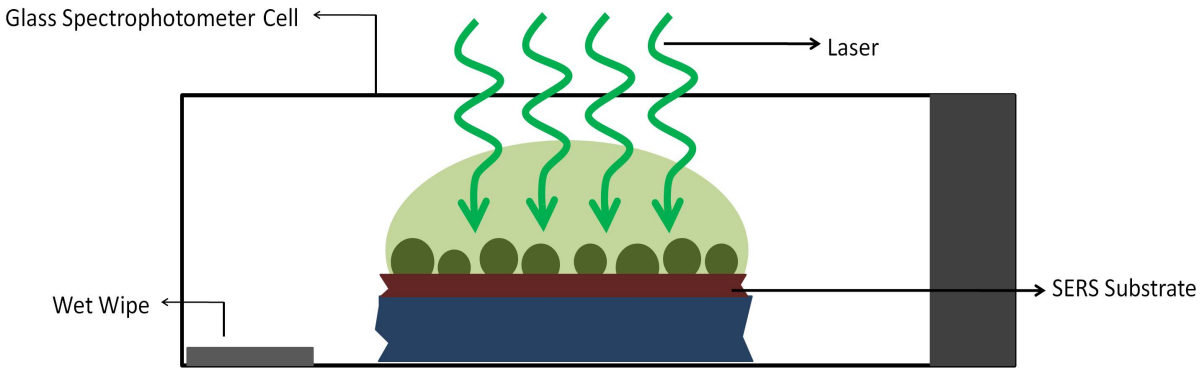

Figure III.3. Schematics of the SM-SERS acquisition.

Ensemble averaged SERS scans were performed using a Renishaw RM 1000 system equipped with a CCD detector. For these measurements, a 514nm Ar^+ ion laser (Spectra-Physics 160 series) was employed to excite SERS. Measurements were carried out with a 20% defocusing of the laser probe to reduce photo-bleaching while keeping the spot size around 20 μm. A 1 μL aliquot of 1.0×10^{-7} M wtGFP was spotted on the SERS substrate and a 20× objective lens with a numerical aperture of 0.4 was focused at the aliquot— substrate interface while conducting the SERS measurements. Three different laser intensities (3.4. 5.5 and 7.5 mW) were employed for ensemble average measurements. The signal integration time was set to 20 s. A grating of 1800 l/mm was used and centered at 1350 cm^{-1}.

CHAPTER IV

RESULTS AND DISCUSSIONS

IV.1. Outline

The present Chapter discloses and analyzes the time series SERS spectra of GFP single molecules. Under 532 nm laser excitation, a minimum of 4 conformational states of the GFP chromophore are observed as trans/cis and protonated/deprotonated combinations. Among these 4 states, the transitions occur in between certain pairs of states, which line-up in a cyclic pattern. Further, population of the 4 states and the probability of transitions (i.e., protonation $\leftrightarrow$ deprotonation and cis $\leftrightarrow$ trans) between them are investigated as a function of laser intensity. Particular transitions are found to be more frequent leading to increasing population of certain states. This effect is pronounced with increasing laser intensity. All results are summarized in the form of histograms at the end of the Chapter.

IV.2. Capturing SM-SERS spectra of GFP molecules

Aliquots of 1×10^{-9} M GFP were spotted on the SERS substrate and excited with the 532 nm Nd:YAG laser at two different incident powers of 100 and 700 μW. A 20× lens with a numerical aperture of 0.4 was focused at the aliquot-substrate interface and the laser spot size was set to around 5 μm. Subsequently, time series SERS spectra were collected with an integration time of 50 or 100 ms. While capturing the SERS spectra, sudden appearance of sharp and narrow

peaks on the weak spectral background were observed once every 30 seconds on the average. These temporal spectra with well resolved narrow peaks are referred as" Jumps", which generally sustain less than a second. These spectral jumps are attributed to single GFP molecule diffusing

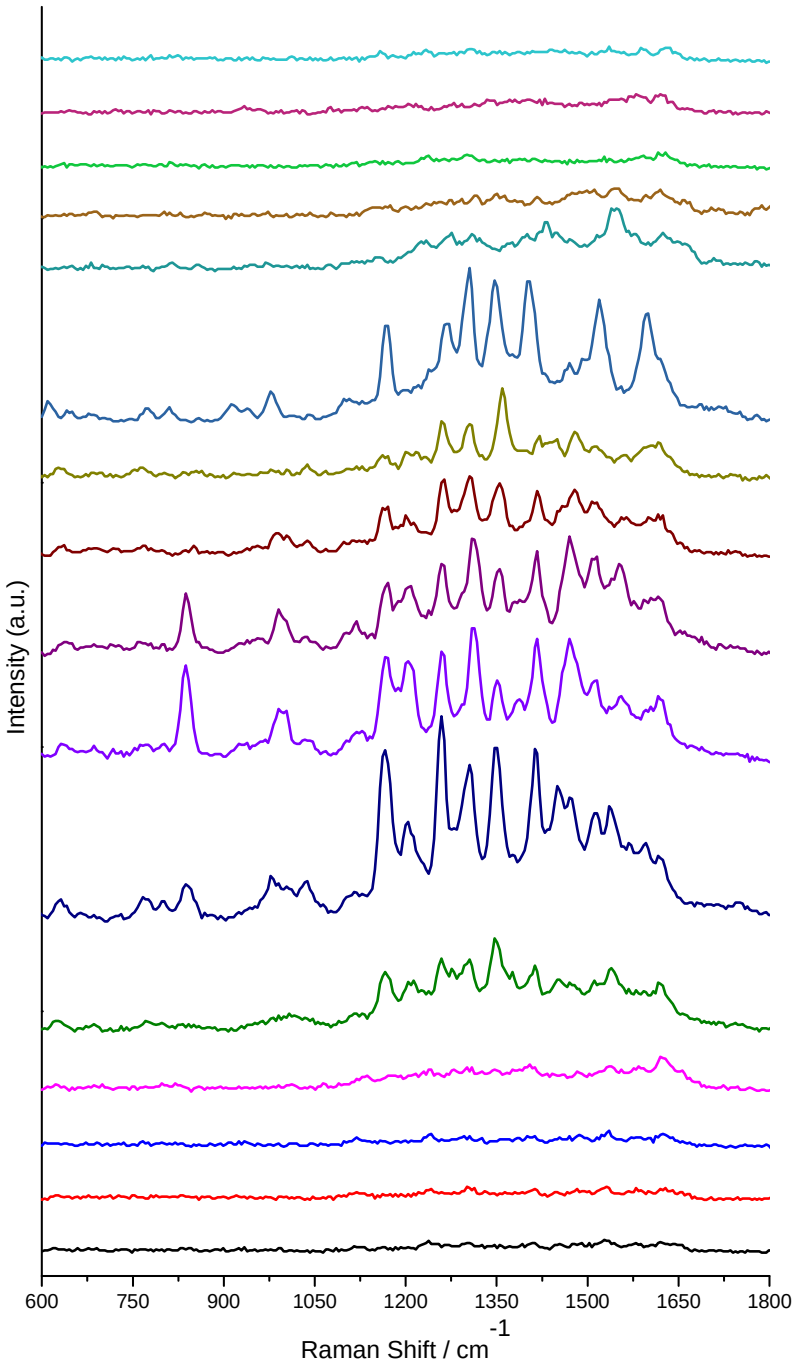

Figure IV.1. Time series SERS spectra demonstrating a single GFP molecule jump at 100 ms intervals.

in/out of the high SERS enhancement factor sites on “nanometal-on-semiconductor” substrates. Such high SERS enhancement factor sites on the substrate involve concentration of electromagnetic fields (as discussed earlier in the background chapter) in proximity of metal nanostructures, are typically known as “hotspots” [18-21]. Several lines of evidence indicate that the aforementioned spectral jumps arise from single GFP molecules adsorbed at the hotspots as discussed below. A representative single GFP SERS jump is shown in Figure IV.1 in terms of time series spectra at 100 ms intervals.

IV.2.1. Minor temporal fluctuations in peak wavenumbers

When a spectral jump as in Figure IV.1 is analyzed, the SERS peaks are observed to undergo temporal and random wavenumber shifts. These spectral fluctuations occur within ±5 cm^{-1} in consecutive spectra as exhibited by the spectral jump of Figure IV.2a. The minor temporal fluctuations are considered as an evidence of capturing single GFP molecules.

When a GFP molecule adsorbs to a Ag nanoparticle surface, it has a certain degree of translational and rotational freedom due to the weak adsorption. The restricted, however not completely inhibited freedom of GFP leads to a slowed-down motion of the molecule on the Ag surface. This motion of the GFP, induces alternating stresses on its β-barrel structure and thereby creates slight alteration in bond lengths and angles of the chromophore inside the barrel. The consequence is minor frequency fluctuations of ±5 cm^{-1}. Such small temporal fluctuations in peaks frequencies were reported in earlier for SM-SERS works and referred as typical characteristics of single molecule SERS [18-21, 71-76].

IV.2.2. Relative intensity fluctuations of the peaks

Time series SERS spectra of GFP as discussed above also reveal relative intensity fluctuations of the Raman peaks during a jump as seen in Figure IV.2b. While a single GFP molecule radiates detectible SERS signal in a hotspot, it may adsorb to the Ag surface in a variety

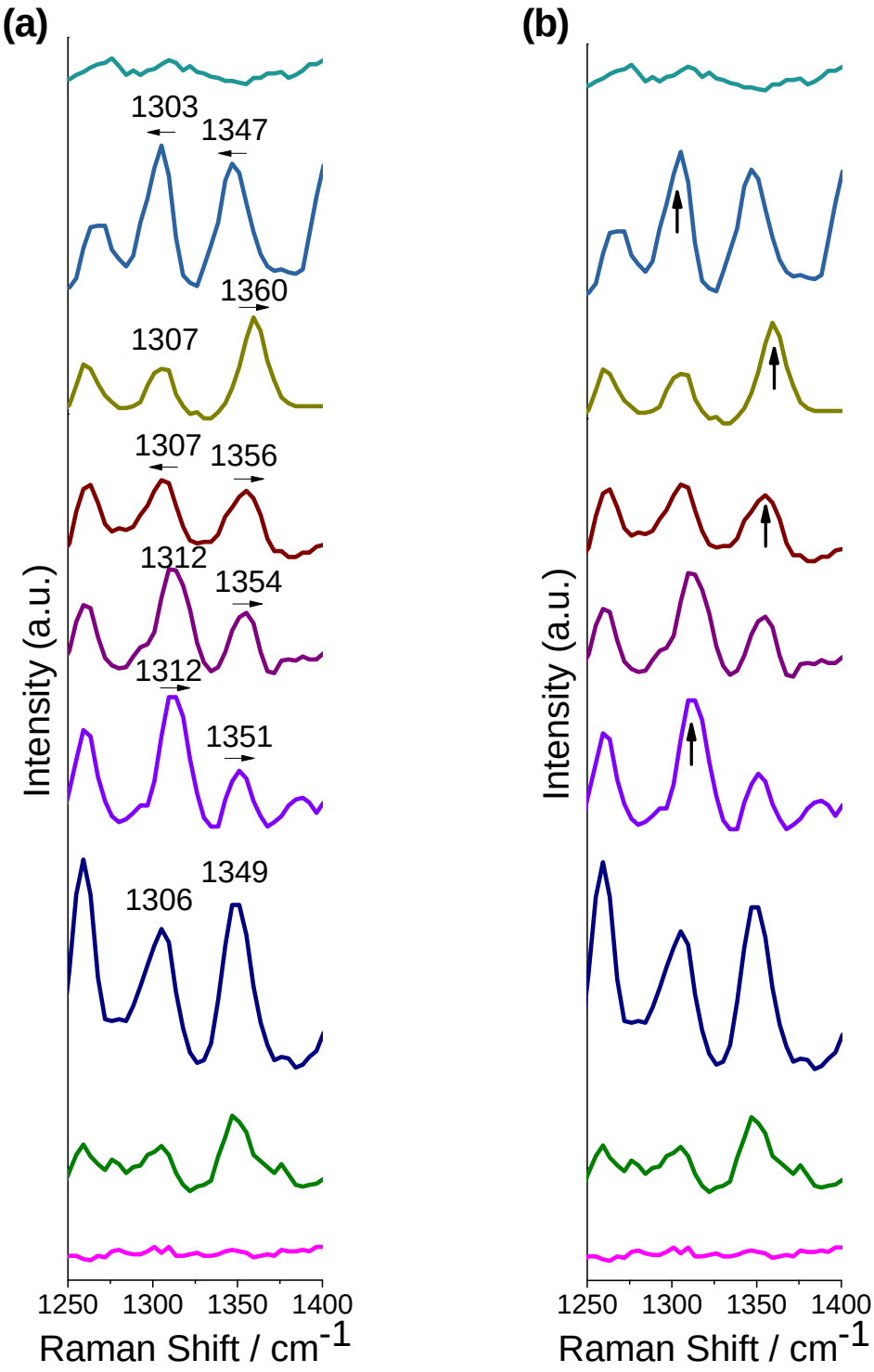

Figure IV.2. Time series SERS spectra of a single GFP molecule (1250 - 1400 cm^{-1} range of Figure IV.1) exhibiting: **(a)** random frequency fluctuations; **(b)** relative intensity fluctuations of the peaks. Arrows indicate (a) relative spectral shifts and (b) relative intensity fluctuations with respect to the previous scan.

of orientations. The surface-enhanced field is normal to the Ag surface. The SERS intensity for a vibrational mode depends on how well the corresponding Raman transition moment aligns with the enhance-field. Accordingly, if the transition moment is normal to the surface too, then the intensity of the SERS peak is maximized. In turn, the direction of Raman transition moment depends on the orientation of the molecule. Further, different vibrational modes have transition moments in different directions. Hence, a particular orientation of the molecule can maximize some Raman peaks, while subdue others. As a result, rotation of the GFP on Ag surface is expected to yield temporal variations in the ratio of peak intensities. In an EA measurement such variations are averaged out yielding a stable spectrum. However, for single molecules, the absence of averaging reveals such heterogeneity. Hence, relative intensity fluctuations in SERS can be considered as an evidence for single molecules.

IV.2.3. Structural transitions

Time series SERS spectra of single GFP molecules also reveal sudden disappearance of certain peaks with concomitant appearance of new peaks (Figure IV.3, spectra 8 and 9). Because a GFP molecule can stand in a single conformation at a time, such spectral changes indicate certain structural transitions between distinct forms of a single GFP molecule chromophore. Unlike, the minor temporal frequency shifts, the shifts discussed here are in the range of at least ± 15 cm^{-1}. Further, they are persistent for a longer period of time. As illustrated by Figure IV.3, the sudden frequency shift between spectra 6 and 8 (from 1560 cm^{-1} to 1530 cm^{-1}) suggests such a transition of a GFP chromophore (here protonated→ deprotonated) [16]. More detailed discussion on different forms of GFP and transitions between the forms will be provided later in this Chapter. Observing such individual molecular activity in consecutive SERS scans also holds strong evidence of capturing single GFP molecules. On the other hand, in EA measurement such transitions cannot be resolved and mutually exclusive peaks appear together due to the co-existence of populations of different forms.

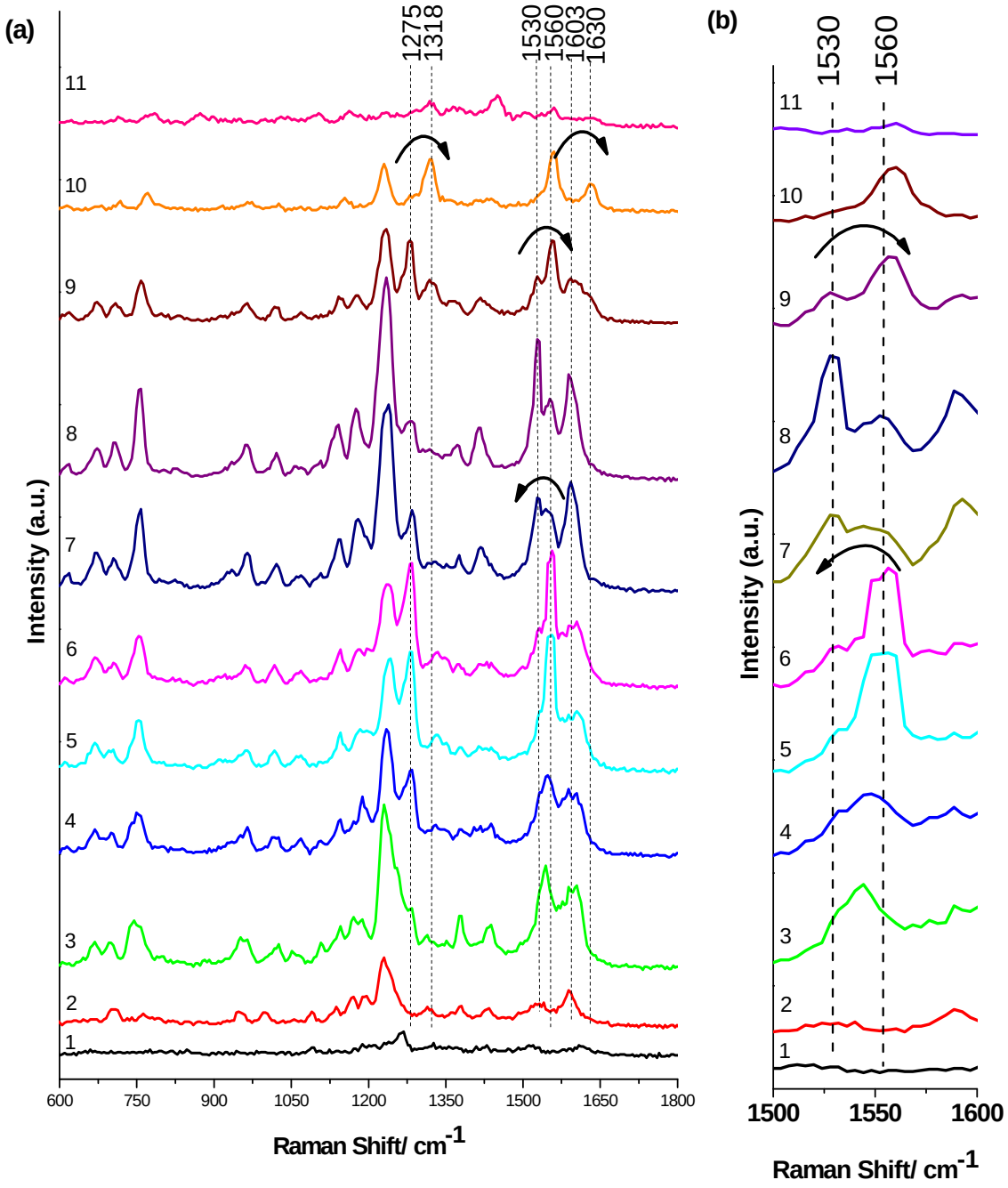

Figure IV.3. Time series SERS spectra of a single GFP molecule illustrating structural transitions: **(a)** 600-1800 cm^{-1}; **(b)** 1500 -1600 cm^{-1} (magnified).

However, in few spectra of Figure IV.3, Raman peaks defining two different forms of the chromophore are found simultaneously (Figure IV.3 spectra 6), which suggest structural transition of the chromophore between two different forms (i.e., here protonated→deprotonated) during that particular time interval [16].

IV.2.4. Elimination of heterogeneous broadening

As seen from the Figure IV.4, our captured single molecule SERS spectra of GFP exhibit sharper and narrower peaks in comparison to the spectrum captured from an ensemble-averaged SERS measurement, which can be considered as yet another evidence of capturing single GFP molecules. As discussed in Section IV.2.1, a GFP molecule at a certain form may also exhibit small variations in Raman peak positions wit in ±5 cm^{-1} as a result of its changing adsorption configurations. In an ensemble-averaged measurement, the signal is averaged from a large number of molecules. Consequently, such diversity of peak positions is averaged out and thereby, heterogeneous broadening in the spectrum is found. On the other hand, heterogeneous broadening exceedingly unlikely in case of single molecule SERS spectrum, as can be noticed from Figure IV.4.

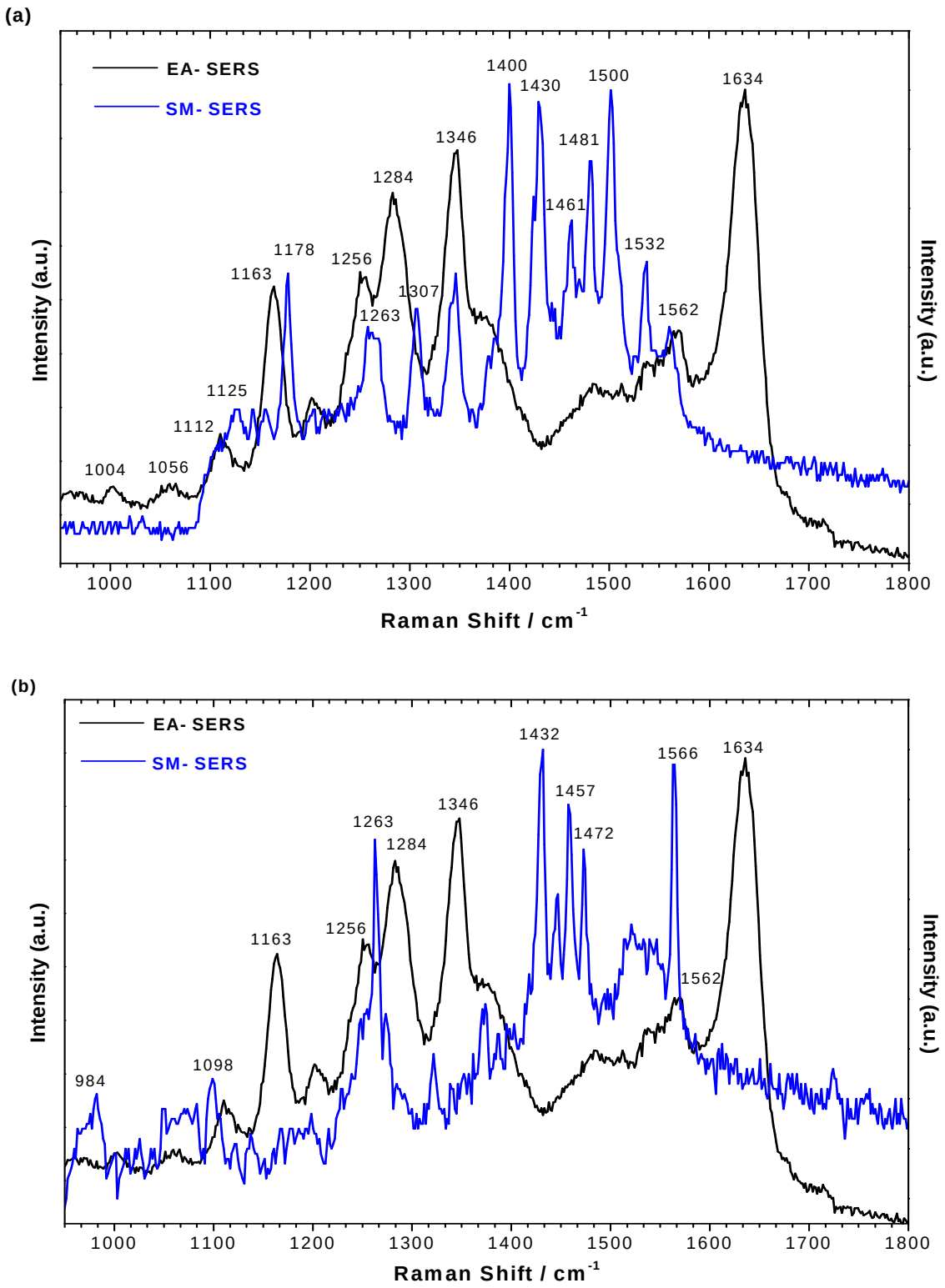

Figure IV.4. Ensemble-averaged SERS (EA-SERS) vs single molecule SERS spectrum (SM-SERS) of GFP. The captured molecules in SM-SERS are exhibiting Raman peaks primarily characterizing **(a)** deprotonated form and **(b)** protonated form of the GFP chromophore.

IV.3. Observing 4 different states

As reported in the literature so far, vibrational mode assignments of GFP chromophore are based on the ensemble-averaged Raman measurements on HBDI (4-hydroxybenzylidene-2, 3-dimethyl-imidazolinone) and HBMIA (ethyl 4-(4-hydroxyphenyl) metheylidene-2-methyl-5-oxoimidazolacetate), synthetic analogs of the GFP chromophore [50, 80]. This sort of Raman measurement on wtGFP is very difficult as its optical excitation in the visible yields a strong fluorescence even far from the resonance [5, 6, 10]. The strong baseline in the signal makes it very difficult to resolve the Raman peaks. Therefore to avoid such difficulty, researchers adopted nonfluorescent HBDI and HBMIA for ensemble-averaged Raman measurements. However, the fluorescence is quenched in SERS due to GFP to silver nanoparticle energy transfer [18-20]. In the absence of fluorescence, the vibrational modes can be clearly resolved. In this present thesis work, to verify the consistency of our results, we performed ensemble-averaged SERS (EA-SERS) measurement on wtGFP at three different laser powers (i.e., 3.4, 5.5 and 7.5 mw) (Figure IV.5). Our EA-SERS spectrum of wtGFP agrees well with the Raman spectrum of wtGFP, EGFP (enhanced green fluorescent protein), HBDI and HBMIA with in a deviation of ±5 cm^{-1} [16, 50, 83-86]. However, few differences were found (Table IV.1). A summary of the vibrational markers assignments for the protonated/ deprotonated and cis/trans forms of GFP and related proteins/chomophores (i.e., wtGFP, RFP, EGFP, HBDI, HBMIA etc) is compiled in the Table IV.1.

In 2003, Habuchi *et al.* reported ensemble-averaged Raman spectrum of neutral (i.e., at pH 5.0) and anionic (i.e., at pH 7.4) forms of EGFP and assigned the vibrational fingerprints for the protonated/deprotonated forms of the EGFP chromophore [16]. They attributed the peaks around 1560 cm^{-1} and 1530 cm^{-1} to the "**protonated**" and "**deprotonated**" form of the chromophore, respectively, based on the isotopic labeling and normal-mode analysis on HBDI by He *et al.*[16, 50, 80]. Both bands have been ascribed to the delocalized imidazolinone/ exocyclic

C=C stretching mode of the chromophore. This mode is dominated by stretching of the C=N double bond of the imidazoline ring and stretching of the C=C double bond linking the two rings and referred to as the "C=N stretch" [16, 50, 80]. Our EA-SERS spectra from wtGFP reveal two peaks at 1562 cm^{-1} (protonated) and 1531 cm^{-1} (deprotonated), which show excellent consistency with the assignments made by Habuchi *et al.*

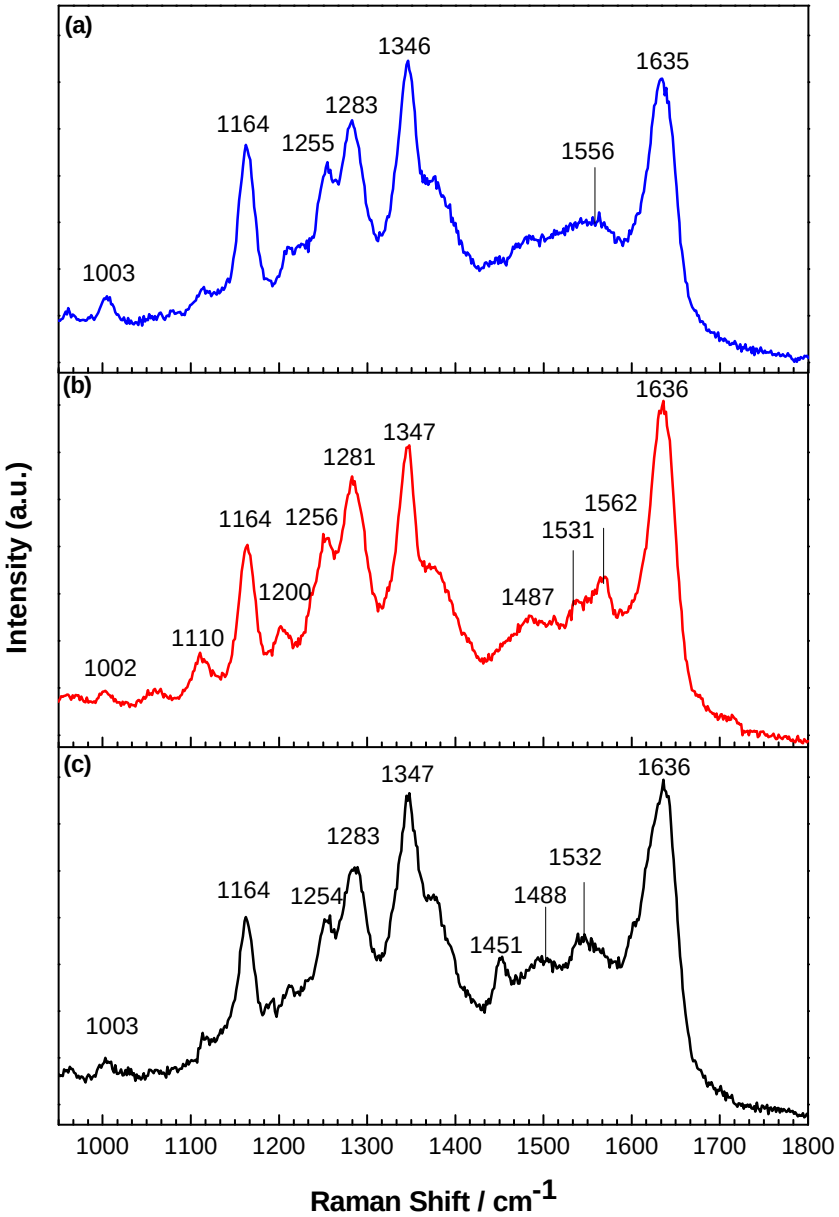

Figure IV.5. Ensemble-averaged SERS spectra of 1×10^{-7} M wtGFP acquired under 514 nm excitation at: (**a**) 7.5 mW; (**b**) 5.5 mW; and (**c**) 3.4 mW excitation.

Table IV.1. Vibrational (Raman) markers of conformational states for the GFP chromophore and its analogs

Group	Analyte	Acquisition conditions	Raman markers (cm^{-1})			
			protonated	deprotonated	cis	trans
He *et al.* [80]	HBDI	Raman (752 nm)	1567[a] 1556[b]	1533[b]	1234[a] 1246[b]	1281[a]
Habuchi *et al.* [16]	EGFP	SM-SERS (488 nm)	1562	1524	1259[c]	1281[c]
Habuchi *et al.* [16]	EGFP	Raman (647 nm)	1556	153	1254[c]	
Loos *et al.* [81]	eqF611	Raman (752 nm)	1562[d]	1526[d]	1258	1281
Loos *et al.* [81]	DsRed	Raman (752 nm)	1568[d]	1509[d]	1263	
Luin *et al.* [99]	GFP (Y66)	Raman (514.5 nm)	1565[d]	1515[d]	1270[c]	1290[c]
Bell *et al.* [50]	HBMIA	Raman (752 nm)	1567[e] 1556[f]	1525[e] 1535[f]	1257[e] 1265[f]	1280[e]
Bell *et al.* [101]	wtGFP	Raman (752 nm)	1566	1539	1244[c]	1278[c]
Bell *et al.* [101]	wtGFP	Raman (752 nm)	1565 1562[g]	1536 1542[g]	1244 1259[g]	1282

Gray: Inferred from the authors data and assigned by us

[a] Data obtained from neutral form of chromophore at pH 5.5. "trans" peak agrees with Loos *et al.* Peak at 1234 cm^{-1} found to be the closest of the "cis" (1260 cm^{-1}) peak suggested by Loos *et al.*

[b] Data obtained from anionic form of chromophore at pH 14.

[c] Bands found to be consistent with cis/trans markers as suggested by Loos *et al.*

[d] Bands found to be consistent with protonation/deprotonation markers as suggested by Habuchi *et al.*

[e] Data obtained from neutral form of chromophore at pH 4.5. "cis" and "trans" bands agree with Loos *et al.*

[f] Data obtained from anionic form of chromophore at pH 11.20. "cis" band agrees with Loos *et al.*

[g] Data obtained after Hg arc lamp (254 nm) irradiation for 90 min.

Later in 2006, Loos *et al.* suggested vibrational fingerprints for the "**cis**" and "**trans**" forms of the red fluorescent protein (RFP) chromophore, based on the Raman spectrum of RFP variants (i.e., eqFP611 and DsRed) from the sea anemone *Entacmaea quadricolor* [81]. Chromophore of these red fluorescent proteins contains an extended π-conjugated system; however, the remaining chemical structure is identical to the chromophore of the wtGFP. X-ray crystallographic studies confirm the chromophore of eqFP611and DsRed to be in a coplanar "trans" and coplanar "cis" configuration, respectively. Upon irradiation (532 nm), variant eqFP611 undergoes a permanent trans to cis isomerization. Consequently, Raman spectrum of

eqFP611 becomes identical to the Raman spectrum of DsRed through a spectral shift from 1281 cm^{-1} to 1263 cm^{-1}. Hence, Loos *et al.* attributed the peaks at around 1260 cm^{-1} and 1280 cm^{-1} to the "**cis**" and "**trans**" form of the red fluorescent protein chromophore, respectively [81, 82]. Our EA-SERS data from wtGFP indicate peaks at around 1256 cm^{-1} and 1281 cm^{-1}, which agree well with the cis/trans assignments on RFP chromophore by Loos *et al*. Although RFP is a different protein than GFP, due to significant similarity between the chemical structure of GFP and RFP chromophore, we adopted these "**cis**" and "**trans**" markers of RFP chromophore for GFP chromophore.

More recently, Luin *et al*. reported Raman spectra of cis and trans forms of GFP(Y66), a synthetic analogue of GFP chromophore and suggested possible vibrational markers for cis/trans forms of the GFP chromophore [99, 100]. Unfortunately, their suggested vibrational modes are not found to be consistent with our spectra. However, as inferred from their data, a shift of vibrational mode at 1270 cm^{-1} to 1290 cm^{-1} is noticed for cis to trans form of the chromophore. Although Luin *et al.* didn't comment on this spectral shift, this observation (by the author of the present thesis) is consistent with the vibrational mode assignments made by Loos *et al.* (i.e., cis marker at 1260 cm^{-1} and trans marker at 1280 cm^{-1}) [99, 100].

Based upon the Raman peaks assignments discussed above, it is apparent that GFP has at least four different conformational states as the combinations of protonation/deprotonation and cis/trans forms (i.e., cis/protonated, cis/deprotonated, trans/protonated and trans/deprotonated). It is well established that cis/protonated and cis/deprotonated forms of the chromophore attributes to the A and B state of GFP, respectively [16, 50, 80]. However, reports on the "trans" version of the chromophore are still limited and also controversial. In 2003, Nifosi *et al.* demonstrated the existence a nonfluorescent dark state, whose optical absorption is at higher energies than state A and B [91]. They claimed this state to be the trans and neutral form of the chromophore and termed it as the C state [91-93]. However, no real evidence of capturing trans/deprotonated form

of the chromophore was reported earlier. In the present work, for the first time, we provide evidence of capturing such a state with trans/deprotonated configuration of the chromophore. For consistency with the present nomenclature, we named this state (i.e., trans/deprotonated) of the chromophore as the D state.

Table IV.2 shows the primary markers that identify different conformational states of GFP chromophore. In addition, Figure IV.6 illustrates SM-SERS spectra captured from single GFP molecules at 4 different conformational states at 100 μW excitation: (**i**) A state (*cis & protonated*); (**ii**) B state (*cis & deprotonated*); (**iii**) C state (*trans & protonated*) and (**iv**) D state (*trans & deprotonated*).

Table IV.2. Vibrational (Raman) markers adopted in the present thesis work for characterizing the 4 different conformational states of GFP chromophore.

	protonated ($1560\ cm^{-1}$)	deprotonated ($1530\ cm^{-1}$)
cis ($1260\ cm^{-1}$)	**A state**	**B state**
trans ($1280\ cm^{-1}$)	**C state**	**D state**

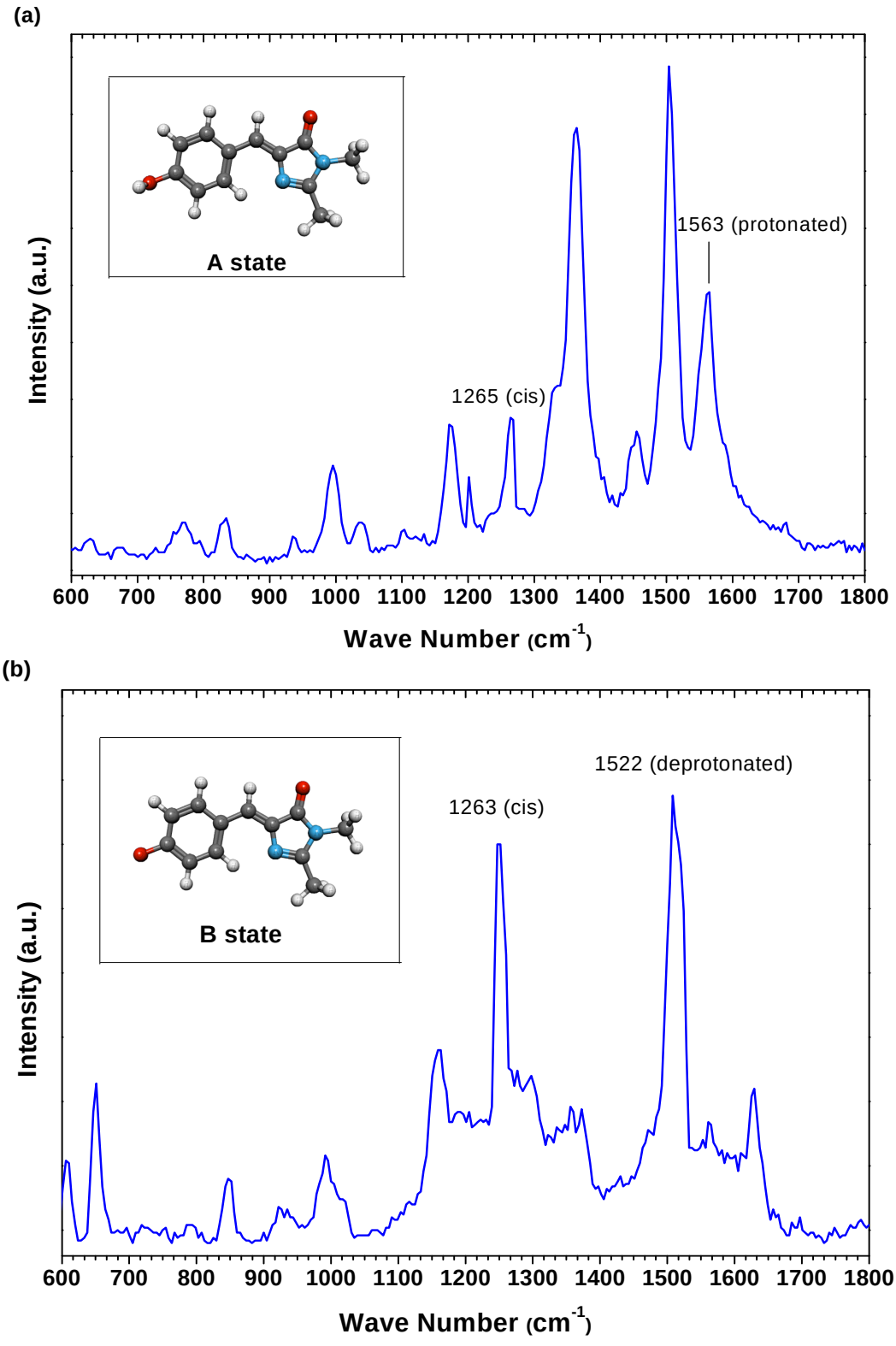
(a)
A state
1563 (protonated)
1265 (cis)
Intensity (a.u.)
600 700 800 900 1000 1100 1200 1300 1400 1500 1600 1700 1800
Wave Number (cm-1)
(b)
B state
1522 (deprotonated)
1263 (cis)
Intensity (a.u.)
600 700 800 900 1000 1100 1200 1300 1400 1500 1600 1700 1800
Wave Number (cm-1)

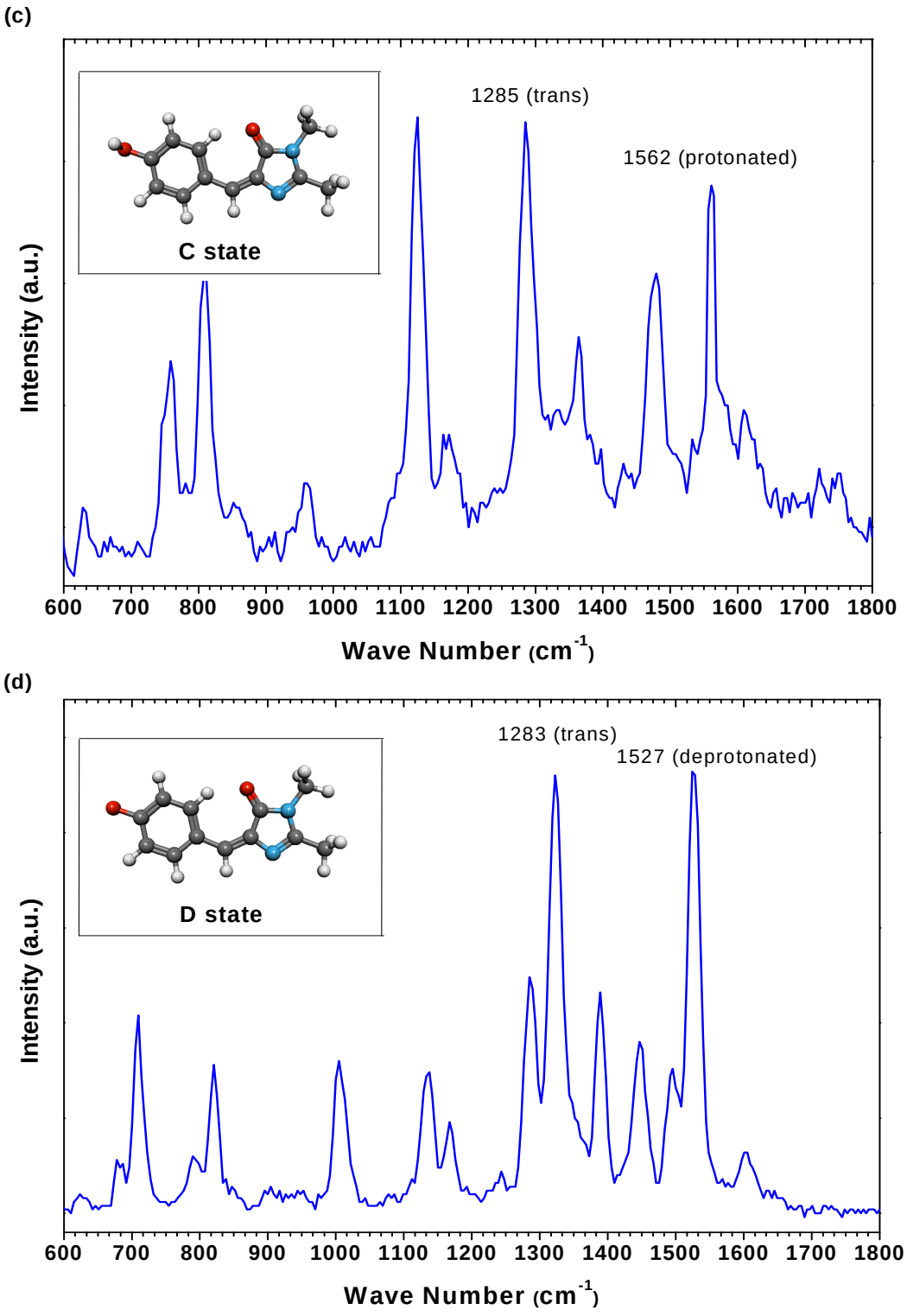

Figure IV.6. SM-SERS spectra captured from individual wtGFP molecules illustrating **(a)** A state, **(b)** B state, **(c)** C state and **(d)** D state. The corresponding chromophore structures are depicted by ball-stick models.

IV.4. Observing transitions between the states

As discussed earlier in Section IV.2.3, time series SERS measurements on single GFP molecules reveal certain structural transitions between distinct forms of its chromophore. Accordingly, we observed transitions between 4 chromophore states (A, B, C and D state) under two different laser excitations (i.e., 100 and 700 μW). Among 4 states of the GFP chromophore, transitions involved between certain pair of states (i.e., A↔B, B↔D, D↔C and C↔A), which line up in cyclic pattern as represented in Figure IV.7.

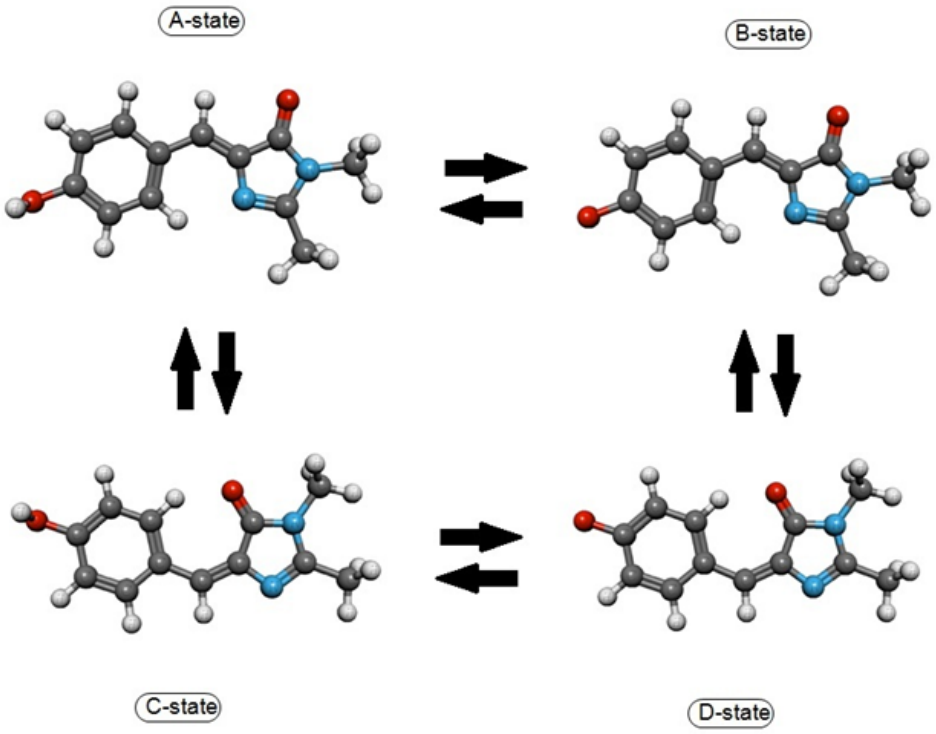

Figure IV.7. Transitions involved with A, B, C and D states of GFP chromophore corresponding to the protonated/deprotonated and cis/trans forms.

IV.4.1. Transitions observed at 100 µW laser excitation

The time evolution of SERS spectra of a single GFP molecule adsorbed at the hotspot is shown in the Figure IV.8. Consecutive SERS scans reveal transitions of the molecule between A and B states through protonation↔deprotonation. Initially, molecule was captured in the B state as confirmed by the cis (1266 cm^{-1}) and deprotonated (1526 cm^{-1}) peaks on the spectrum 2. An important observation within the series of spectra is the sudden frequency shift from 1526 cm^{-1} to 1565 cm^{-1} between spectra 3 and 4. This shift in the peak position has been attributed to the transition of the GFP chromophore from deprotonated to protonated form by Habuchi *et al* [16]. However, as this specific GFP molecule's chromophore stays in the cis (peak at 1266 cm^{-1}) configuration throughout the transition period, it confirms molecule's conversion from the B (cis/deprotonated) to A (cis/protonated) state. An opposite transition is observed between the spectra 6 and 7, where the peak at 1565 cm^{-1} (protonated) shifts to 1526 cm^{-1} (deprotonated), consequently indicating GFP molecule's transition from A to B state. More evidence of transitions between the states A and B are exemplified in the Figure IV.9.

Interestingly, similar kinds of transitions were also observed for the trans state of the GFP chromophore, namely C and D state. Time series SERS spectra in the Figure IV.10 illustrates GFP molecule's transition from the D to C state. In this particular case, GFP molecule was captured in the D state which is confirmed by the trans (1288 cm^{-1}) and deprotonated (1526 cm^{-1}) peaks in the spectrum 2. Consecutive SERS scans reveal sudden spectral shift from 1526 cm^{-1} (deprotonated) to 1565 cm^{-1} (protonated) between spectra 4 and 5, which confirms GFP molecule's transition from D (trans/ deprotonated) to C (trans/protonated) state. Moreover, the spectral series depicted in the Figure IV.11 clearly display the reversibility of the transformation between these two states (i.e., C→D). Further evidence of transitions between the states C and D are represented in the Figure IV.12.

So far discussed transitions (i.e., A⇌B and C⇌D) are based on the protonation⇌deprotonation of the GFP chromophore. Previously, Habuchi *et al.* observed these sorts of transitions for the EGFP chromophore at single molecule level [16]. However, they didn't distinguish between the cis/trans forms of the EGFP chromophore. In an addition, in this present thesis work, we also observed conversions between the cis/trans forms of the GFP chromophore, which involves transitions of the molecules between A⇌C and B⇌D states.

Time series SERS spectra illustrated in the Figure IV.13 reveal transitions between the states A and C of the GFP chromophore. Here molecule was captured in the C state as confirmed by the trans (1286 cm^{-1}) and protonated (1561 cm^{-1}) peaks in the spectrum 2. Spectral shift is noticed form 1286 cm^{-1} to 1268 cm^{-1} between spectra 3 and 4, which indicates trans→cis isomerization of the GFP chromophore, while staying in the protonated form. Hence, this particular shift in the wavenumber (i.e., from 1286 cm^{-1} to 1268 cm^{-1}) indicates conversion of the molecule from C (trans/ protonated) to A (cis/protonated) state. Further, spectra also display the reversibility of the conversion (i.e., A→C) between the two states between spectra 17 and 18. Few more evidences of similar conversions are exemplified in the Figure IV.14.

Moreover, transitions between the states B and D of the GFP chromophore were also observed as illustrated in the Figure IV.15. Time series SERS spectra show molecule was captured in the B state (cis/ deprotonated) and eventually it converted into the D state (trans/ deprotonated) under laser excitation. Spectral shift from 1266 cm^{-1} to 1285 cm^{-1} between spectra 2 and 3 indicates cis→trans isomerization of this particular GFP molecule, while holding the deprotonated configuration. Reversibility of this transition was also observed for a different GFP molecule and reported in the Figure IV.16.

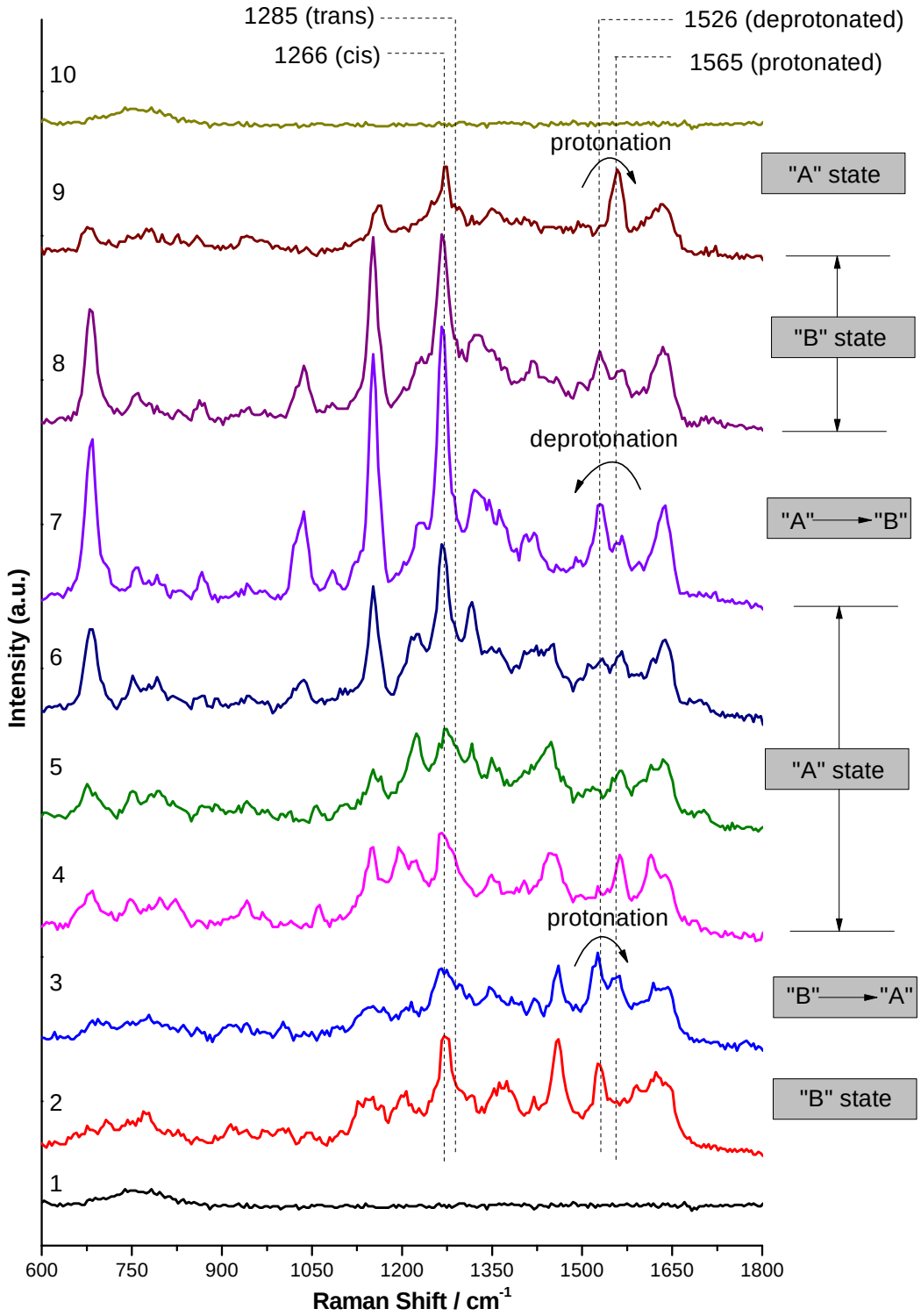

Figure IV.8. Time series SERS spectra of a single GFP molecule at 100 μW laser excitation (100 ms integration time). Molecule captured in the B state (cis/deprotonated) and converts into the A state (cis/protonated).

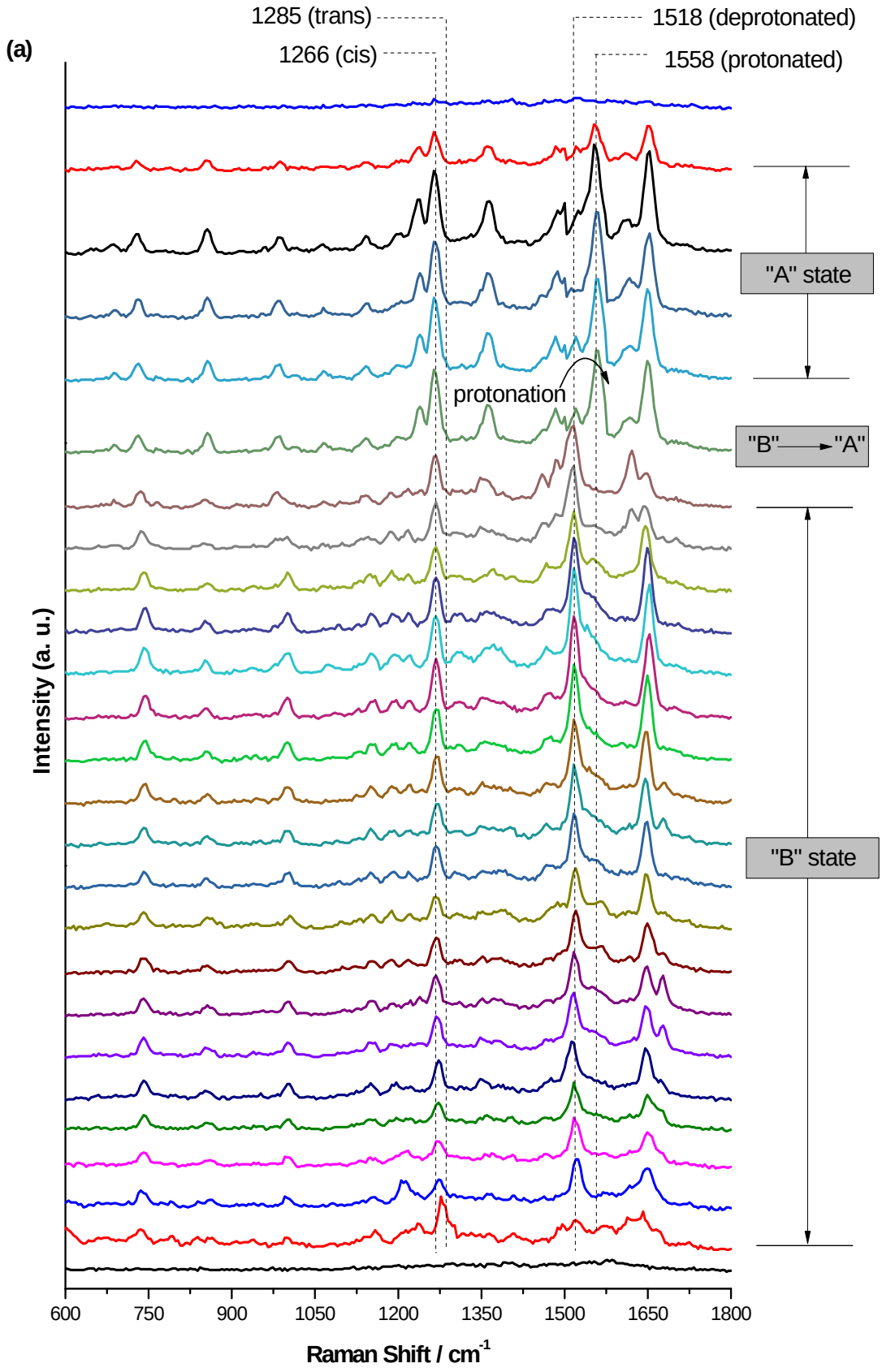
(a)
1285 (trans)
1266 (cis)
1518 (deprotonated)
1558 (protonated)
"A" state
protonation
"B" → "A"
"B" state
Intensity (a. u.)
600
750
900
1050
1200
1350
1500
1650
1800
Raman Shift / cm-1

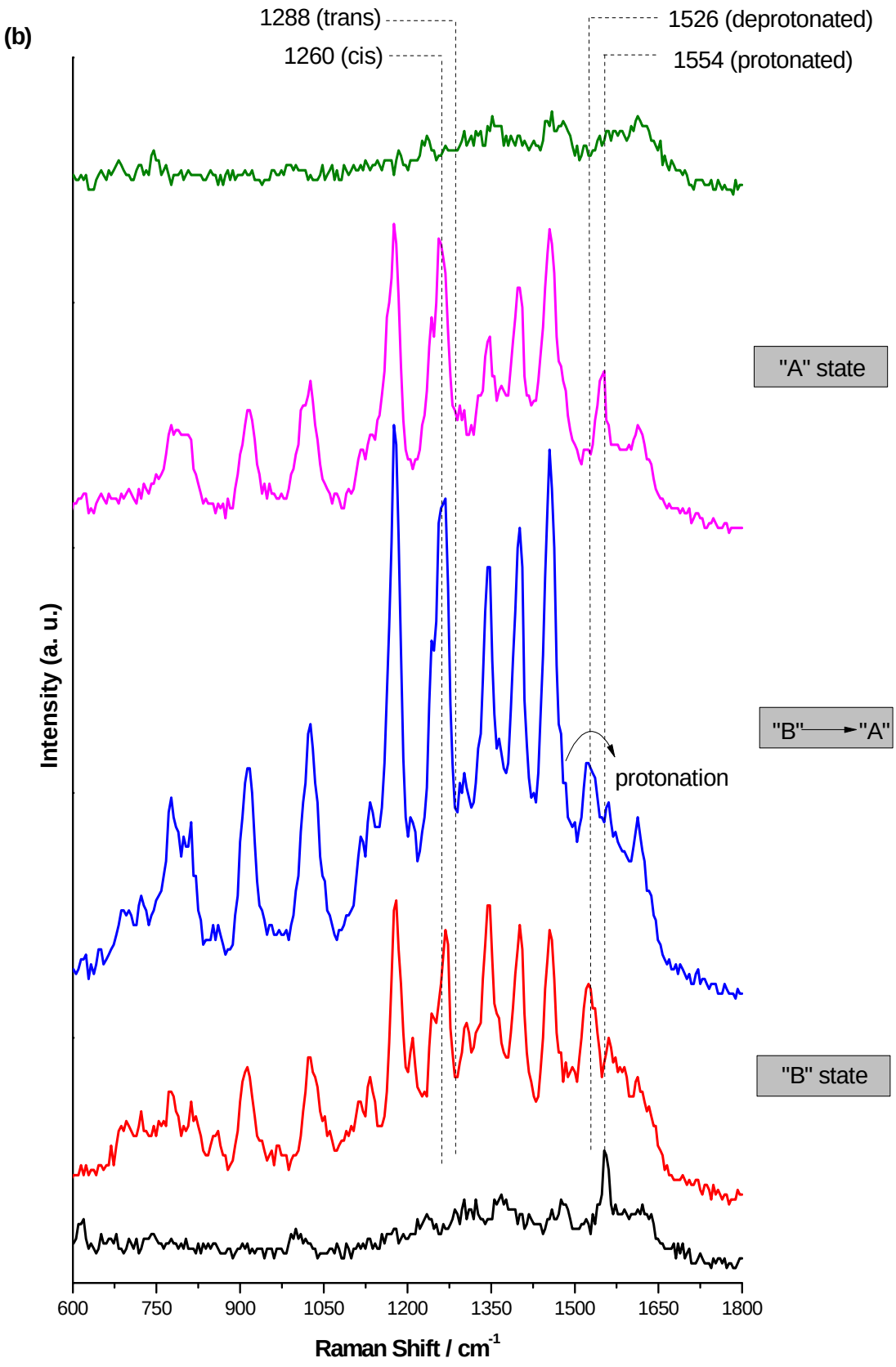
(b)
1288 (trans)
1260 (cis)
1526 (deprotonated)
1554 (protonated)
"A" state
"B"→"A"
protonation
"B" state
Intensity (a. u.)
600
750
900
1050
1200
1350
1500
1650
1800
Raman Shift / cm-1

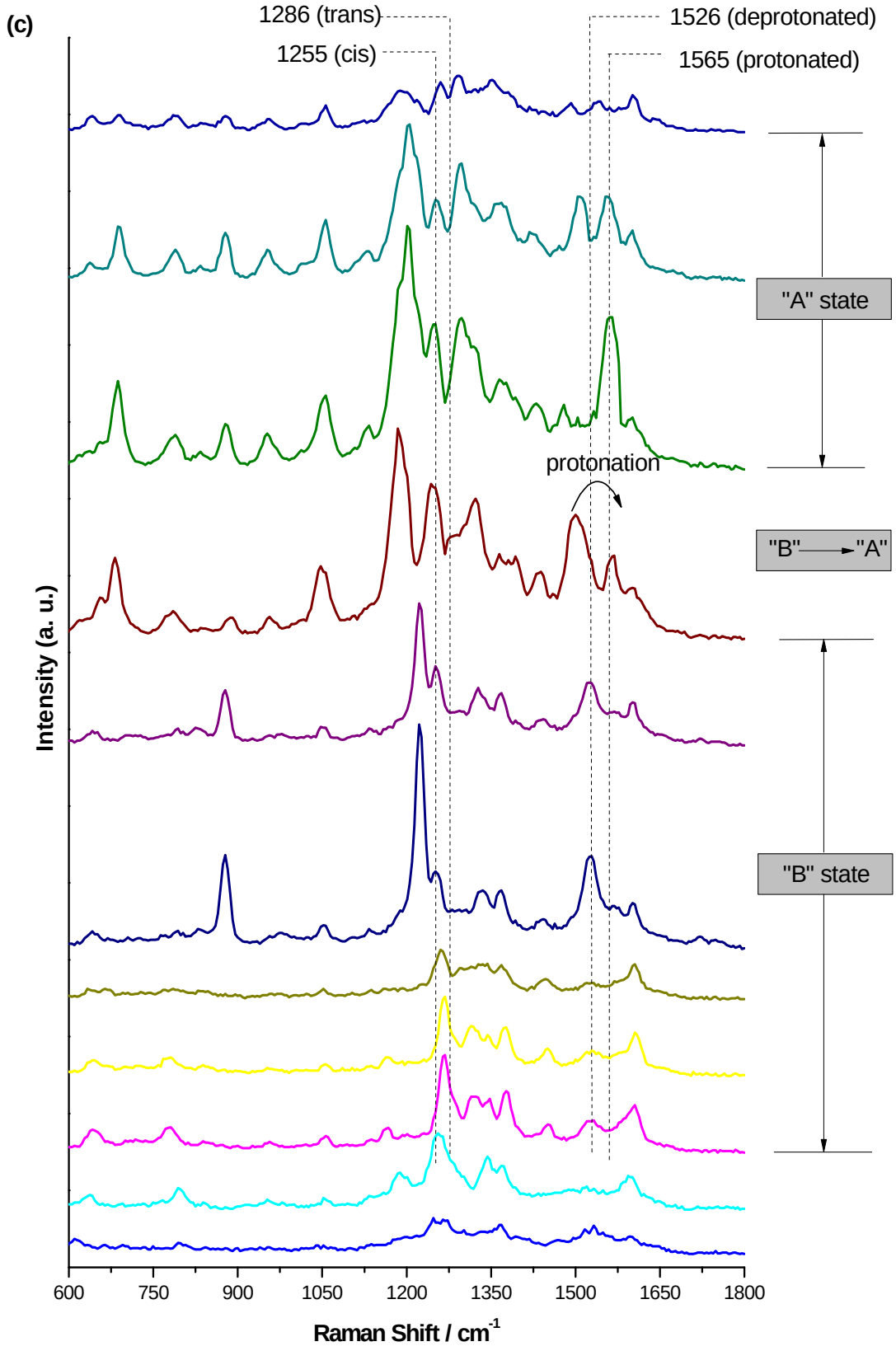
(c)
1286 (trans)
1255 (cis)
1526 (deprotonated)
1565 (protonated)
"A" state
protonation
"B"→"A"
"B" state
Intensity (a. u.)
600
750
900
1050
1200
1350
1500
1650
1800
Raman Shift / cm-1

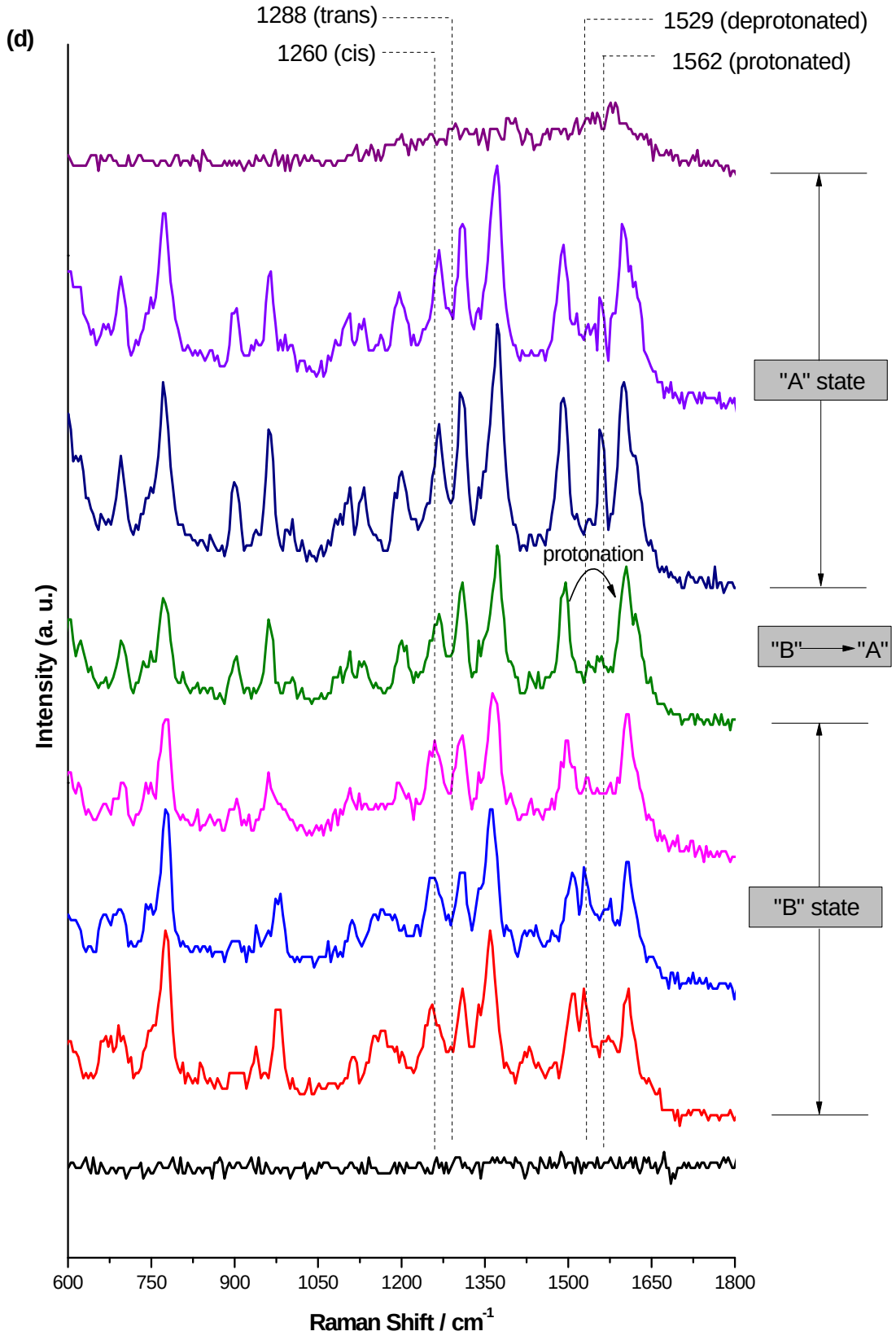
(d)
1288 (trans)
1260 (cis)
1529 (deprotonated)
1562 (protonated)
"A" state
protonation
"B"→"A"
"B" state
Intensity (a. u.)
600
750
900
1050
1200
1350
1500
1650
1800
Raman Shift / cm-1

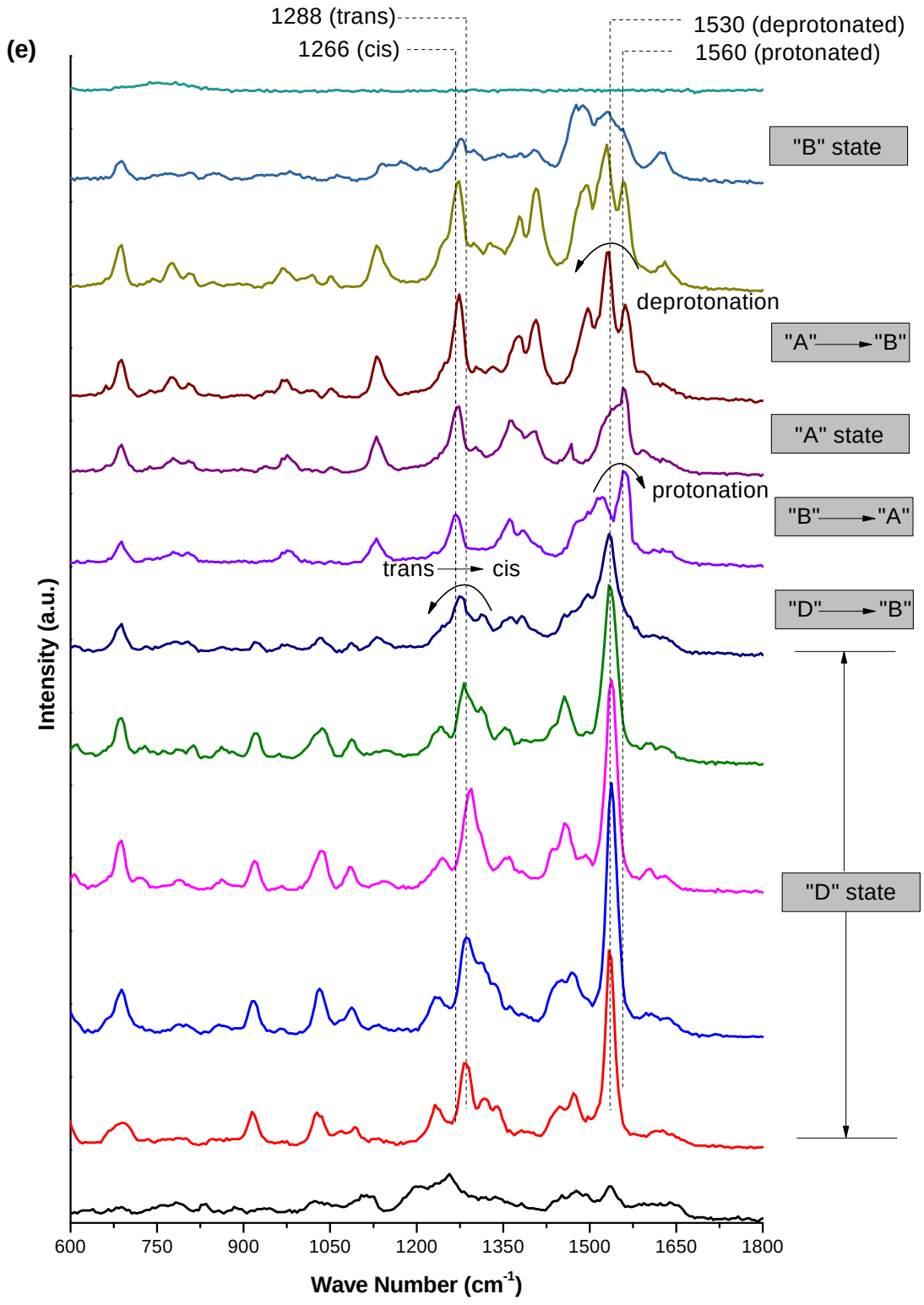

Figure IV.9. Time series SERS spectra illustrating transitions between the states A and B of individual GFP molecules (100 ms integration time, 100 μW laser intensity).

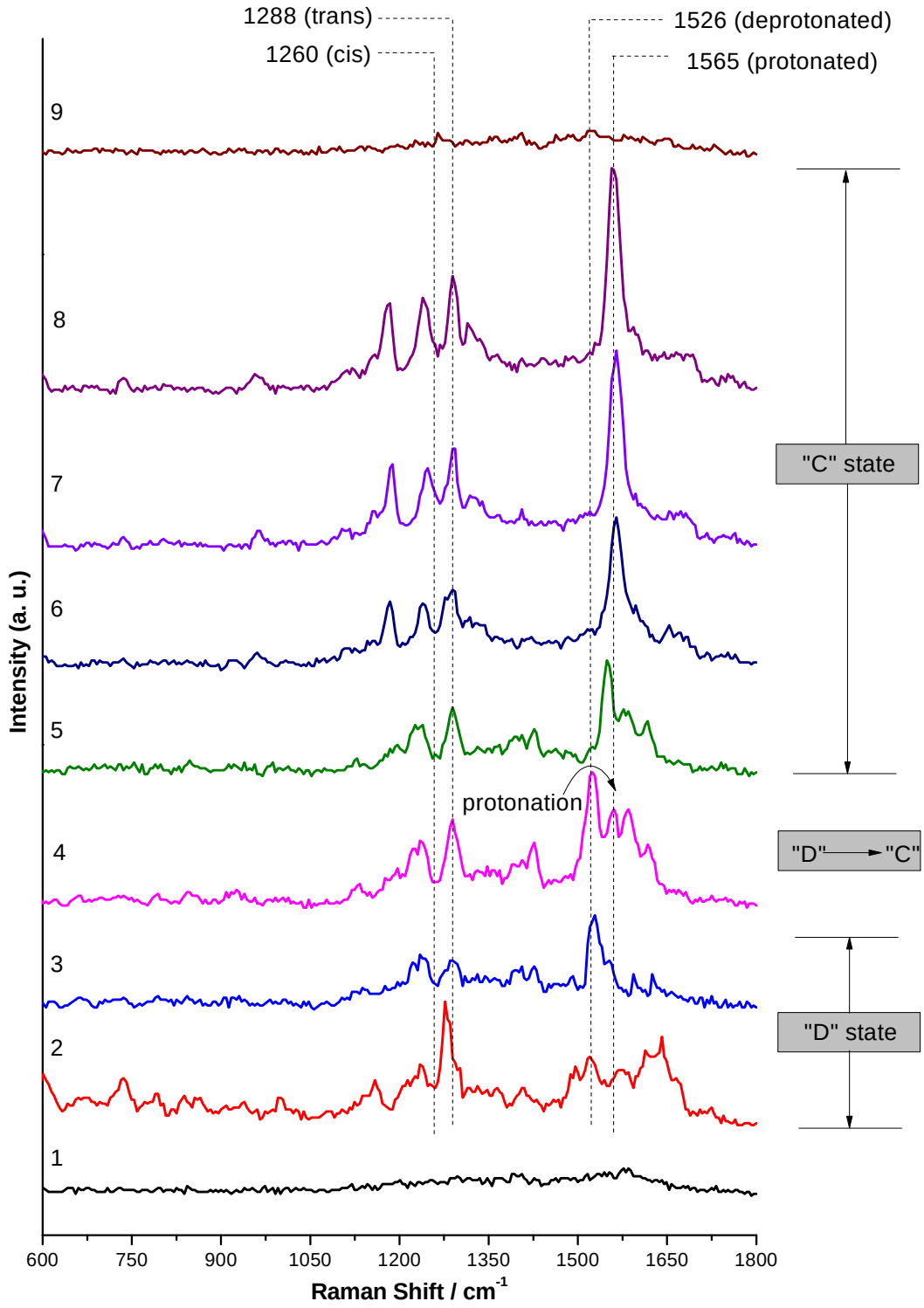

Figure IV.10. Time series SERS spectra of a single GFP molecule at 100 μW laser excitation (100 ms integration time). Molecule captured in the D state (trans/deprotonated) and converts into the C state (trans/protonated).

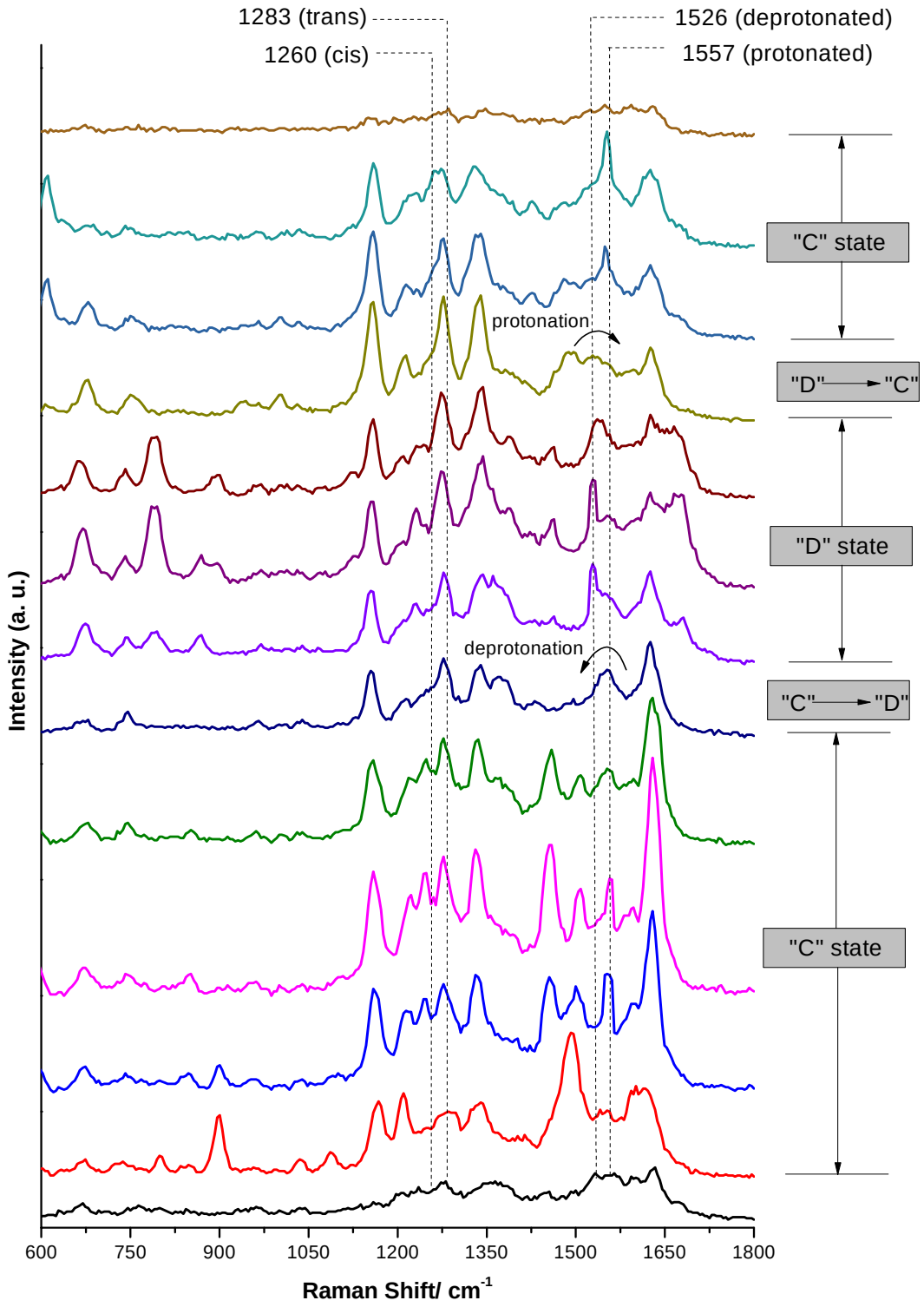

Figure IV.11. Time series SERS spectra of a single GFP molecule at 100 μW laser excitation (100 ms integration time). Graph shows transitions between the C (trans/protonated) and D (trans/deprotonated) state of the GFP chromophore.

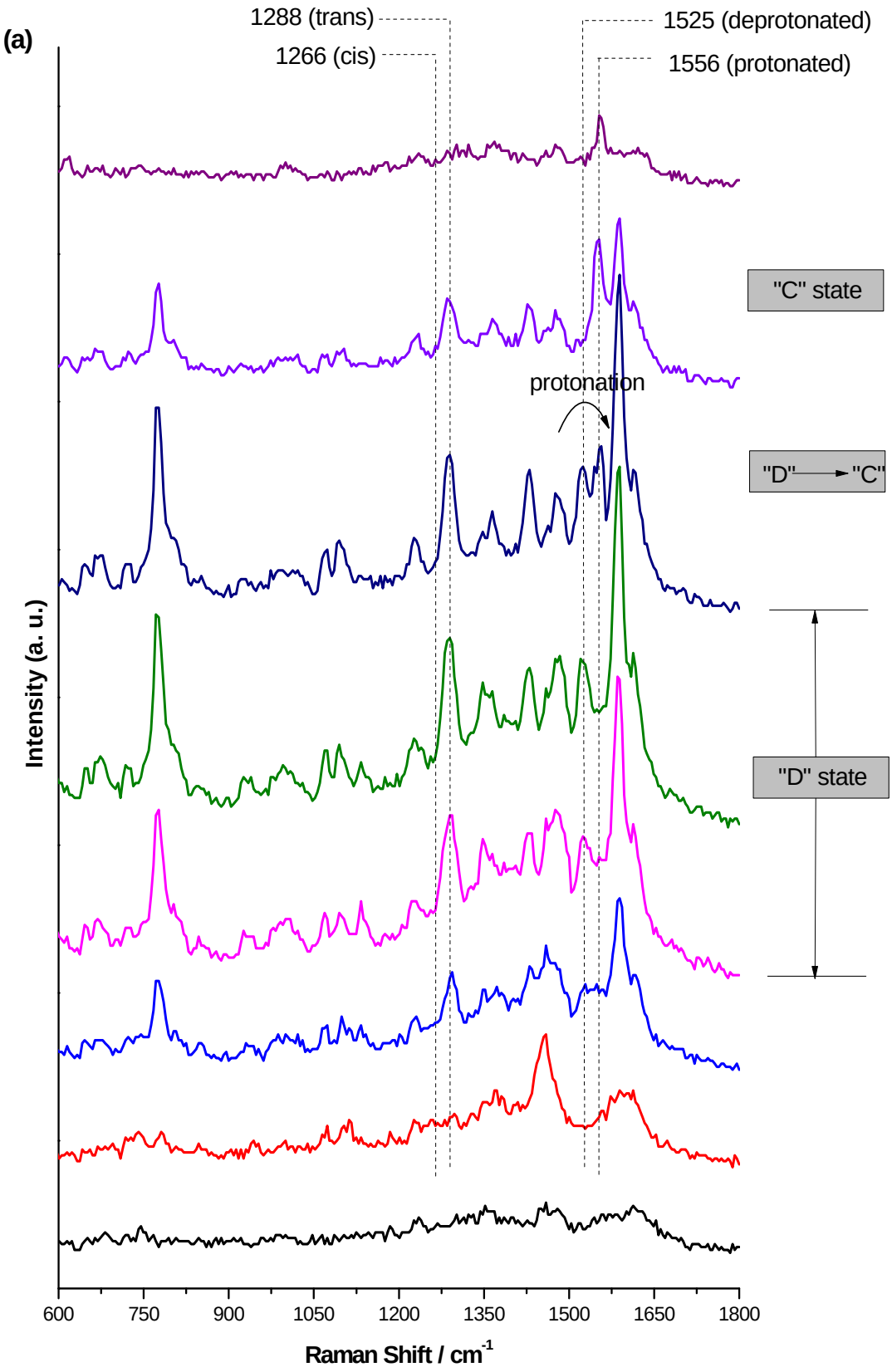
(a)
1288 (trans)
1266 (cis)
1525 (deprotonated)
1556 (protonated)
"C" state
protonation
"D"→"C"
"D" state
Intensity (a. u.)
600
750
900
1050
1200
1350
1500
1650
1800
Raman Shift / cm-1

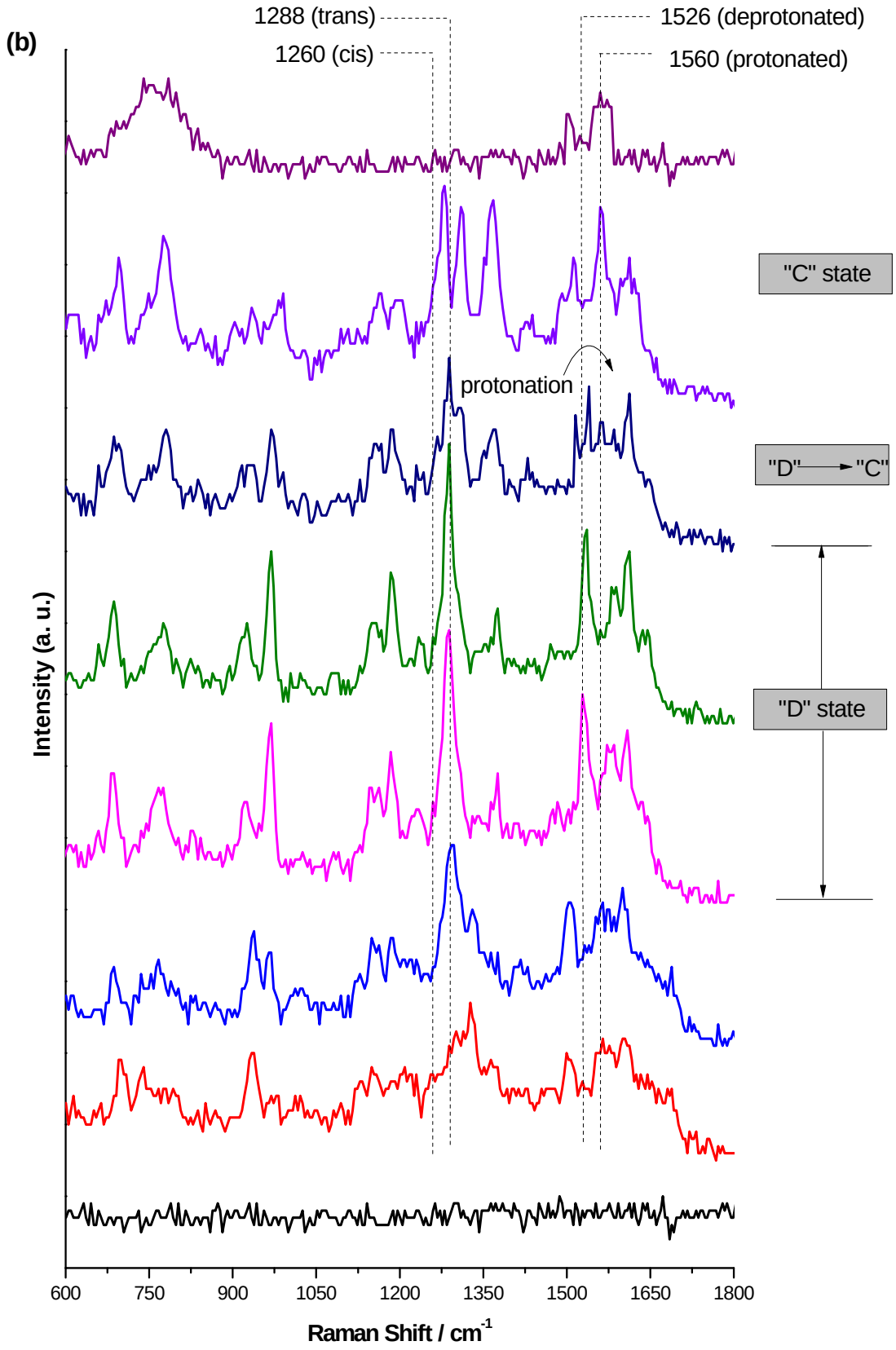
(b)
1288 (trans)
1260 (cis)
1526 (deprotonated)
1560 (protonated)
"C" state
protonation
"D"→"C"
"D" state
Intensity (a. u.)
600
750
900
1050
1200
1350
1500
1650
1800
Raman Shift / cm-1

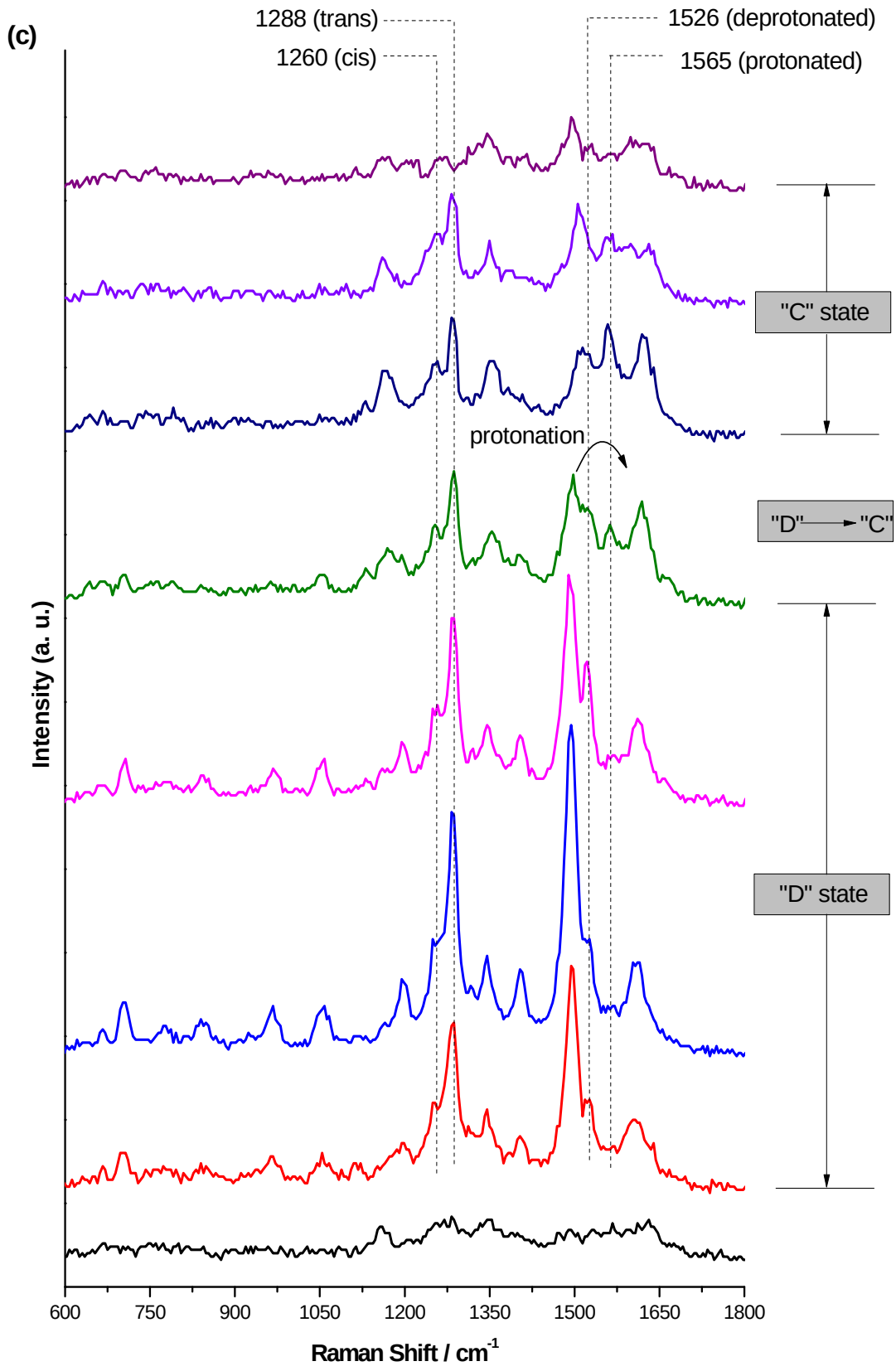
(c)
1288 (trans)
1260 (cis)
1526 (deprotonated)
1565 (protonated)
"C" state
protonation
"D"→"C"
"D" state
Intensity (a. u.)
600
750
900
1050
1200
1350
1500
1650
1800
Raman Shift / cm-1

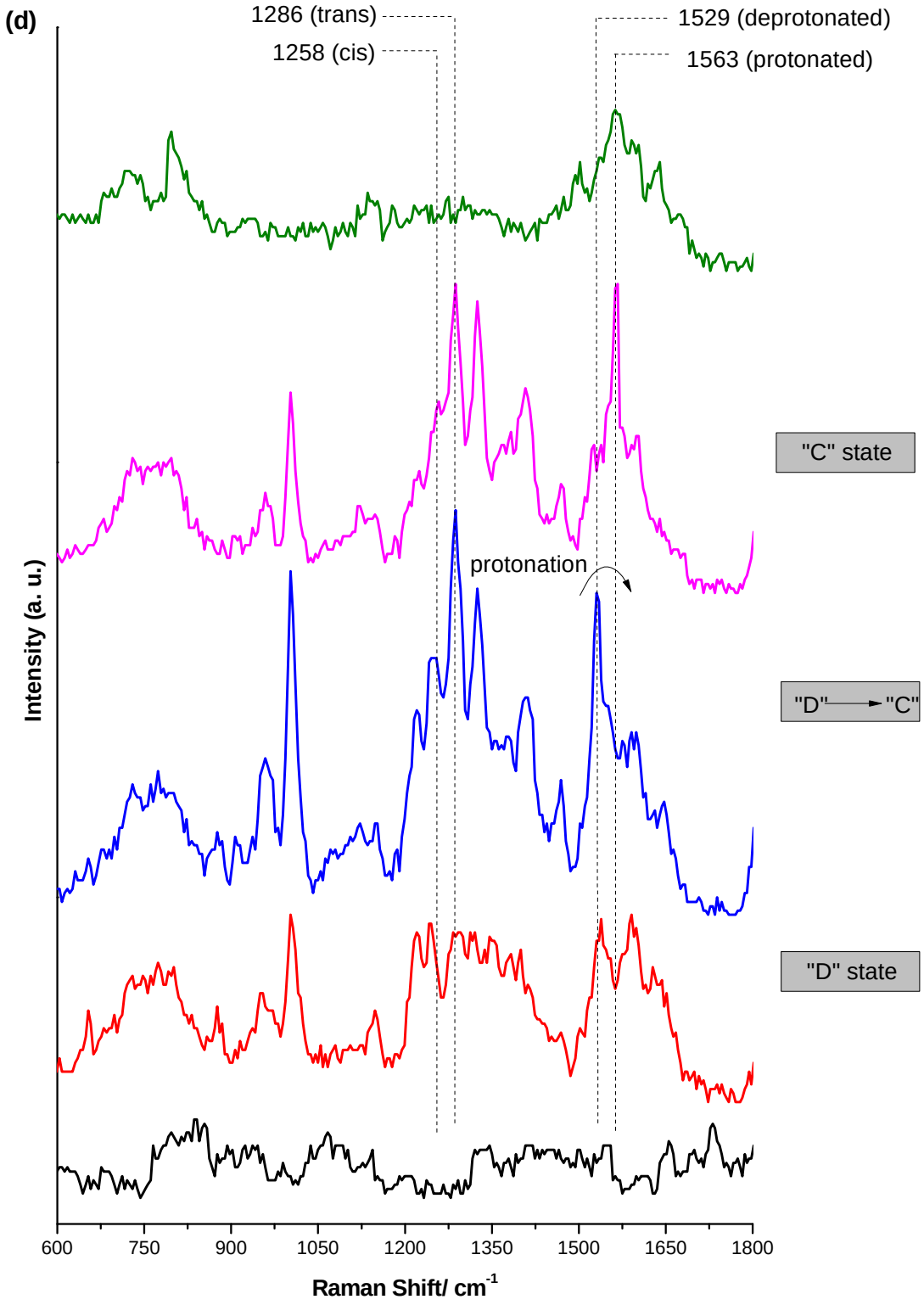

Figure IV.12. Time series SERS spectra illustrating transitions between the states C and D of individual GFP molecules (100 ms integration time, 100 μW laser intensity).

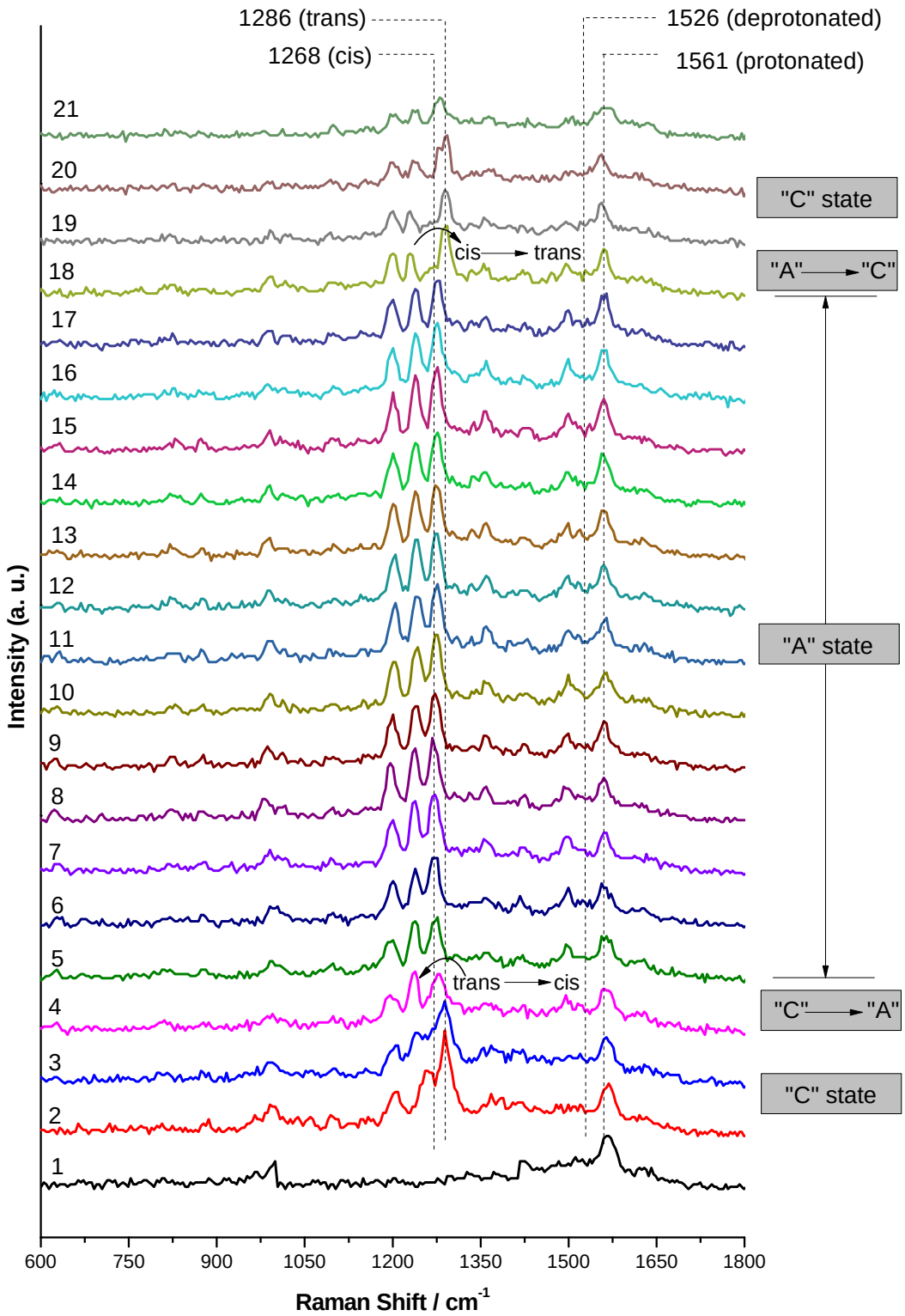

Figure IV.13. Time series SERS spectra of a single GFP molecule at 100 μW laser excitation (100 ms integration time). Graph shows transitions between the C (trans/protonated) and A (cis/protonated) state of the chromophore.

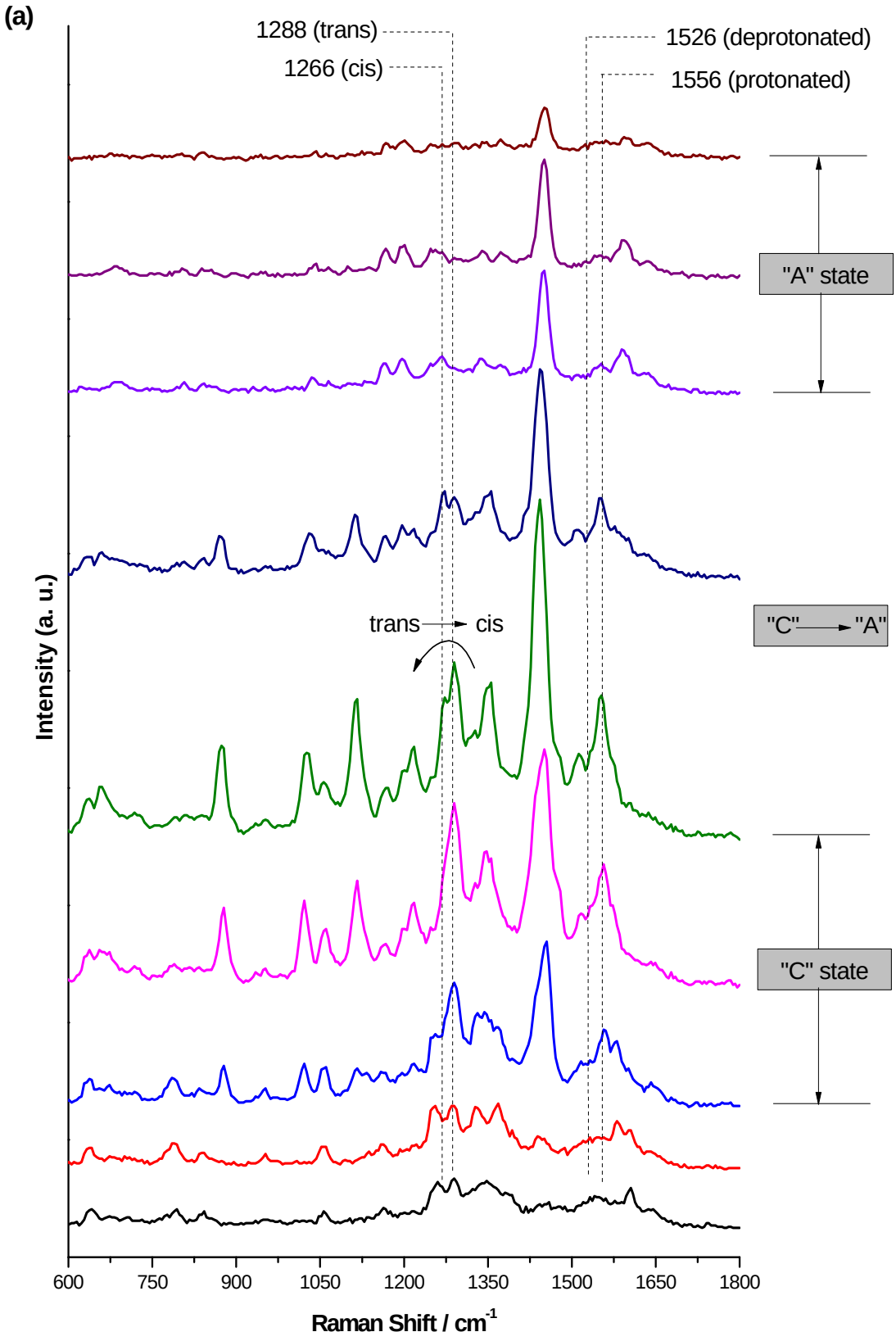
(a)
1288 (trans)
1266 (cis)
1526 (deprotonated)
1556 (protonated)
"A" state
trans
cis
"C"
"A"
"C" state
Intensity (a. u.)
600
750
900
1050
1200
1350
1500
1650
1800
Raman Shift / cm-1

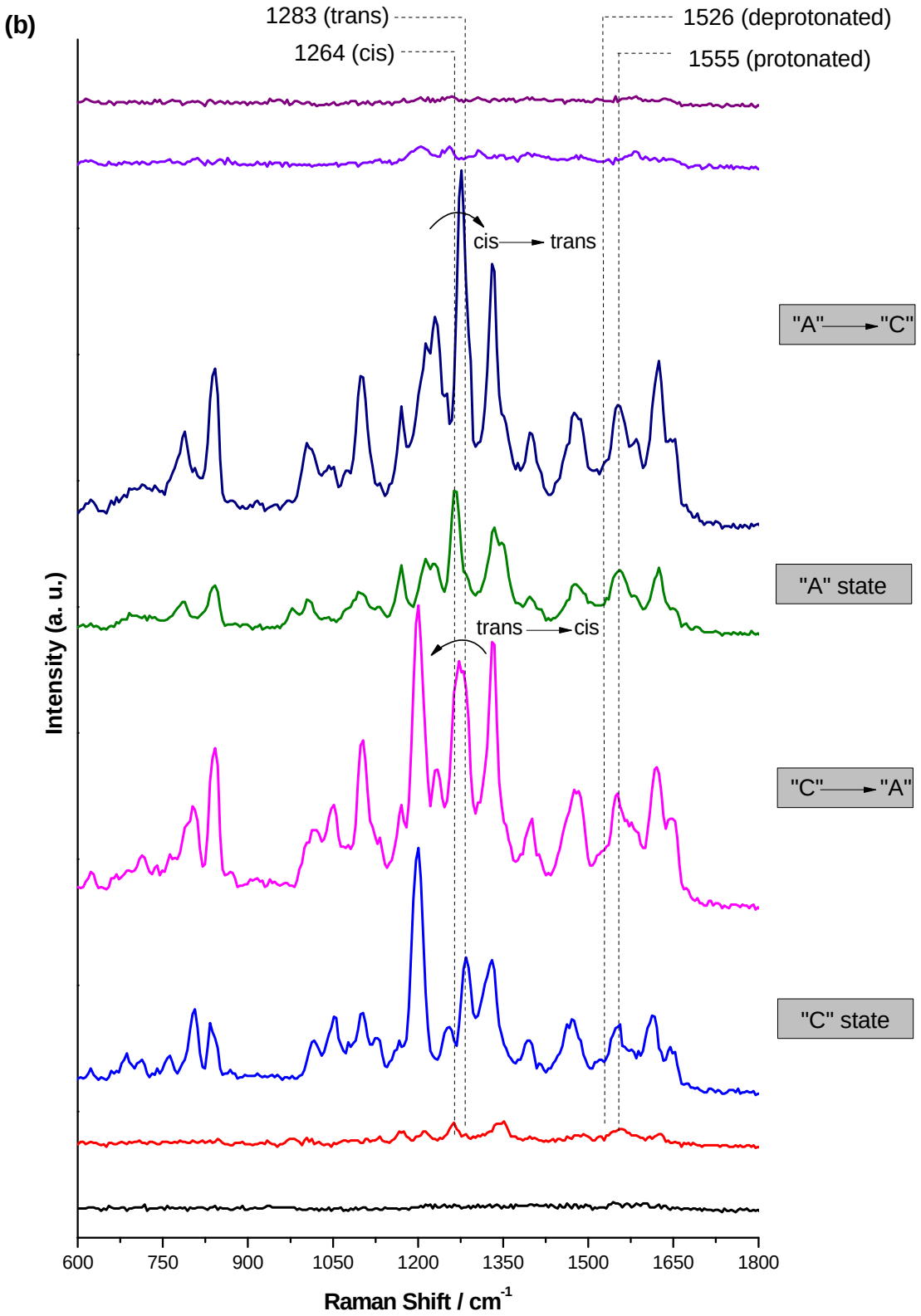

Figure IV.14. Time series SERS spectra illustrating transitions between the states C and A of individual GFP molecules (100 ms integration time, 100 μW laser intensity).

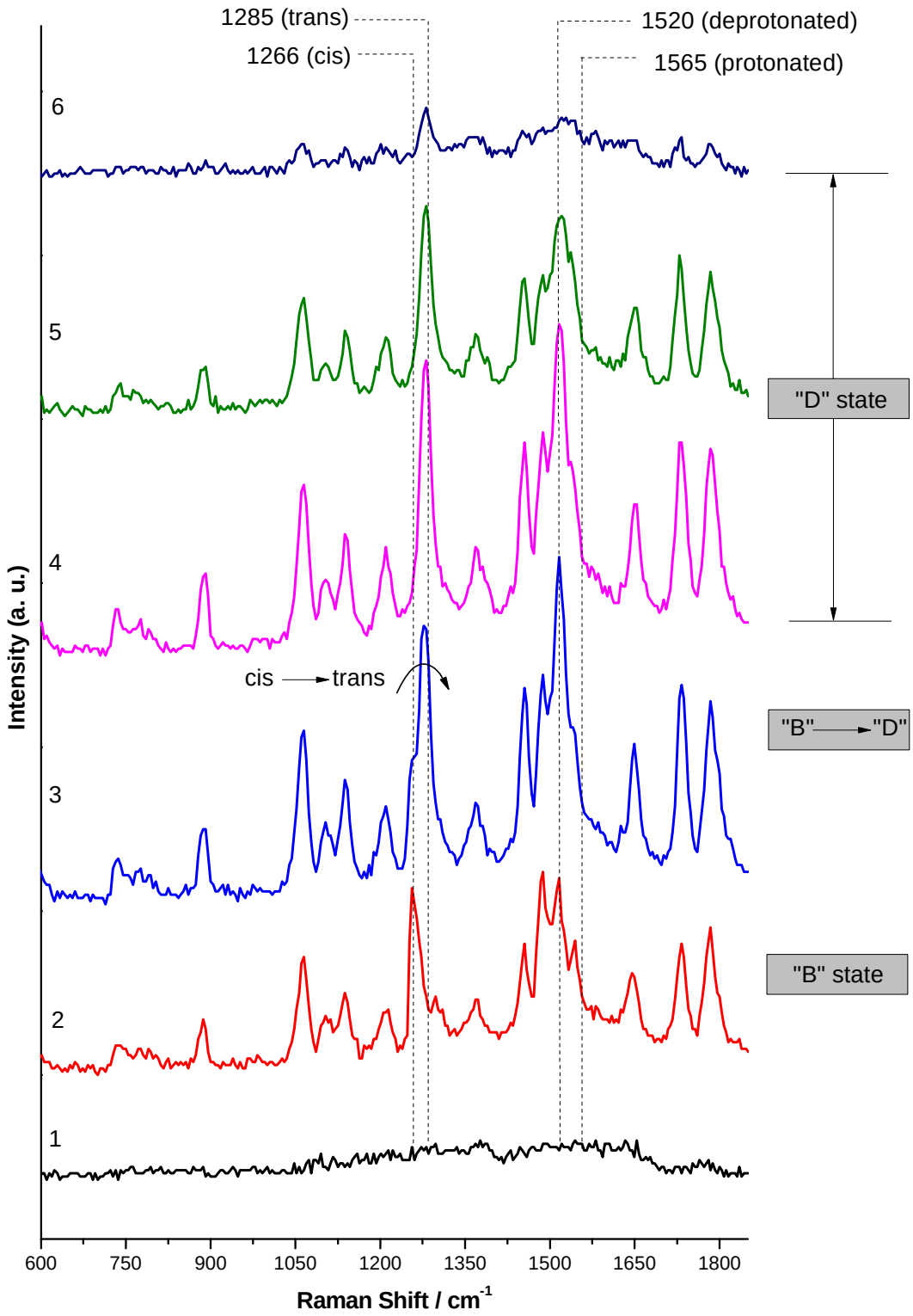

Figure IV.15. Time series SERS spectra of a single GFP molecule at 100 μW laser excitation (100 ms integration time). Molecule captured in the B state (cis/deprotonated) and converts into the D state (trans/deprotonated).

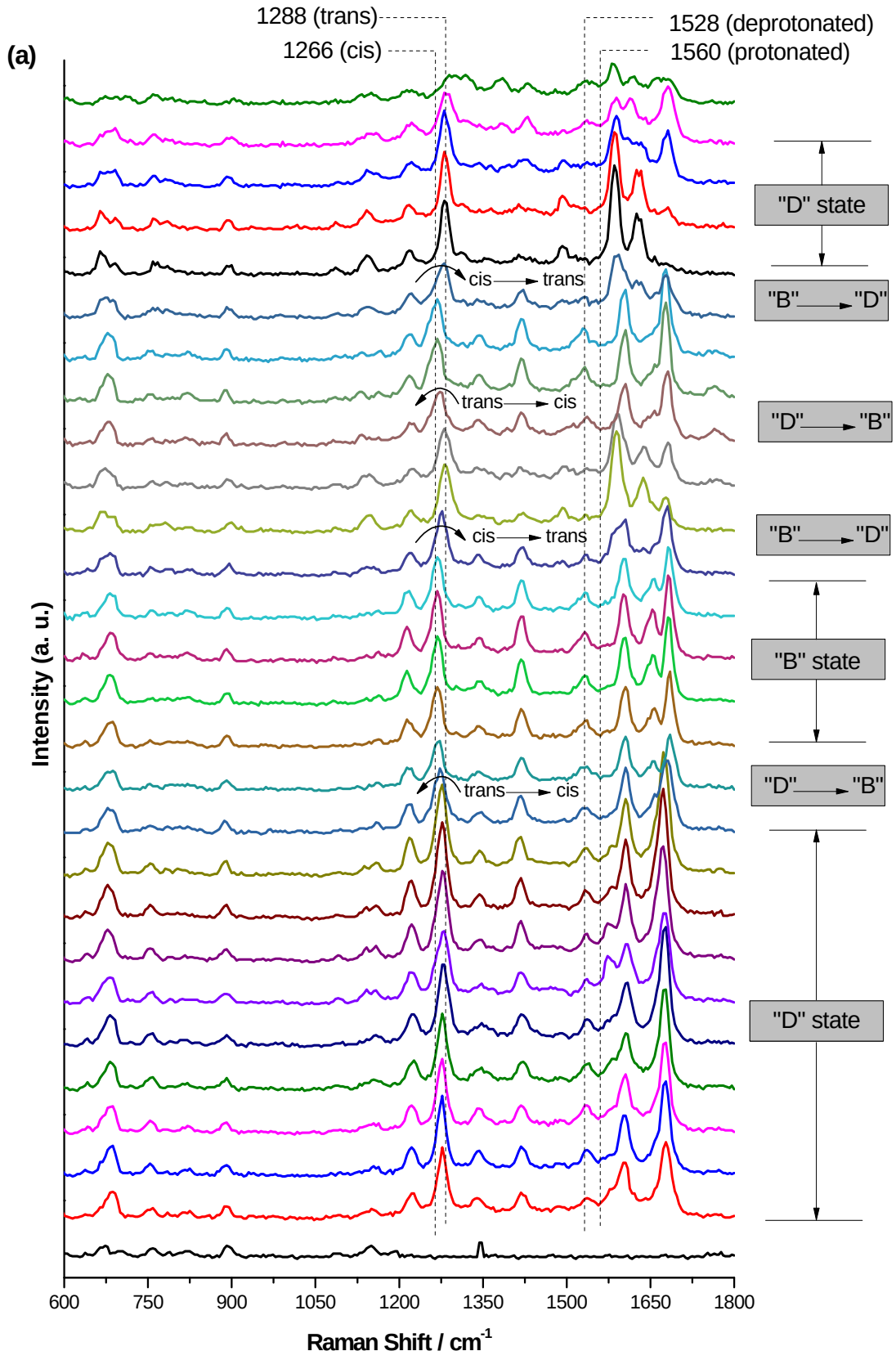
(a)
1288 (trans)
1266 (cis)
1528 (deprotonated)
1560 (protonated)
cis → trans
trans → cis
cis → trans
trans → cis
"D" state
"B" → "D"
"D" → "B"
"B" → "D"
"B" state
"D" → "B"
"D" state
Intensity (a. u.)
600
750
900
1050
1200
1350
1500
1650
1800
Raman Shift / cm-1

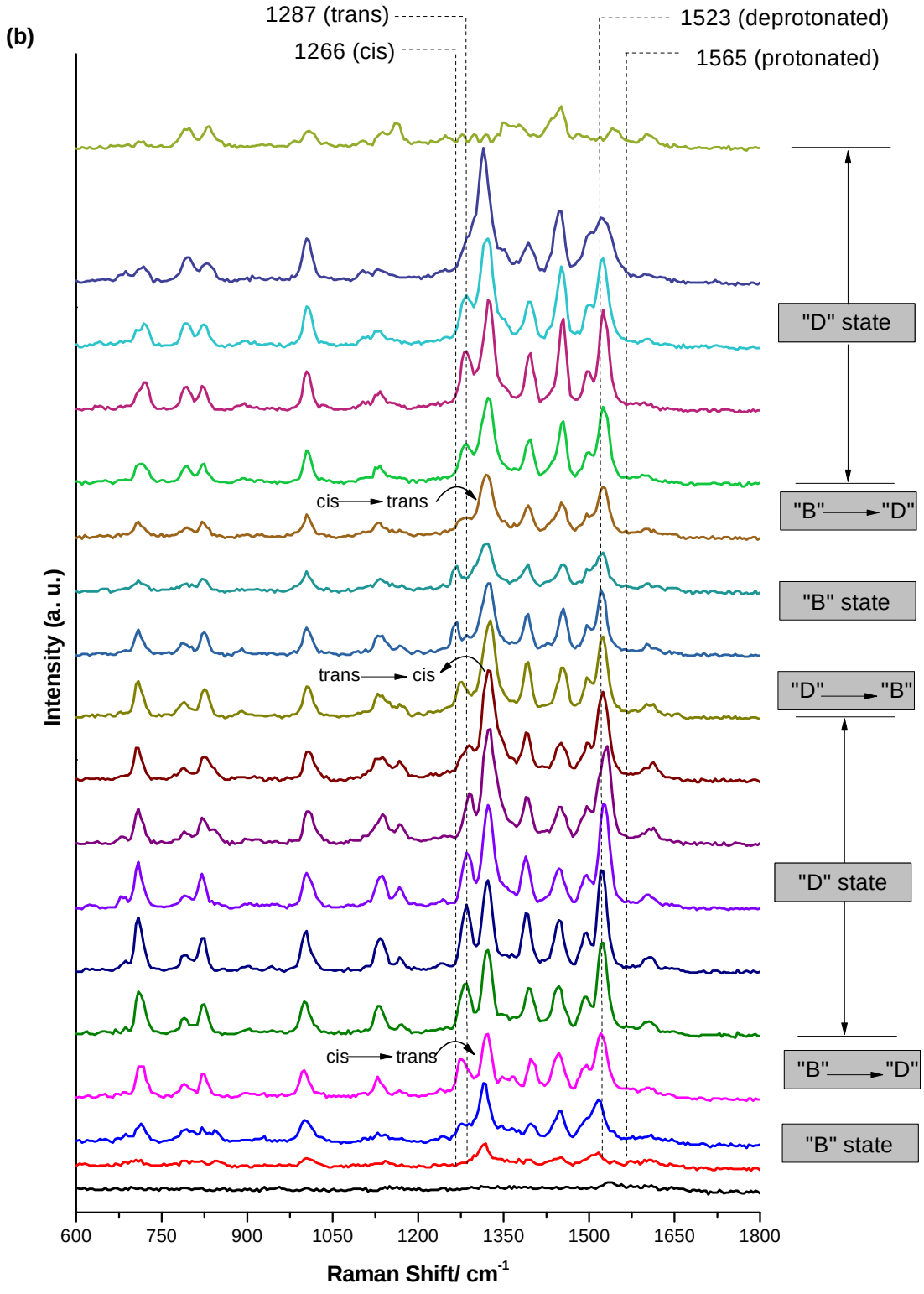

Figure IV.16. Time series SERS spectra illustrating transitions between the states B and D of individual GFP molecules (100 ms integration time, 100 μW laser intensity).

IV.4.2. Transitions observed at 700 μW laser excitation

We captured another set of time series SERS spectra from single GFP molecules while changing the laser power to 700 μW and acquisition time to 50 ms. Interestingly, frequency of capturing single molecule jumps in the SERS scans increased at higher laser excitation. Time series SERS spectra obtained under high laser excitation (700 μW), show similar transition patterns (i.e., A↔B, B↔D, D↔C and C↔A) of GFP chromophore as observed under lower laser excitation (100 μW). However, frequency of capturing transitions between the states of the GFP chromophore increased significantly at higher laser power.

Time series SERS spectra of single GFP molecules illustrated in the Figure IV.17 show evidence of transitions between the state B (cis/deprotonated) and A (cis/protonated) of the GFP chromophore at elevated laser excitation (700 μW) . As discussed earlier in the previous section, transitions between these two states are based on protonation⁄deprotonation of the GFP chromophore while holding the cis configuration. A spectral shift from 1560 cm^{-1} to 1530 cm^{-1} indicates deprotonation of the GFP chromophore and the opposite (i.e., to 1530 cm^{-1} →1560 cm^{-1}) addresses protonation of the chromophore. In case of the transitions between the states C (trans/protonated) and D (trans/deprotonated), it involves similar kinds of conversions (i.e., protonation⁄deprotonation), however, GFP chromophore stays in the trans form. Time series SERS spectra illustrated in the Figure IV.18a reveal transitions between the C (trans/protonated) state and the D (trans/deprotonated) state of the GFP chromophore. Molecule was captured initially in the C state as suggested by the peaks at around 1282 cm^{-1} (trans) and 1562 cm^{-1} (prototnated). A sudden frequency shift from 1562 cm^{-1} (protonated) to 1523 cm^{-1}(deprotonated) between spectra 4 and 5 confirms molecule's transition to the D state. Further, peak shift from 1523 cm^{-1} (deprotonated) to 1562 cm^{-1} (protonated) between spectra 6 and 7 exemplifies the reversibility of the transition (i.e., D→C) of the GFP chromophore.

In previous Section it's been observed that specific transitions between the states (i.e., B⇄D and A⇄C) of GFP molecule involve cis⇄trans isomerization of the chromophore. At higher laser excitation we observed similar transitions, however, a little bit more frequently. Time series SERS spectra of a single GFP molecule depicted in the Figure IV.19a illustrates transitions between the states C and A of the GFP chromophore. Sudden shift in the peak position from 1286 cm^{-1} (trans) to 1268 cm^{-1}(cis), while holding the protonated form (as confirmed by the peak at around 1561 cm^{-1}) indicates conversion of the GFP chromophore from the C state to the A state between spectra 3 and 4. Further, molecule hits back to its original C state later on, as can be noticed from the spectral shift from 1268 cm^{-1} to 1286 cm^{-1} between spectra 6 and 7. Similar transitions are shown in the Figure IV.19. Moreover, transitions between the states B (cis/deprotonated) and D (trans/deprotonated) of the GFP chromophore through cis⇄trans isomerization were also observed at 700 μW laser excitation and illustrated in the Figure IV.20.

Therefore, time series SERS scans of single GFP molecules obtained in this present thesis work, provide significant evidence of transitions between the 4 conformational states (i.e., A, B, C and D) through protonation↔deprotonation and cis↔trans isomerization. Although Habuchi *et al.* demonstrated conversions between the protonated and the deprotonated form of the EGFP molecule's chromophore by SM-SERS [16], no real evidence of transitions between distinct GFP chromophore states (i.e., A⇄B⇄D⇄C⇄A) has been published yet. Here, in this present thesis work, for the first time, we provide significant evidence of such GFP chromophore transitions by our unique single molecule SERS approach.

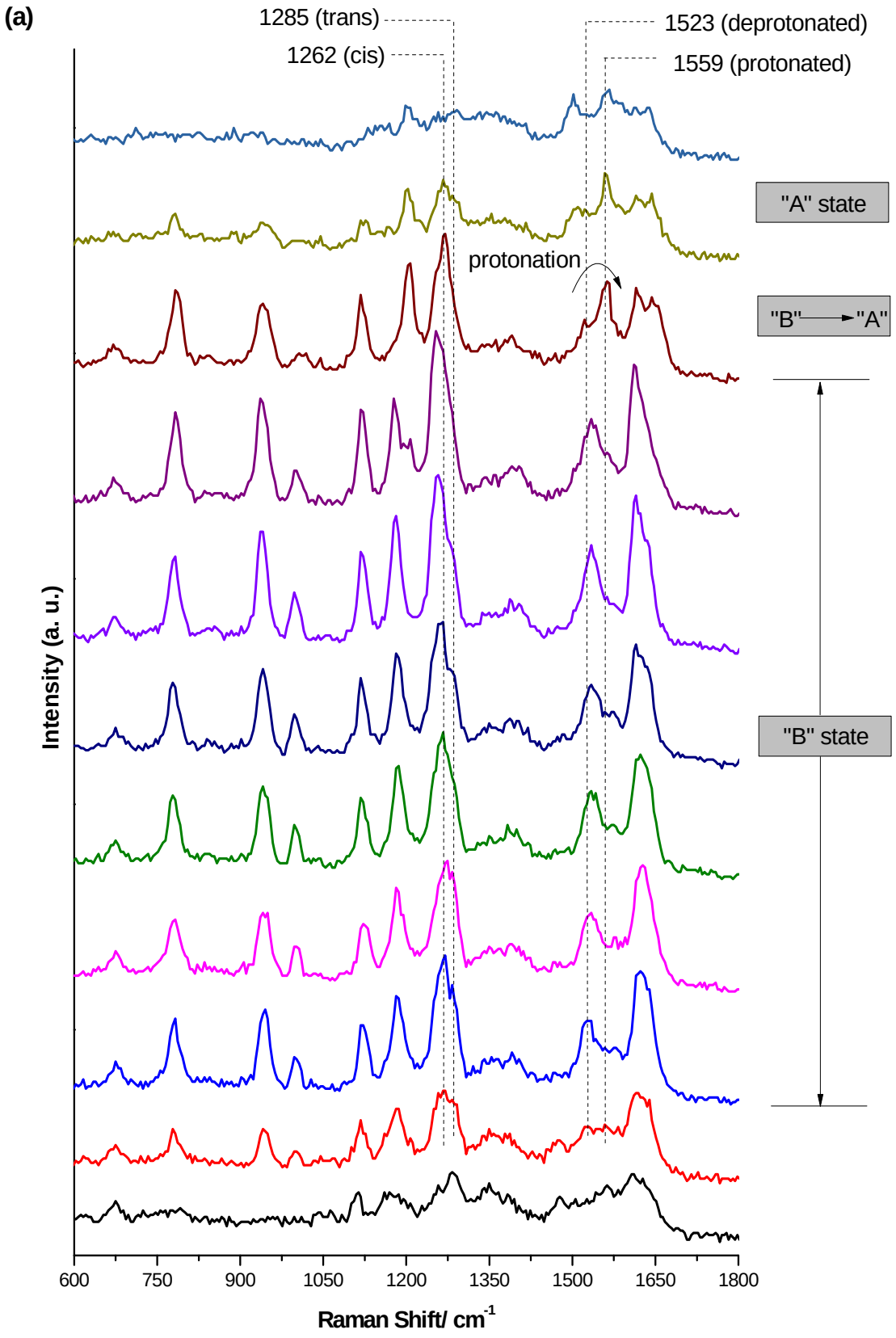
(a)
1285 (trans)
1262 (cis)
1523 (deprotonated)
1559 (protonated)
"A" state
protonation
"B"→"A"
"B" state
Intensity (a. u.)
600
750
900
1050
1200
1350
1500
1650
1800
Raman Shift/ cm-1

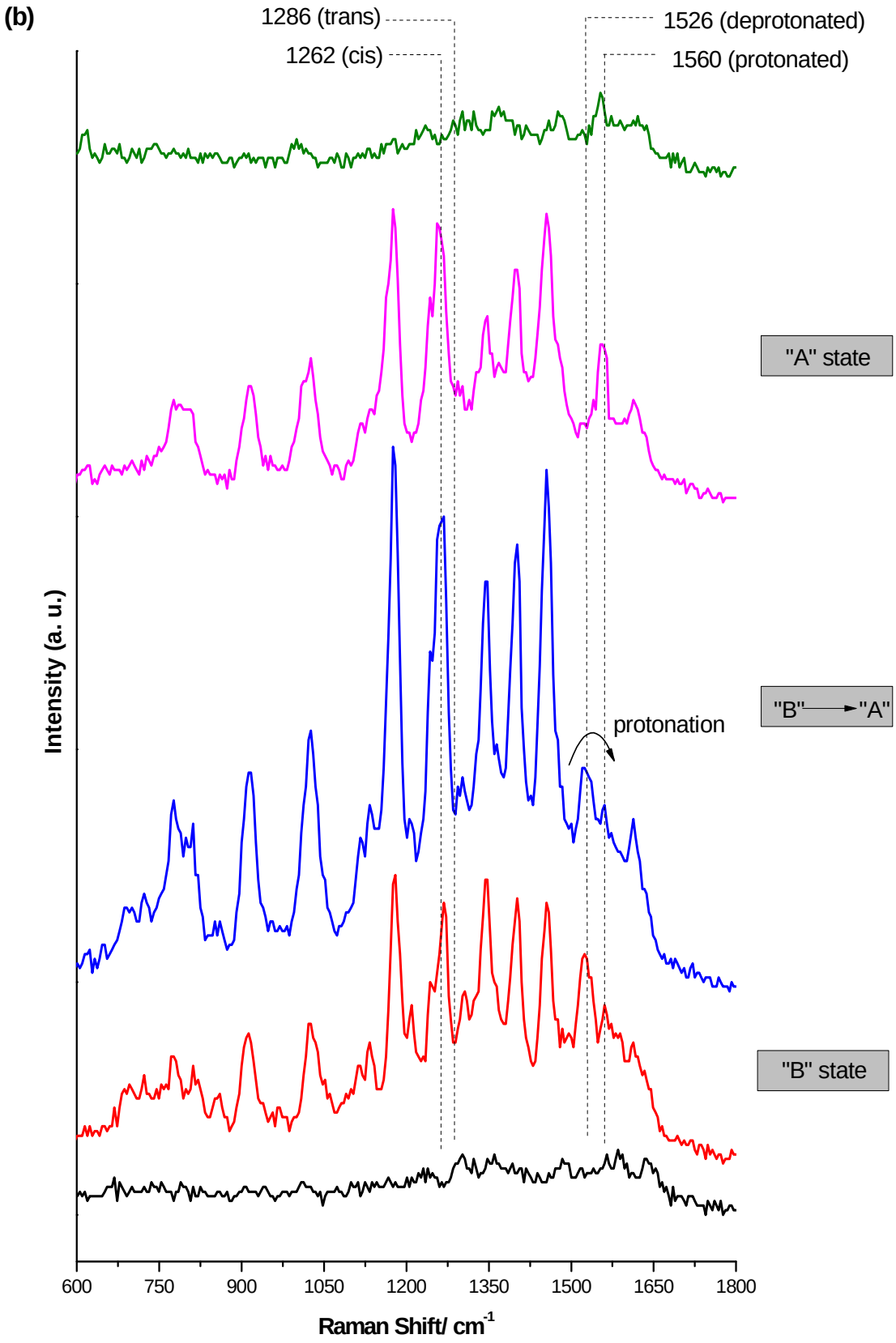
(b)
1286 (trans)
1262 (cis)
1526 (deprotonated)
1560 (protonated)
"A" state
"B"⟶"A"
protonation
"B" state
Intensity (a. u.)
600
750
900
1050
1200
1350
1500
1650
1800
Raman Shift/ cm-1

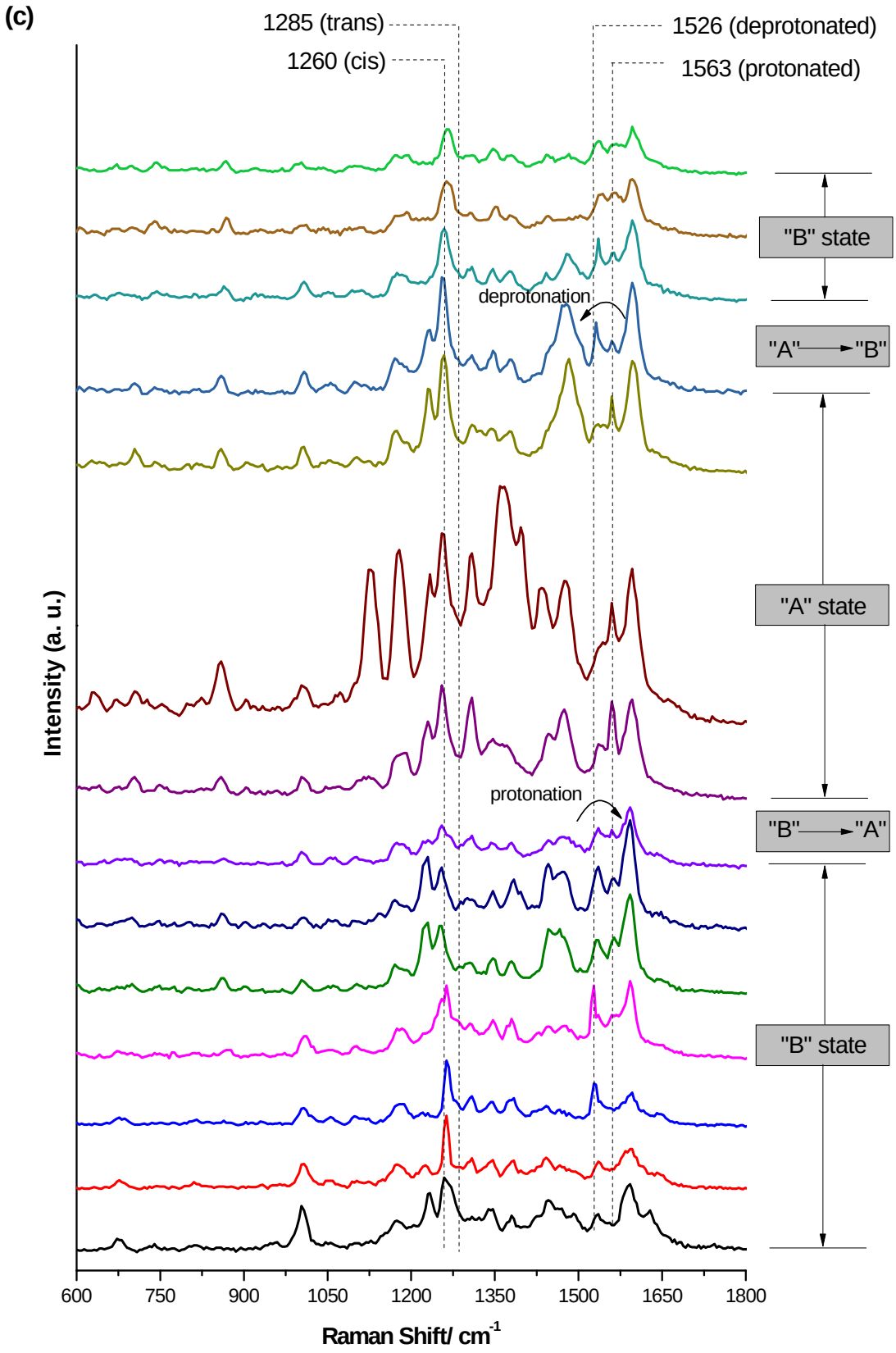
(c)
1285 (trans)
1260 (cis)
1526 (deprotonated)
1563 (protonated)
"B" state
deprotonation
"A"→"B"
"A" state
protonation
"B"→"A"
"B" state
Intensity (a. u.)
600
750
900
1050
1200
1350
1500
1650
1800
Raman Shift/ cm-1

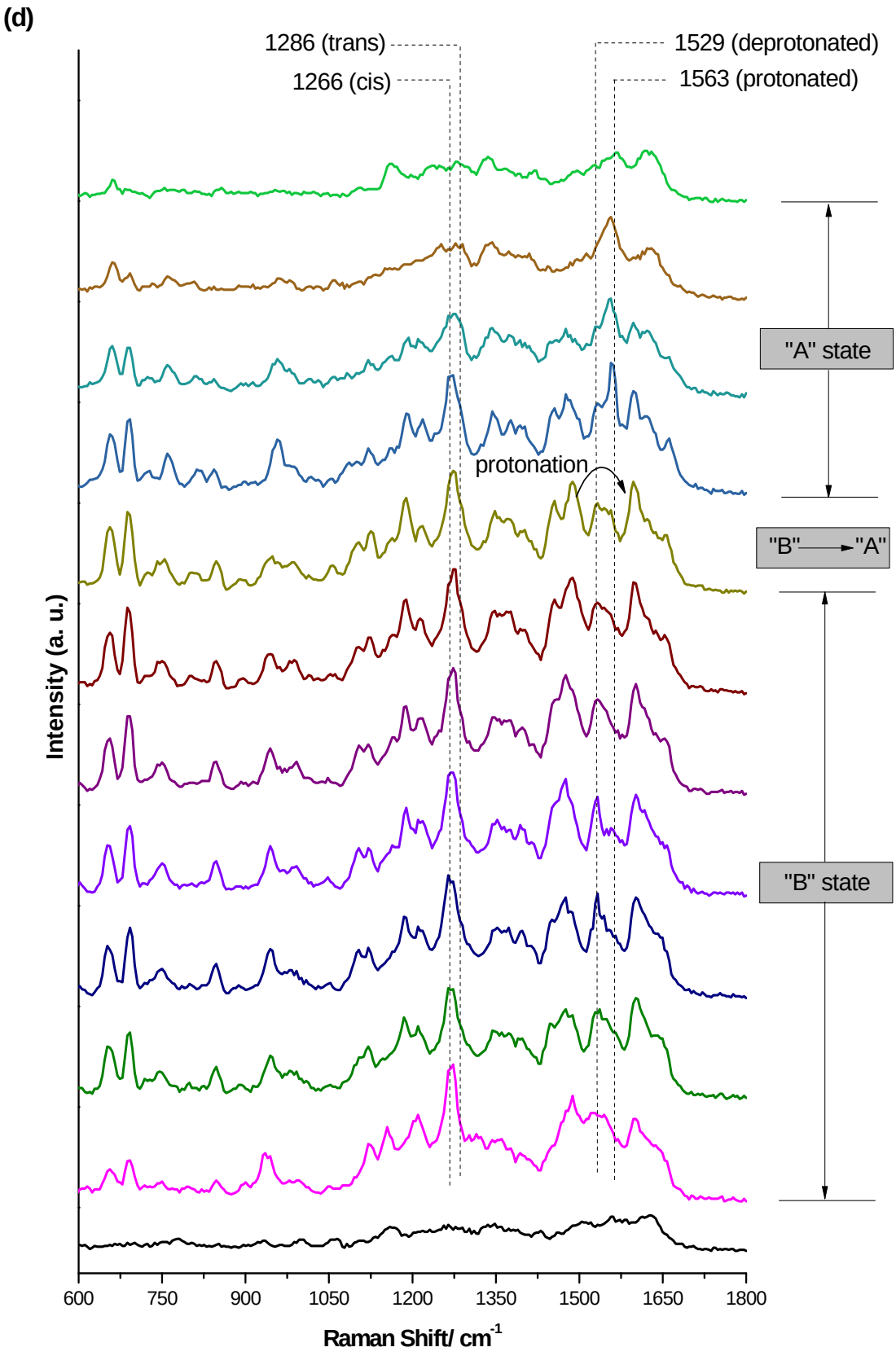
(d)
1286 (trans)
1266 (cis)
1529 (deprotonated)
1563 (protonated)
"A" state
protonation
"B"→"A"
"B" state
Intensity (a. u.)
600
750
900
1050
1200
1350
1500
1650
1800
Raman Shift/ cm-1

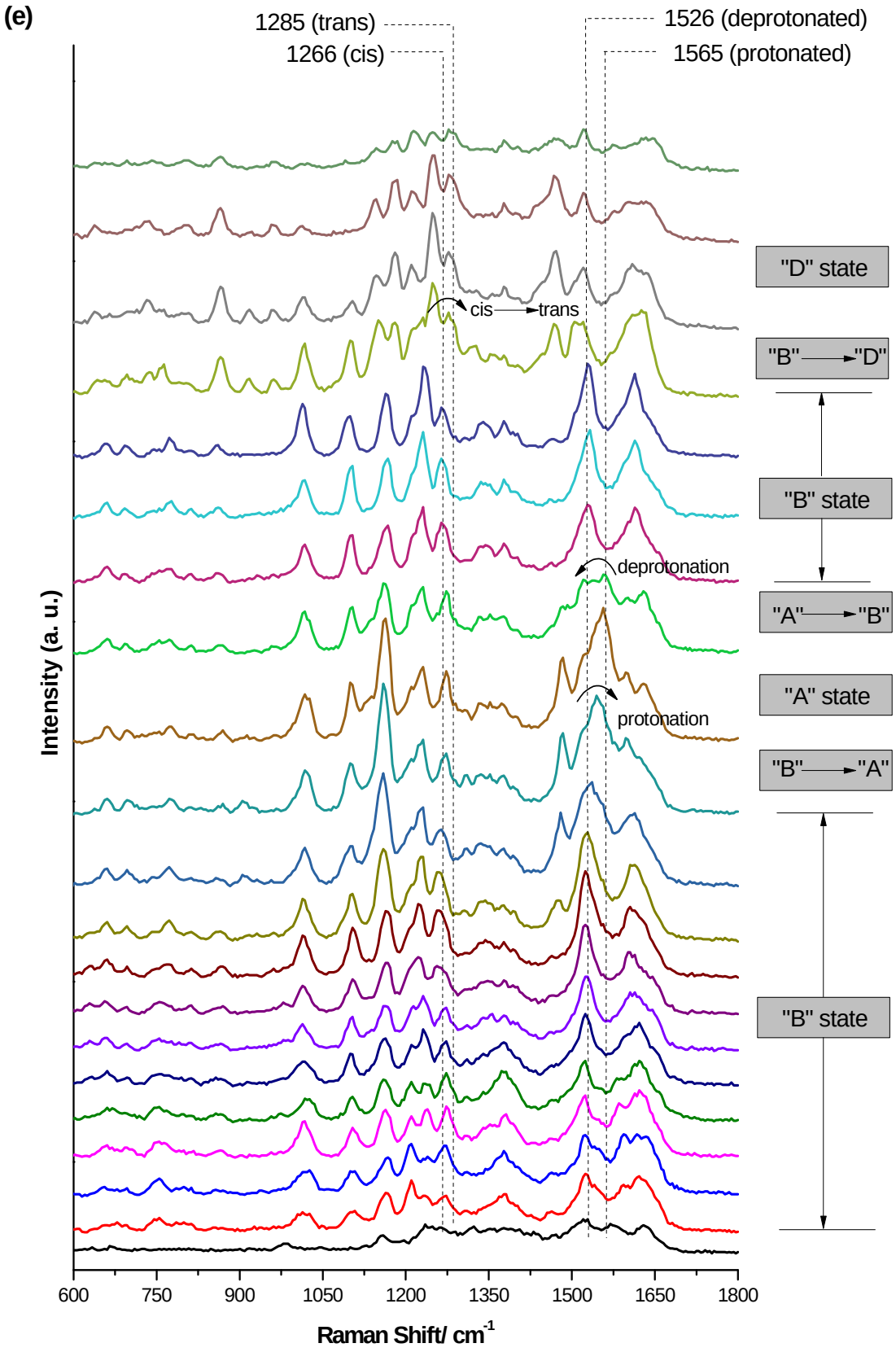
(e)
1285 (trans)
1266 (cis)
1526 (deprotonated)
1565 (protonated)
cis
trans
deprotonation
protonation
"D" state
"B"
"D"
"B" state
"A"
"B"
"A" state
"B"
"A"
"B" state
Intensity (a. u.)
600
750
900
1050
1200
1350
1500
1650
1800
Raman Shift/ cm-1

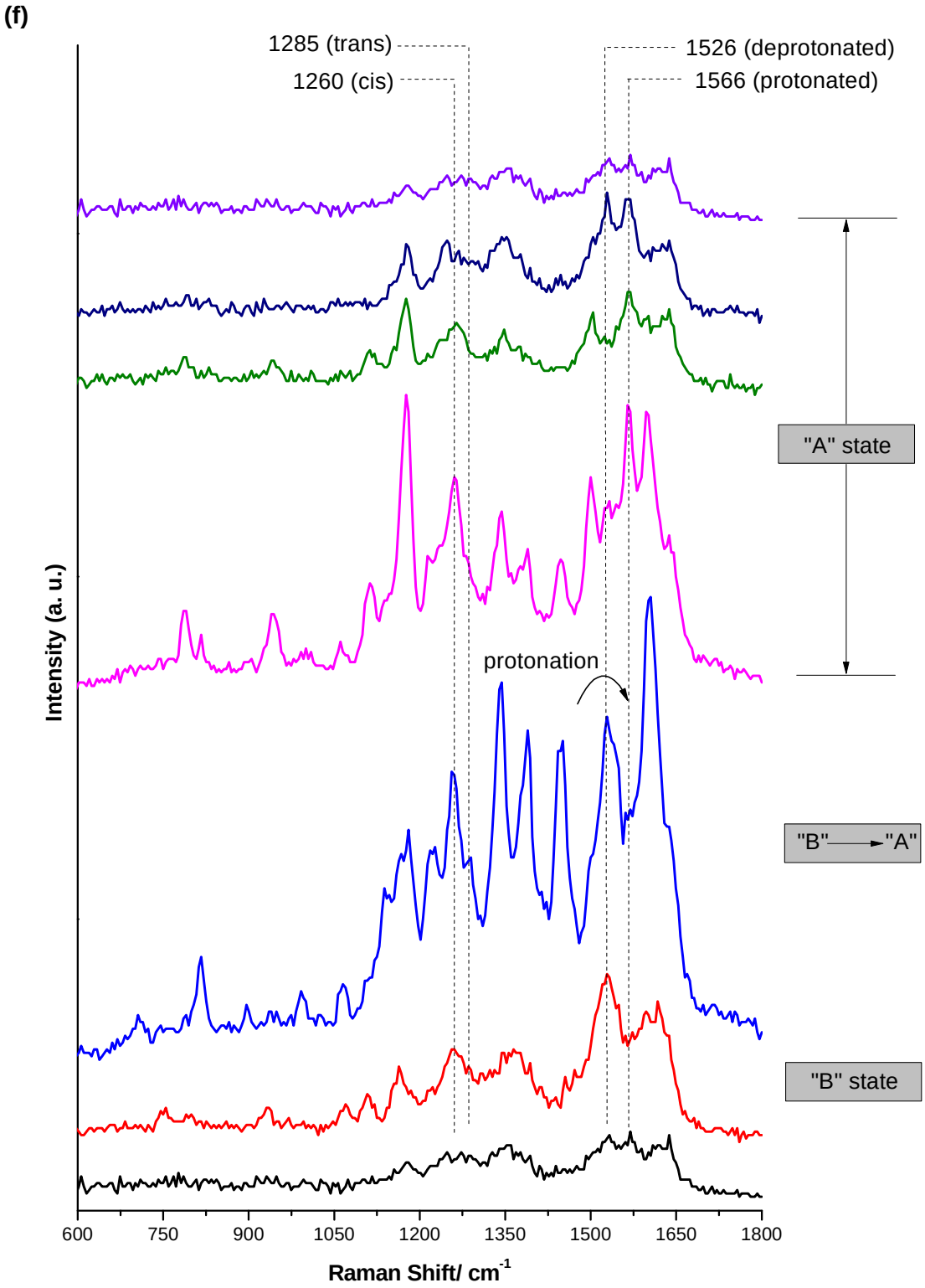

Figure IV.17. Time series SERS spectra illustrating transitions between the states B and A of individual GFP molecules (50 ms integration time, 700 μW laser intensity).

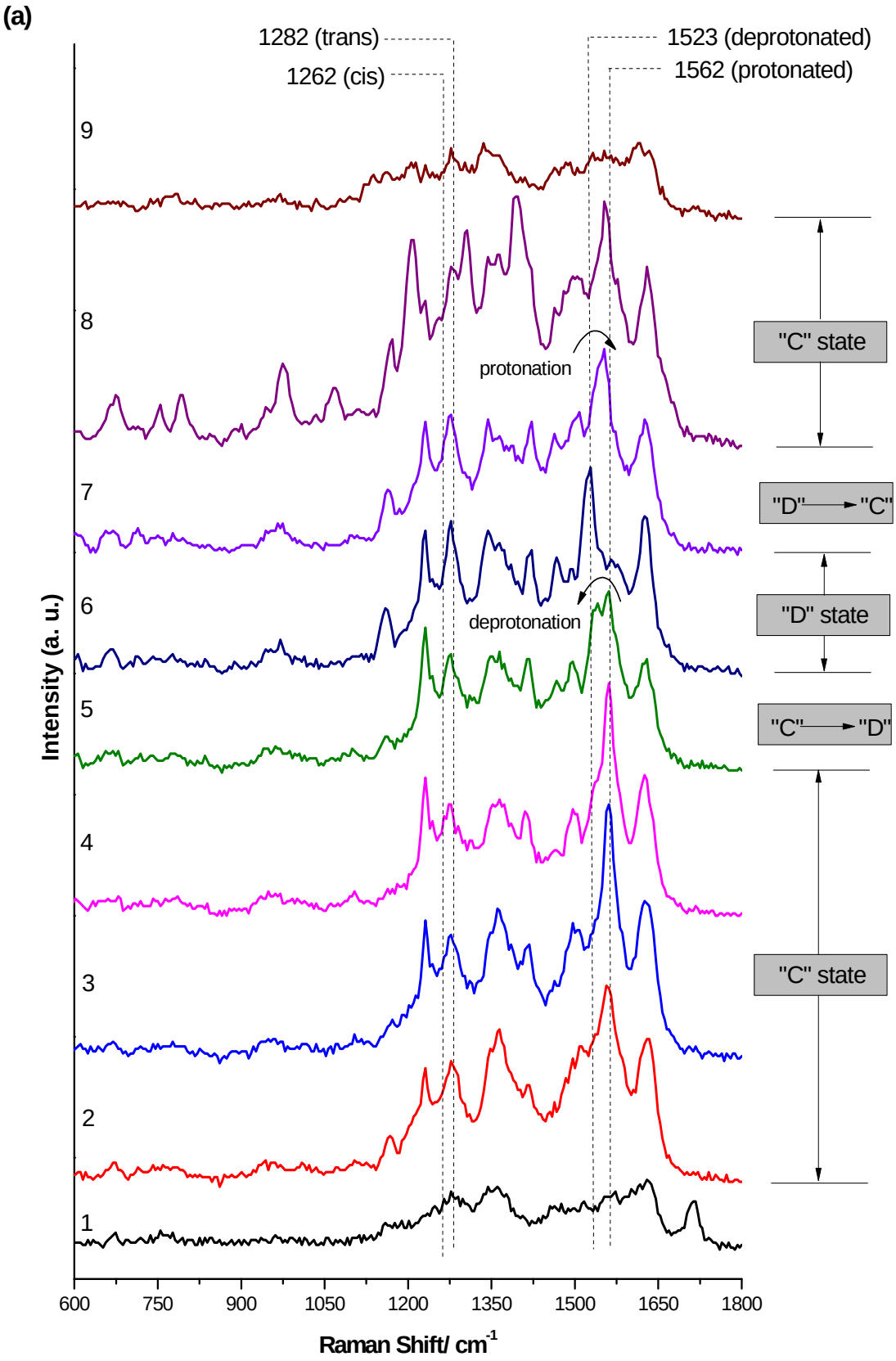
(a)
1282 (trans)
1262 (cis)
1523 (deprotonated)
1562 (protonated)
9
8
7
6
5
4
3
2
1
protonation
deprotonation
"C" state
"D"→"C"
"D" state
"C"→"D"
"C" state
Intensity (a. u.)
600
750
900
1050
1200
1350
1500
1650
1800
Raman Shift/ cm-1

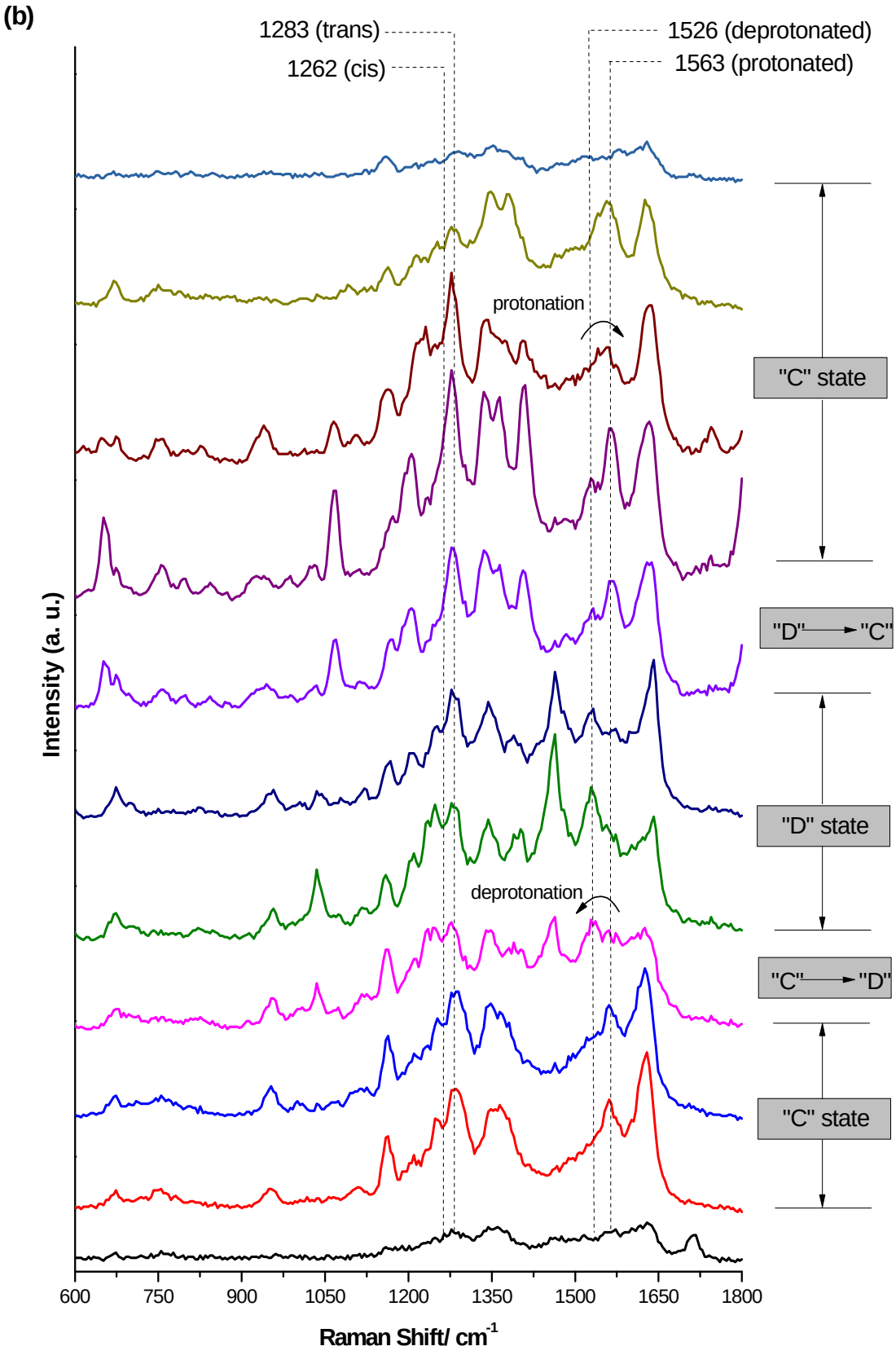
(b)
1283 (trans)
1262 (cis)
1526 (deprotonated)
1563 (protonated)
protonation
deprotonation
"C" state
"D"→"C"
"D" state
"C"→"D"
"C" state
Intensity (a. u.)
600
750
900
1050
1200
1350
1500
1650
1800
Raman Shift/ cm-1

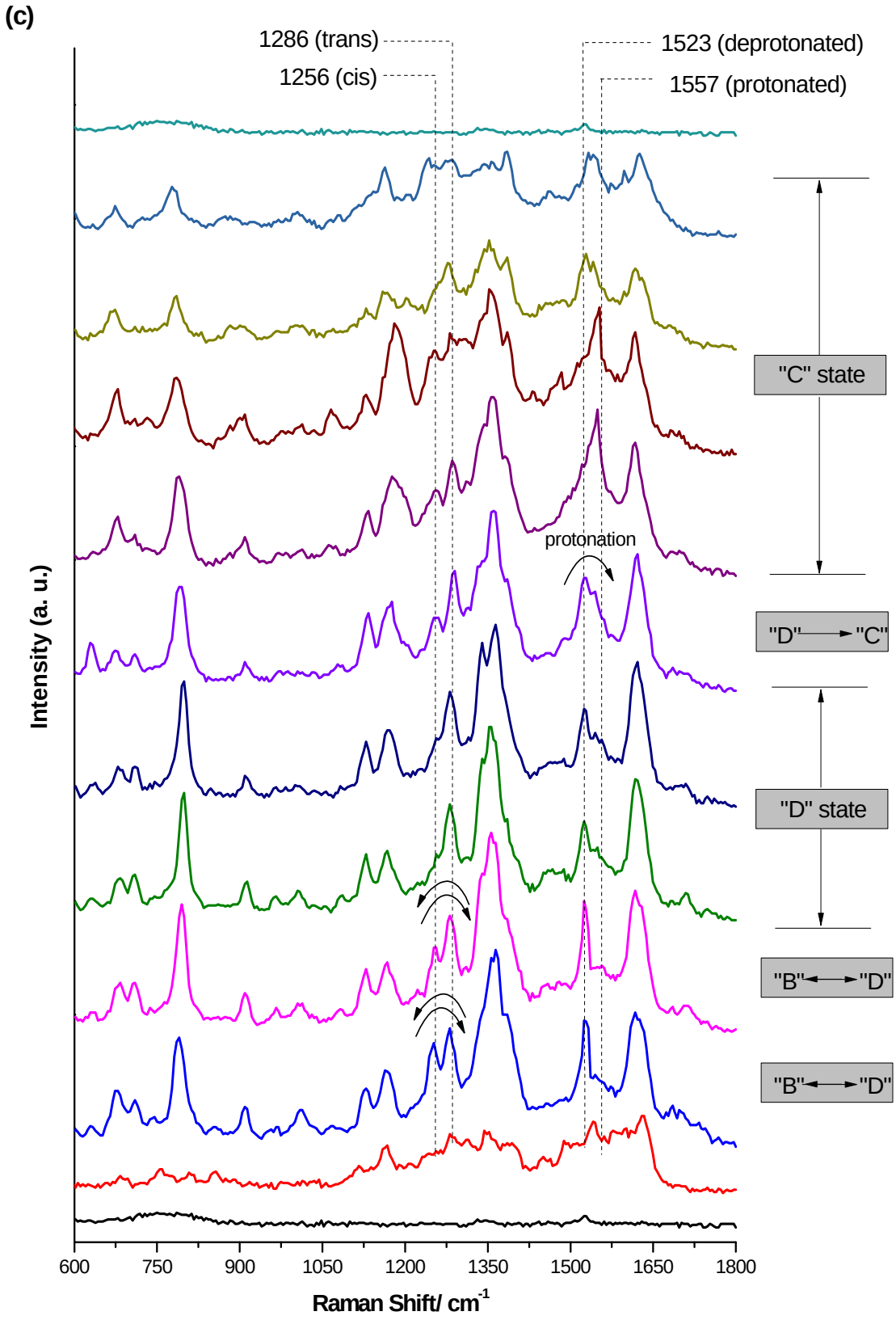
(c)
1286 (trans)
1256 (cis)
1523 (deprotonated)
1557 (protonated)
"C" state
protonation
"D"→"C"
"D" state
"B"→"D"
"B"→"D"
Intensity (a. u.)
600
750
900
1050
1200
1350
1500
1650
1800
Raman Shift/ cm-1

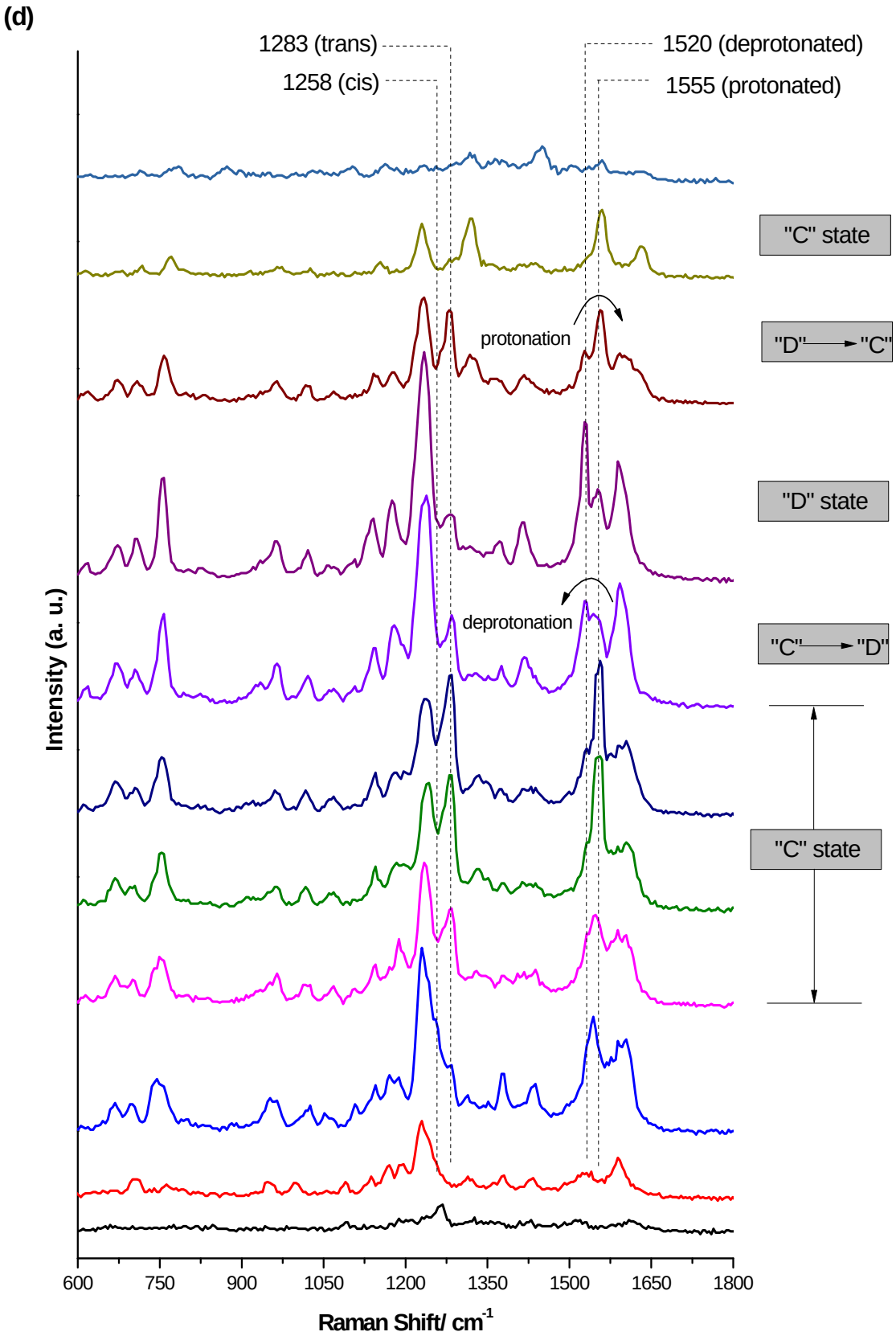
(d)
1283 (trans)
1258 (cis)
1520 (deprotonated)
1555 (protonated)
"C" state
protonation
"D"→"C"
"D" state
deprotonation
"C"→"D"
"C" state
Intensity (a. u.)
600
750
900
1050
1200
1350
1500
1650
1800
Raman Shift/ cm-1

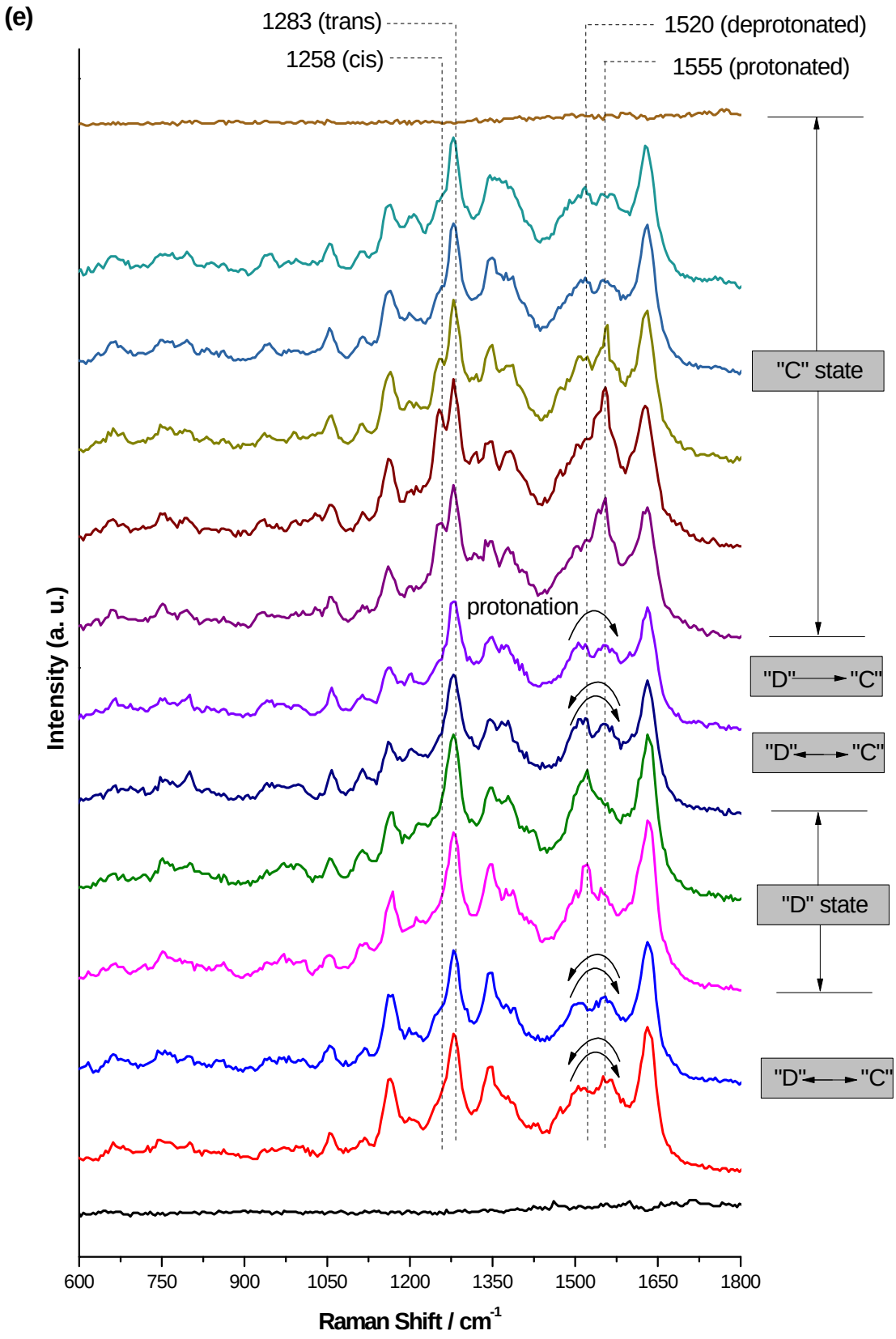
(e)
1283 (trans)
1258 (cis)
1520 (deprotonated)
1555 (protonated)
"C" state
protonation
"D"→"C"
"D"←→"C"
"D" state
"D"←→"C"
Intensity (a. u.)
600
750
900
1050
1200
1350
1500
1650
1800
Raman Shift / cm-1

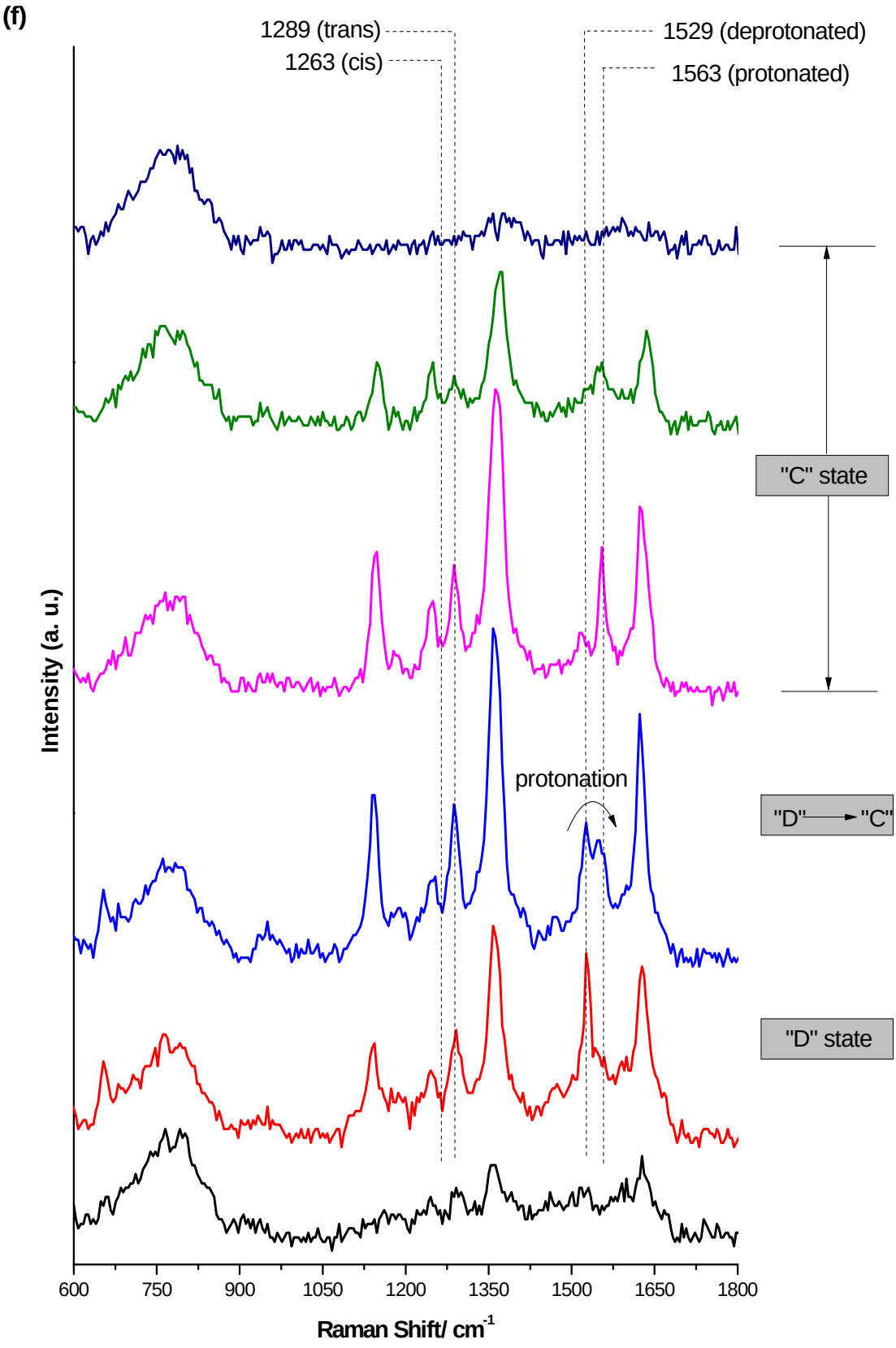
(f)
1289 (trans)
1263 (cis)
1529 (deprotonated)
1563 (protonated)
"C" state
protonation
"D"→"C"
"D" state
Intensity (a. u.)
600
750
900
1050
1200
1350
1500
1650
1800
Raman Shift/ cm-1

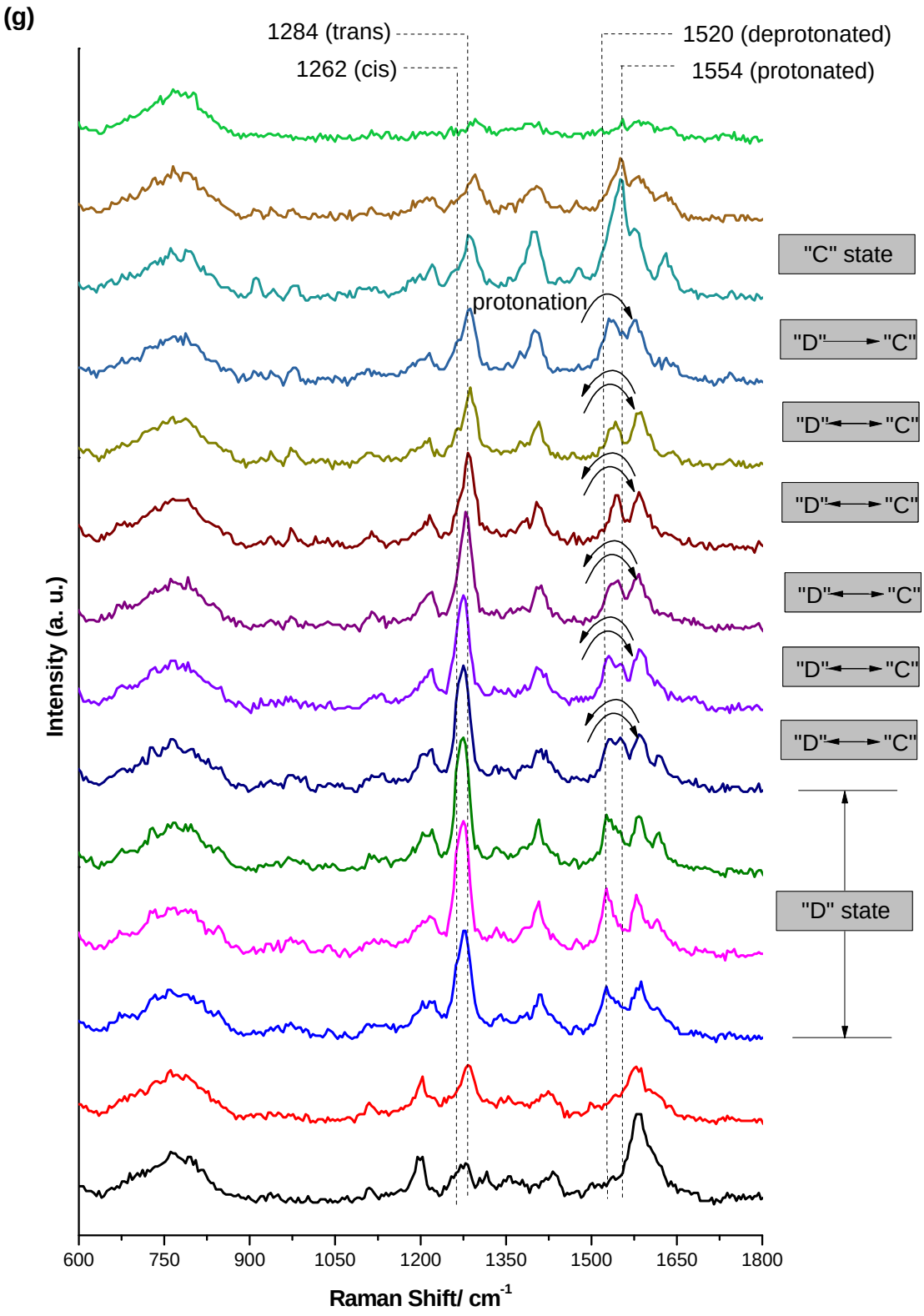

Figure IV.18. Time series SERS spectra illustrating transitions between the states D and C of individual GFP molecules (50 ms integration time, 700 μW laser intensity).

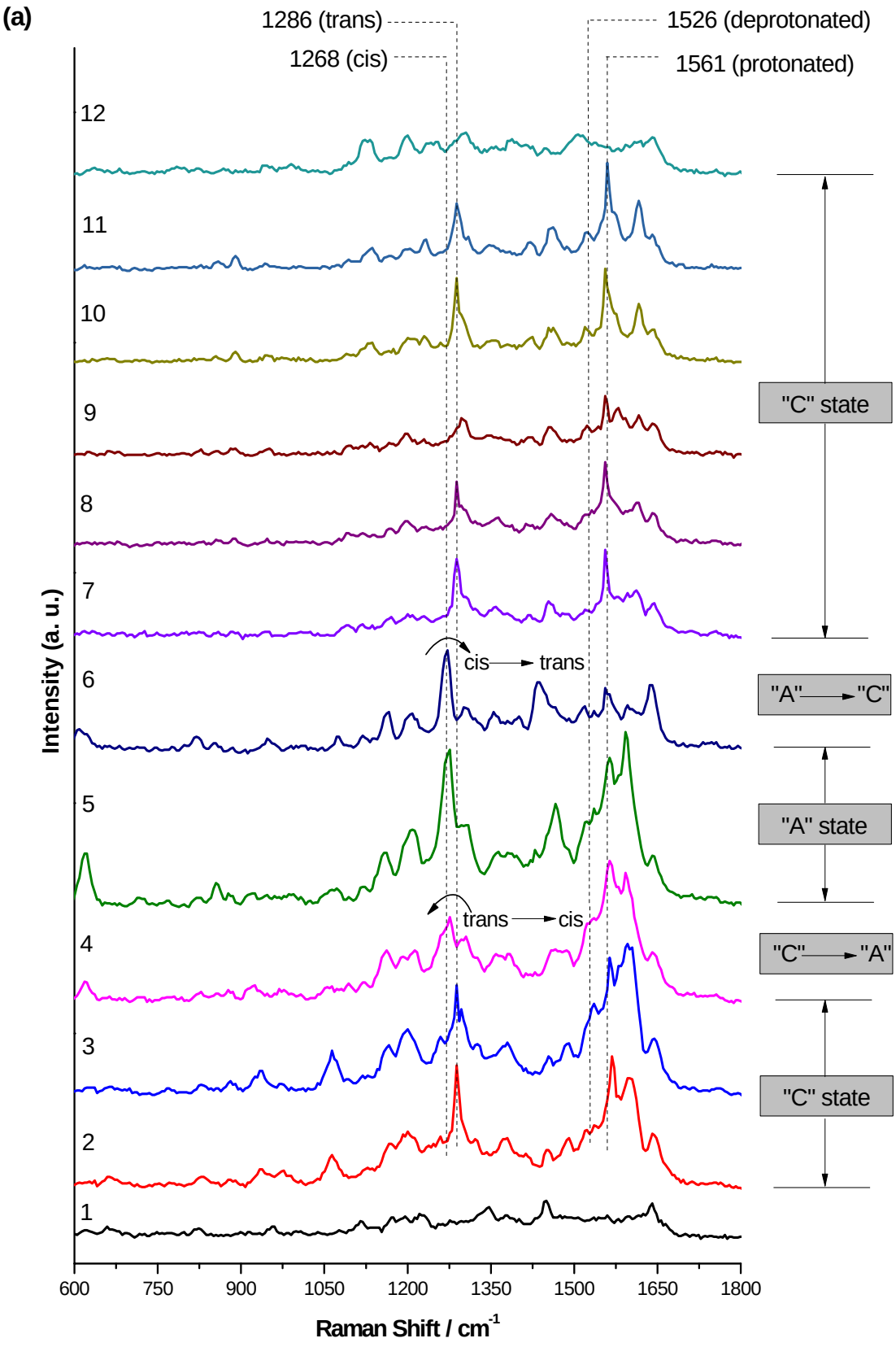
(a)
1286 (trans)
1268 (cis)
1526 (deprotonated)
1561 (protonated)
12
11
10
9
8
7
6
5
4
3
2
1
cis → trans
trans → cis
"C" state
"A" → "C"
"A" state
"C" → "A"
"C" state
Intensity (a. u.)
600
750
900
1050
1200
1350
1500
1650
1800
Raman Shift / cm-1

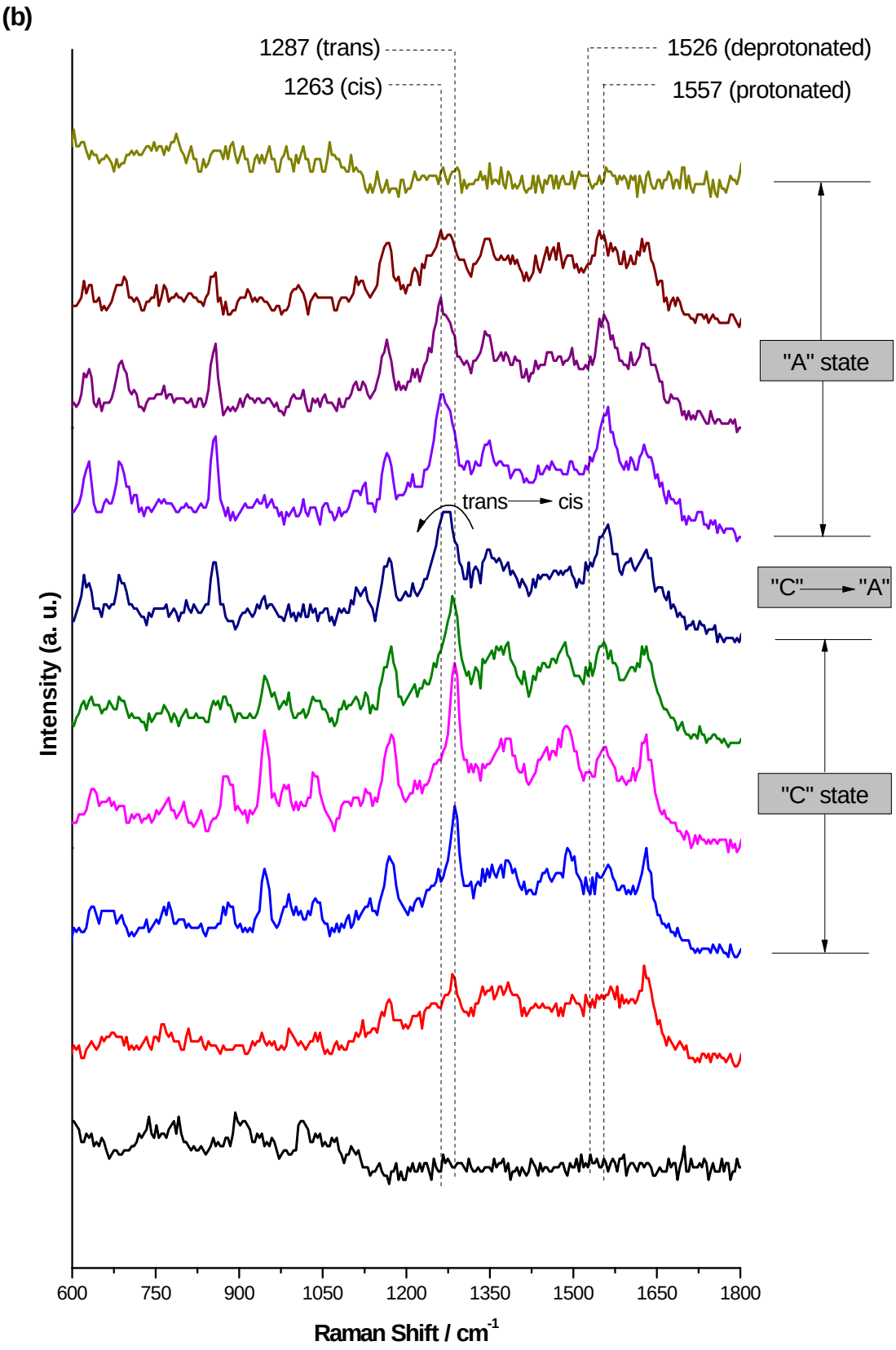
(b)
1287 (trans)
1263 (cis)
1526 (deprotonated)
1557 (protonated)
"A" state
trans
cis
"C"
"A"
"C" state
Intensity (a. u.)
600
750
900
1050
1200
1350
1500
1650
1800
Raman Shift / cm-1

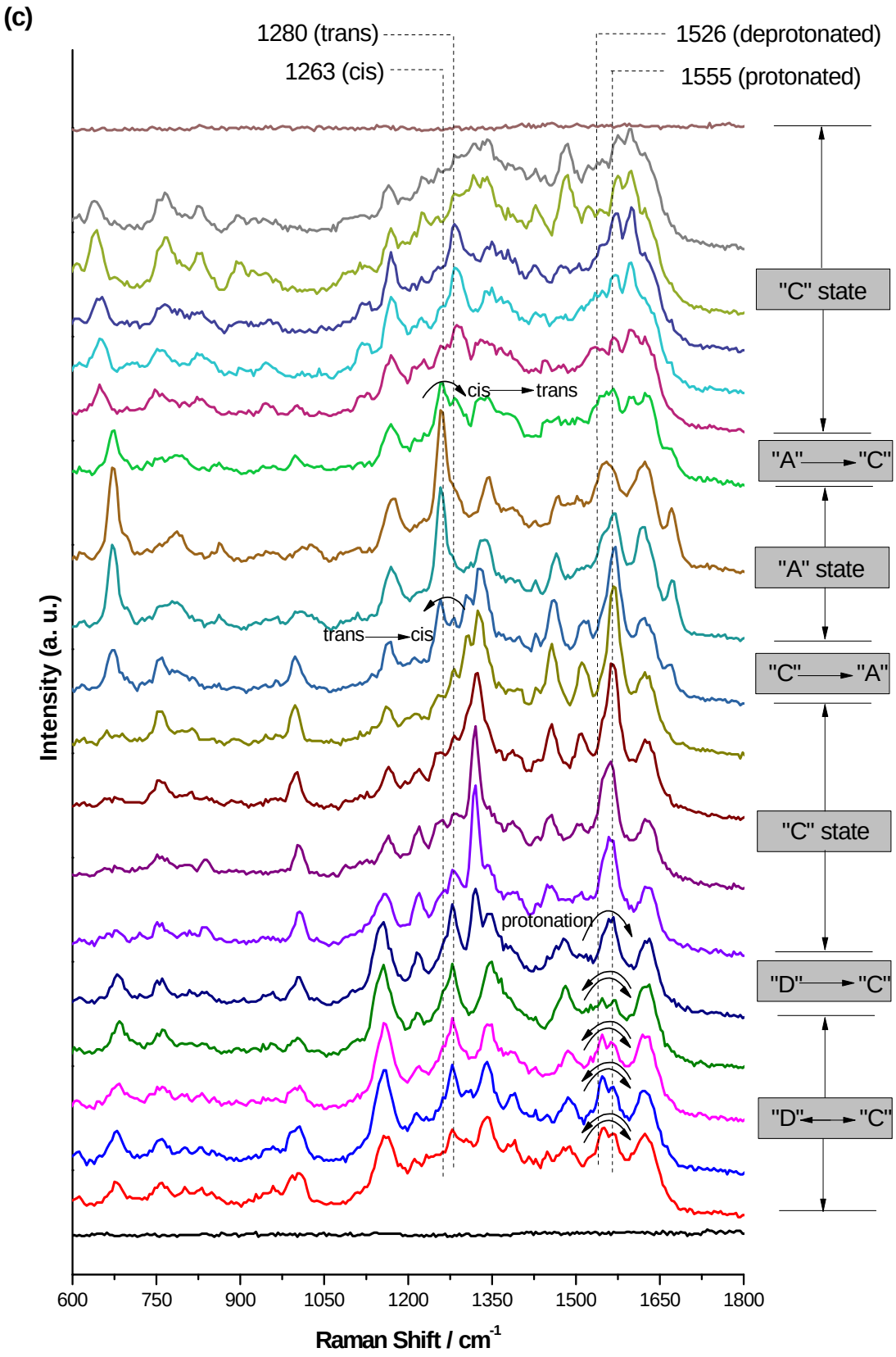
(c)
1280 (trans)
1263 (cis)
1526 (deprotonated)
1555 (protonated)
cis
trans
trans
cis
protonation
"C" state
"A"
"C"
"A" state
"C"
"A"
"C" state
"D"
"C"
"D"
"C"
Intensity (a. u.)
600
750
900
1050
1200
1350
1500
1650
1800
Raman Shift / cm-1

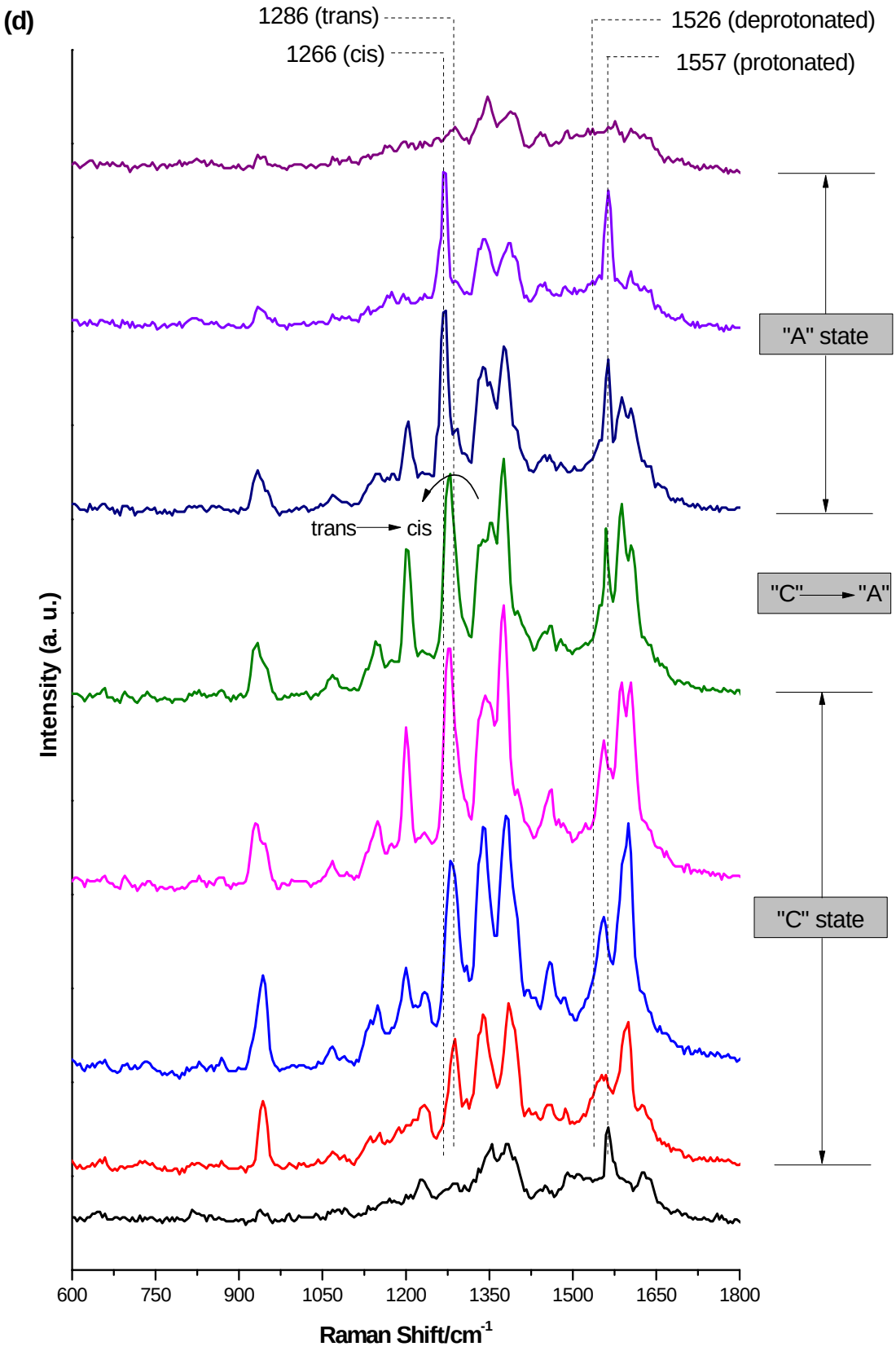
(d)
1286 (trans)
1266 (cis)
1526 (deprotonated)
1557 (protonated)
"A" state
trans
cis
"C"
"A"
"C" state
Intensity (a. u.)
600
750
900
1050
1200
1350
1500
1650
1800
Raman Shift/cm-1

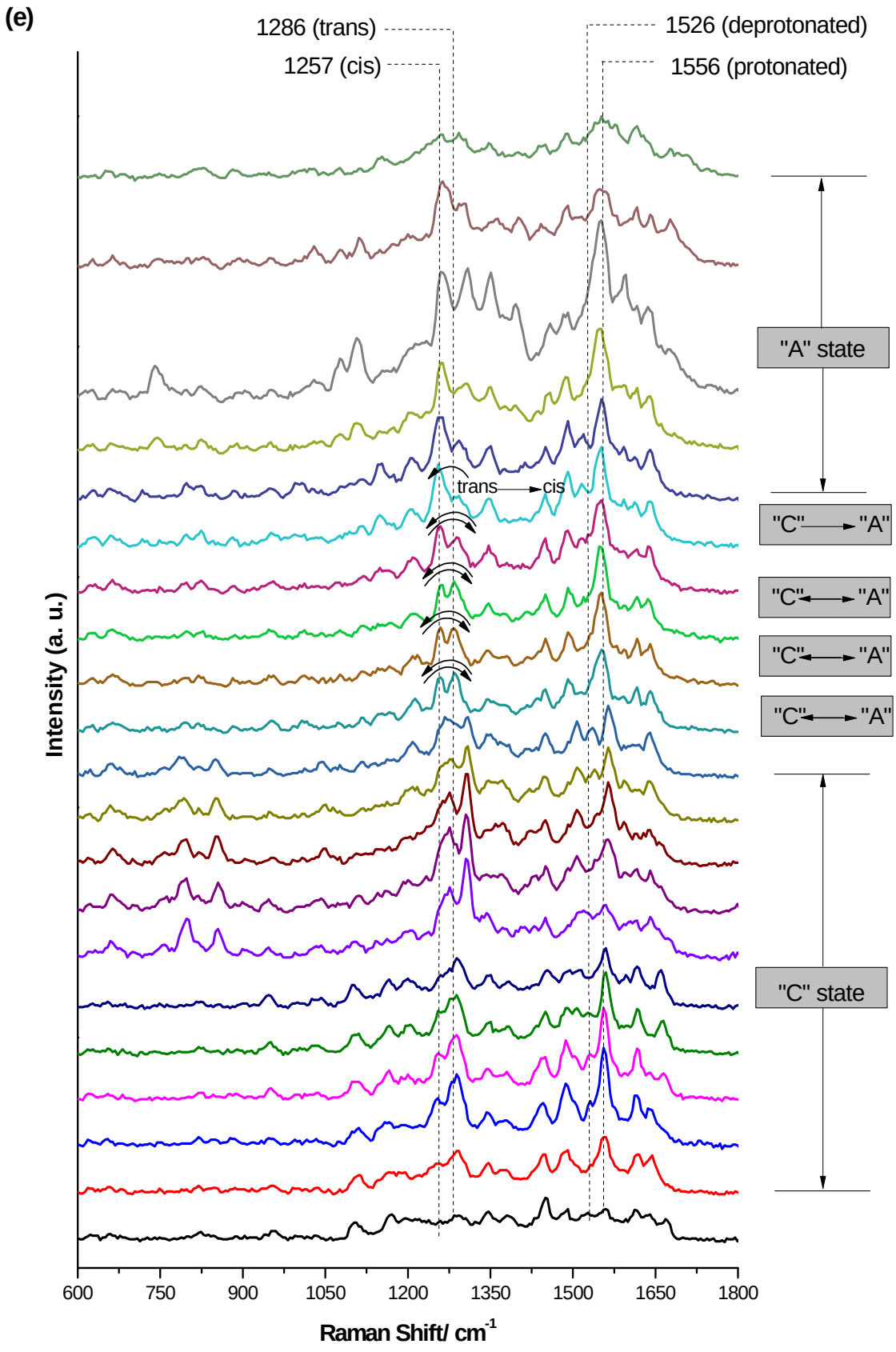
(e)
1286 (trans)
1257 (cis)
1526 (deprotonated)
1556 (protonated)
"A" state
trans
cis
"C"
"A"
"C"
"A"
"C"
"A"
"C"
"A"
"C" state
Intensity (a. u.)
600
750
900
1050
1200
1350
1500
1650
1800
Raman Shift/ cm-1

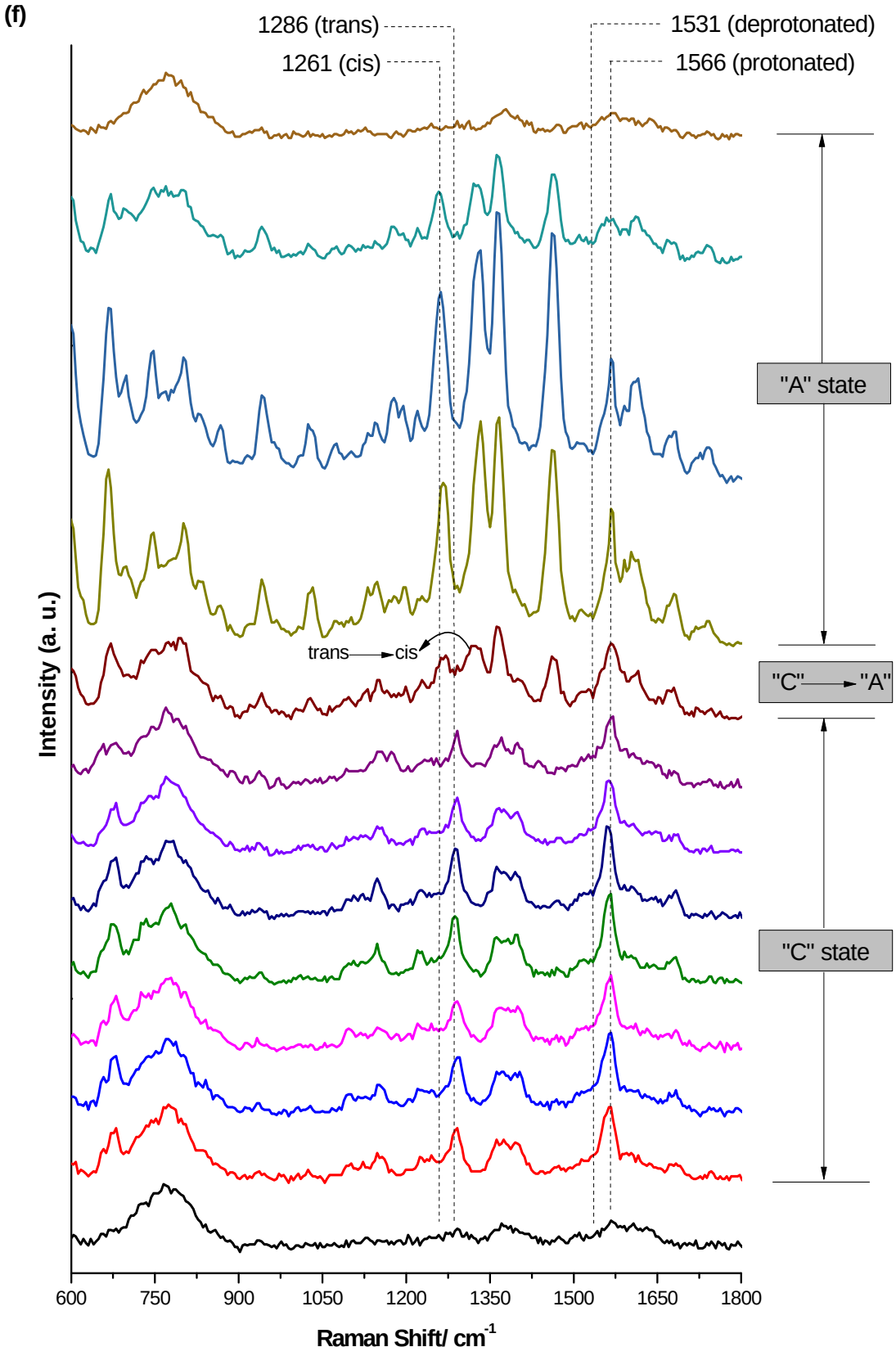
(f)
1286 (trans)
1261 (cis)
1531 (deprotonated)
1566 (protonated)
"A" state
"C"→"A"
"C" state
trans→cis
Intensity (a. u.)
600
750
900
1050
1200
1350
1500
1650
1800
Raman Shift/ cm-1

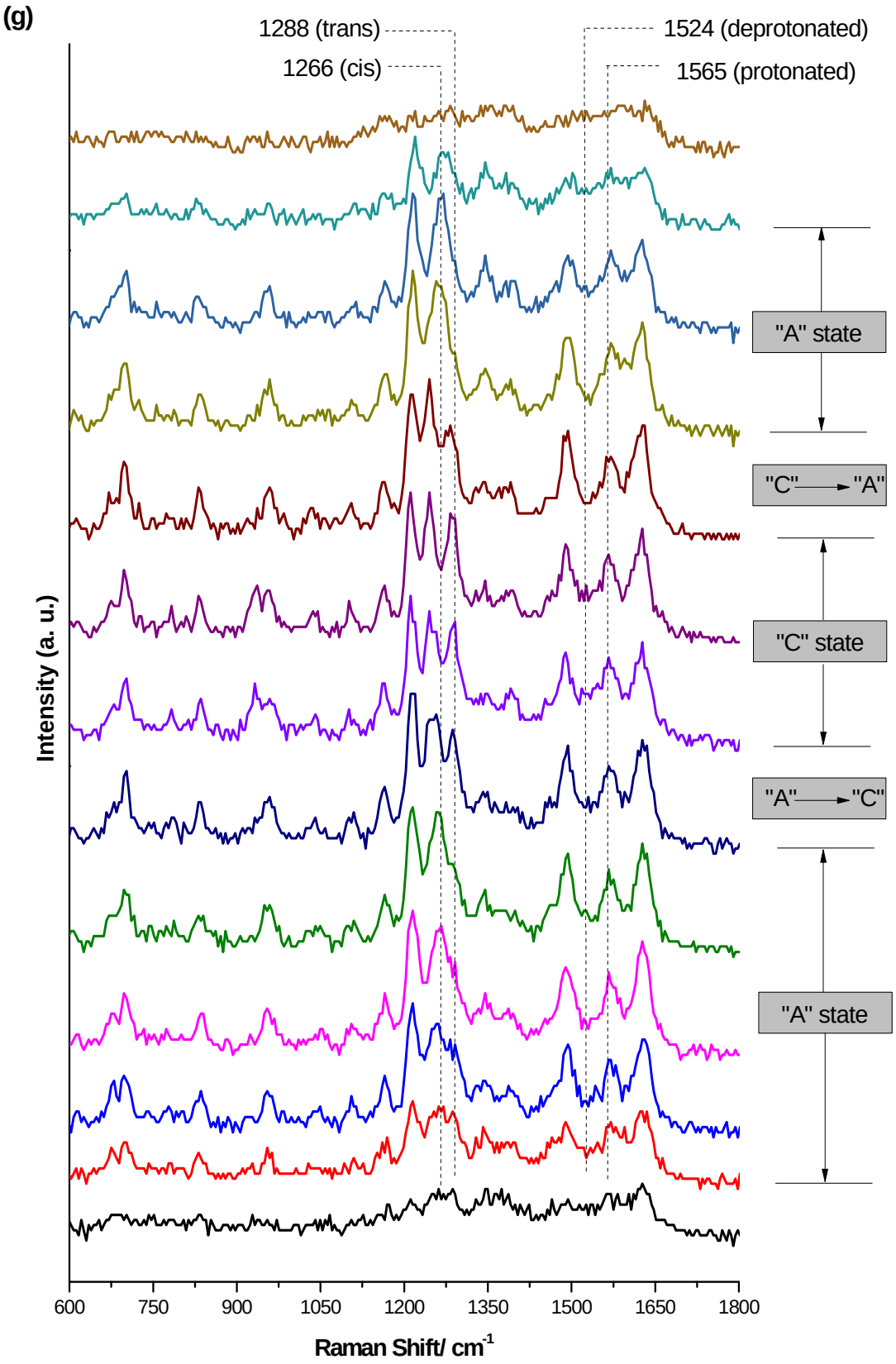
(g)
1288 (trans)
1266 (cis)
1524 (deprotonated)
1565 (protonated)
"A" state
"C"→"A"
"C" state
"A"→"C"
"A" state
Intensity (a. u.)
600
750
900
1050
1200
1350
1500
1650
1800
Raman Shift/ cm-1

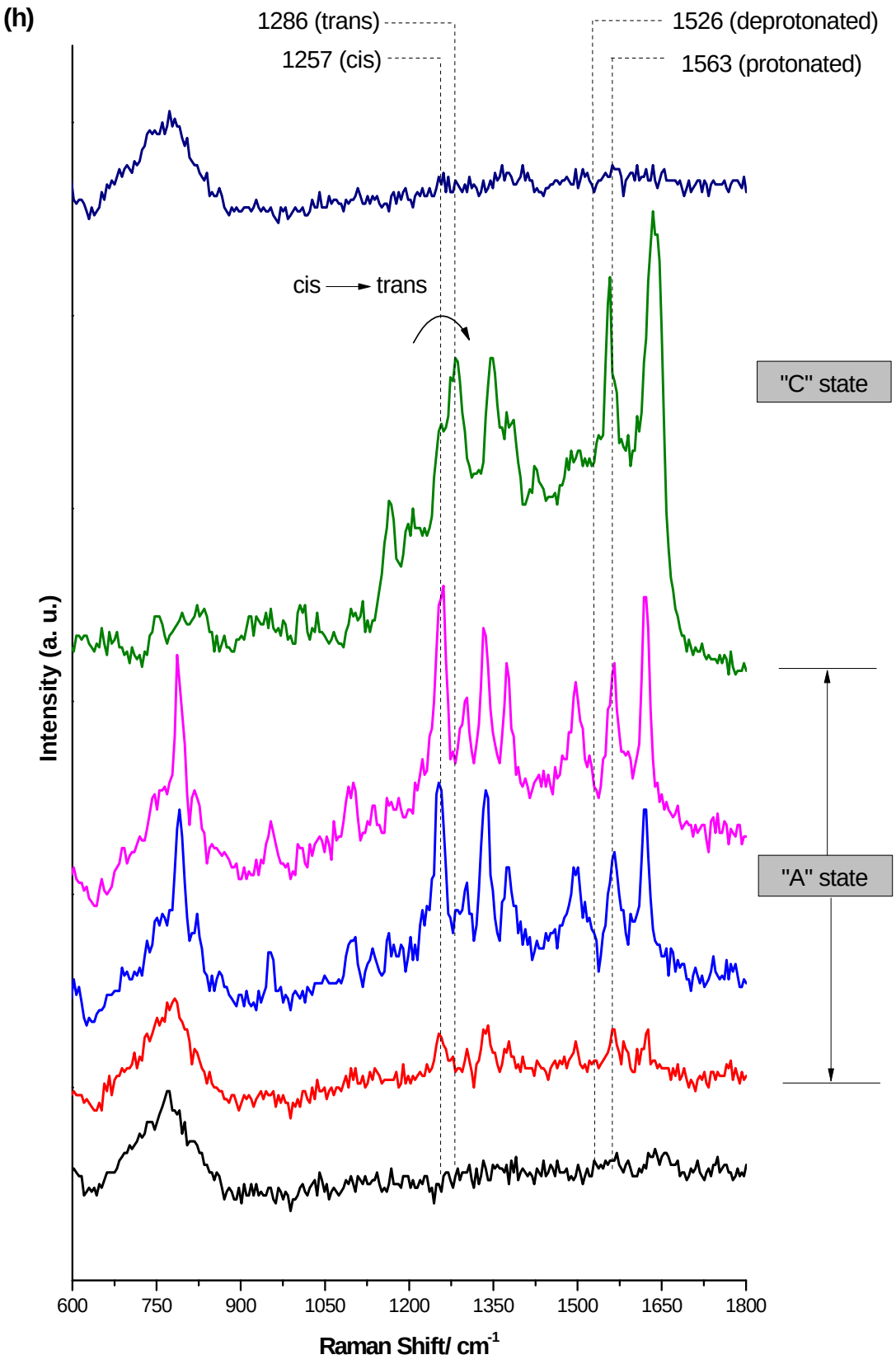
(h)
1286 (trans)
1257 (cis)
1526 (deprotonated)
1563 (protonated)
cis → trans
"C" state
"A" state
Intensity (a. u.)
600
750
900
1050
1200
1350
1500
1650
1800
Raman Shift/ cm-1

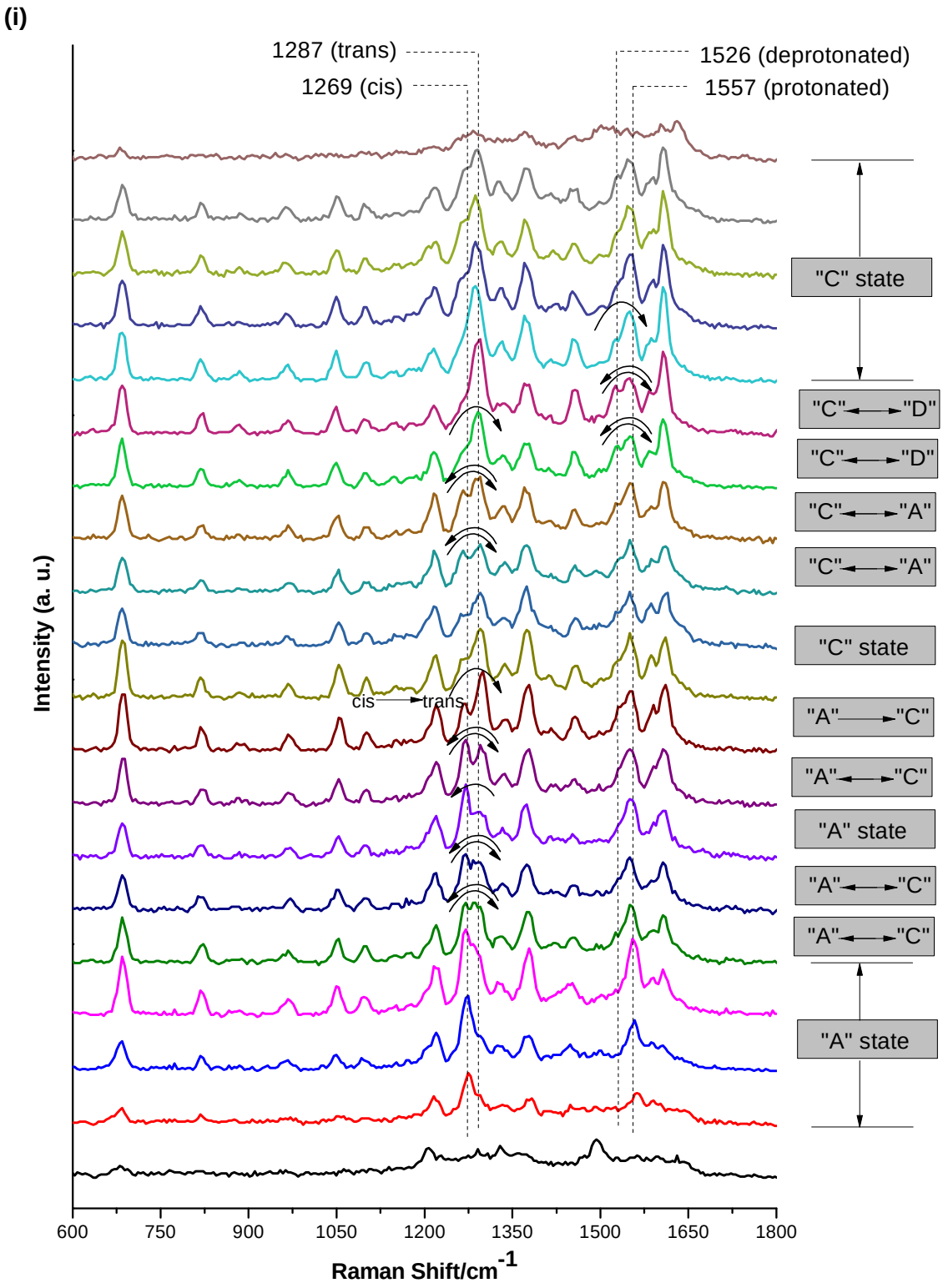

Figure IV.19. Time series SERS spectra illustrating transitions between the states A and C of individual GFP molecules (50 ms integration time, 700 μW laser intensity).

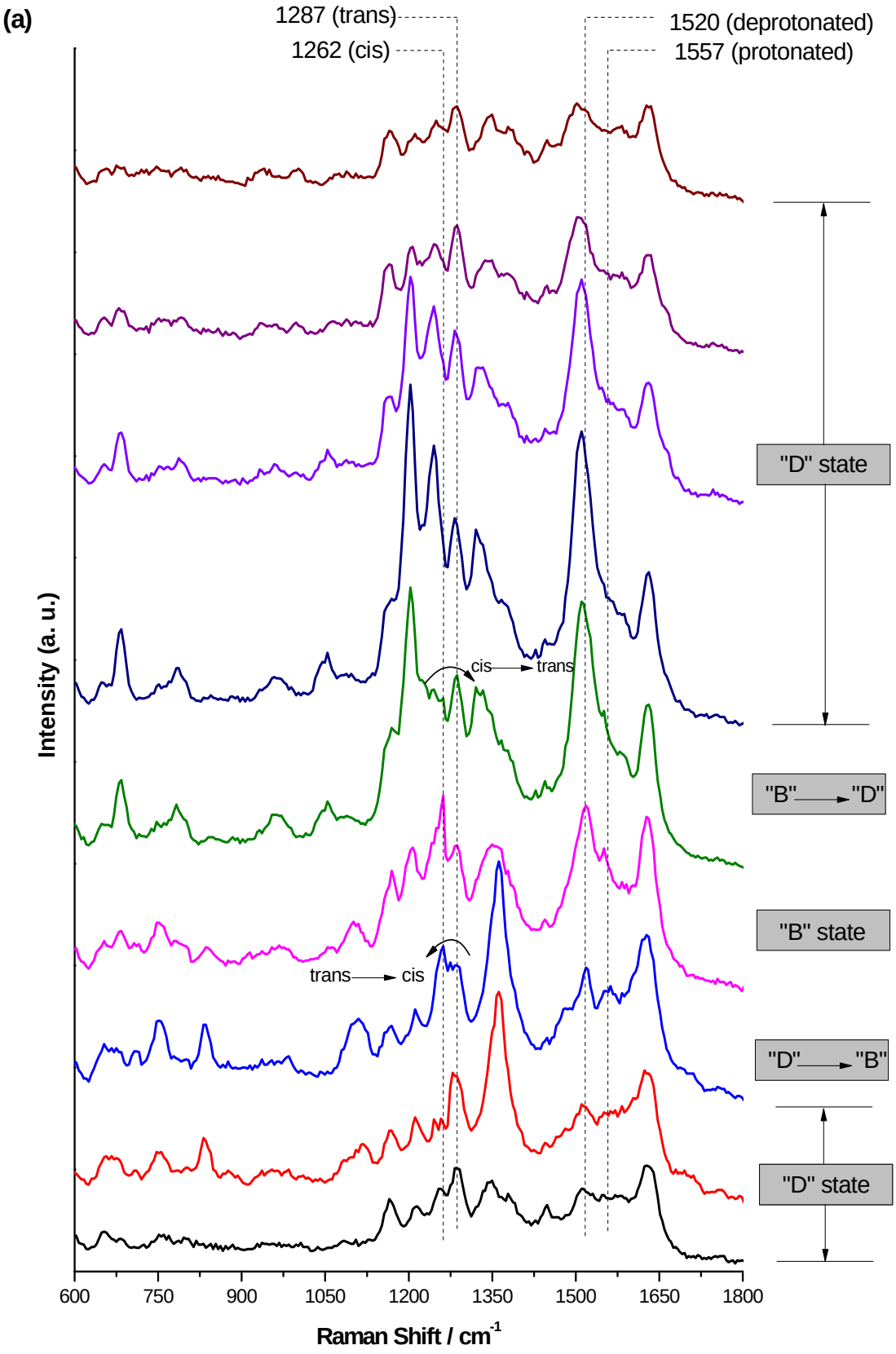
(a)
1287 (trans)
1262 (cis)
1520 (deprotonated)
1557 (protonated)
"D" state
cis
trans
"B"
"D"
"B" state
trans
cis
"D"
"B"
"D" state
Intensity (a. u.)
600
750
900
1050
1200
1350
1500
1650
1800
Raman Shift / cm-1

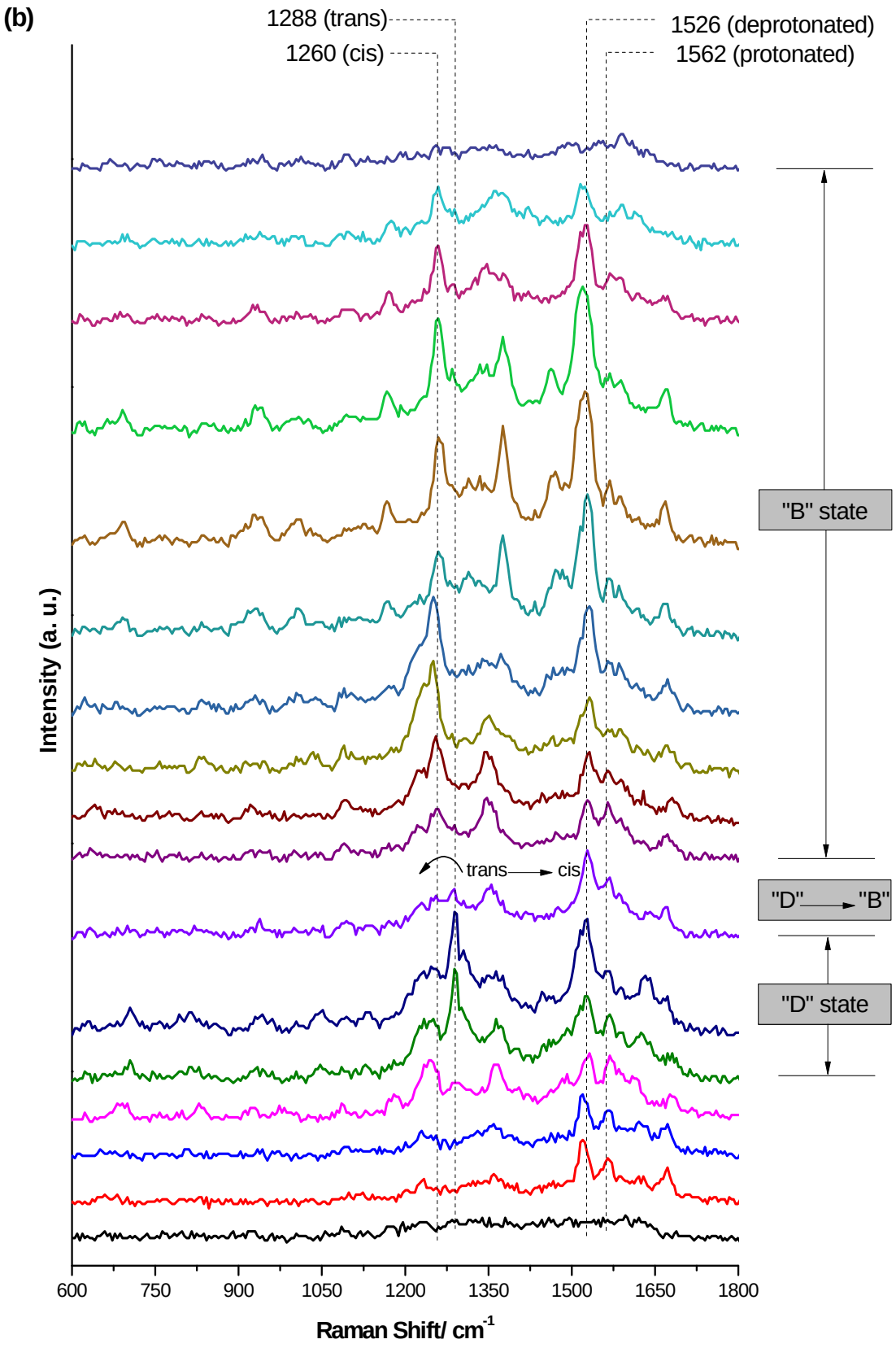
(b)
1288 (trans)
1260 (cis)
1526 (deprotonated)
1562 (protonated)
"B" state
trans
cis
"D"
"B"
"D" state
Intensity (a. u.)
600
750
900
1050
1200
1350
1500
1650
1800
Raman Shift/ cm-1

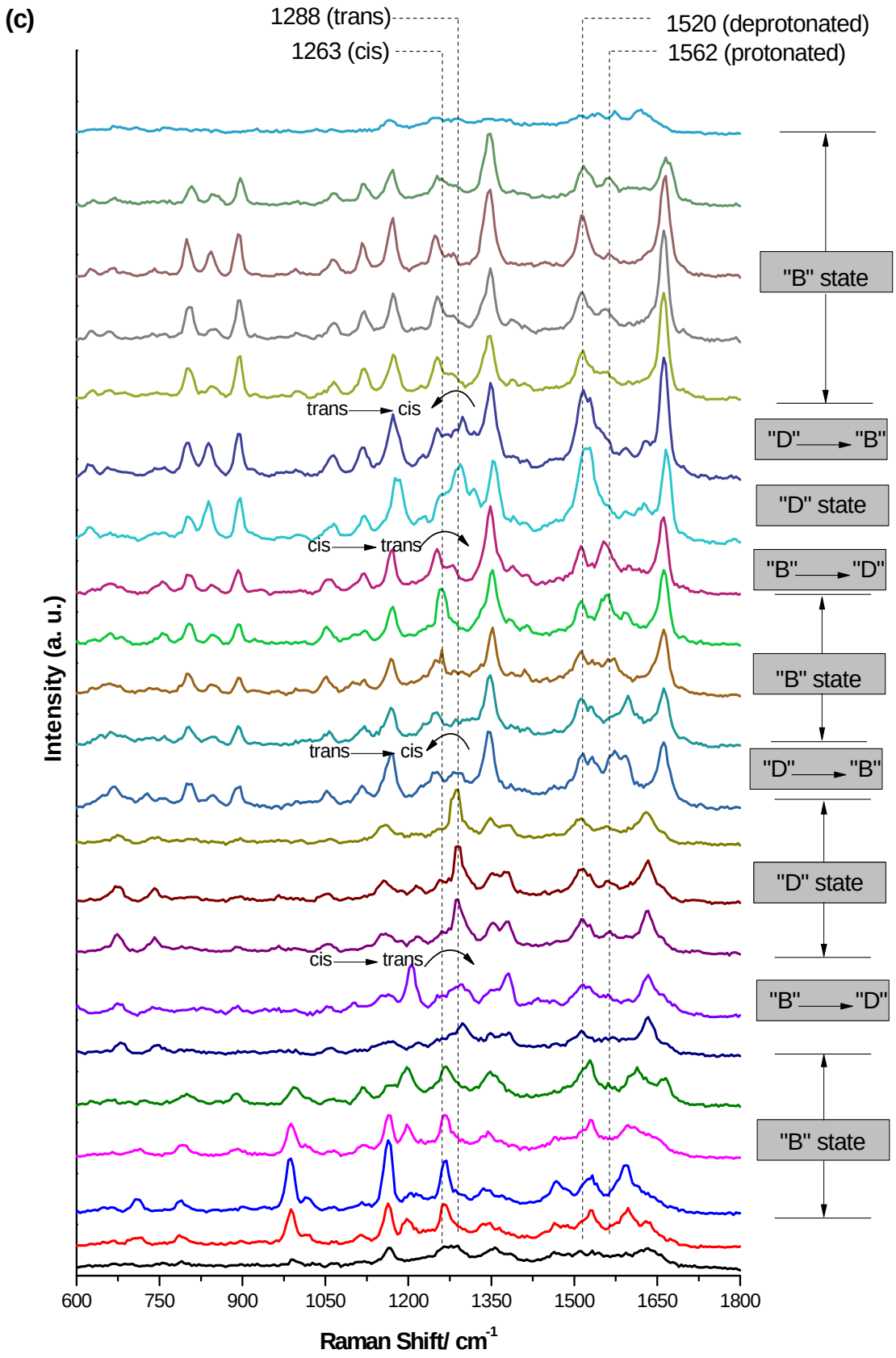
(c)
1288 (trans)
1263 (cis)
1520 (deprotonated)
1562 (protonated)
trans → cis
cis → trans
trans → cis
cis → trans
"B" state
"D" → "B"
"D" state
"B" → "D"
"B" state
"D" → "B"
"D" state
"B" → "D"
"B" state
Intensity (a. u.)
600
750
900
1050
1200
1350
1500
1650
1800
Raman Shift/ cm-1

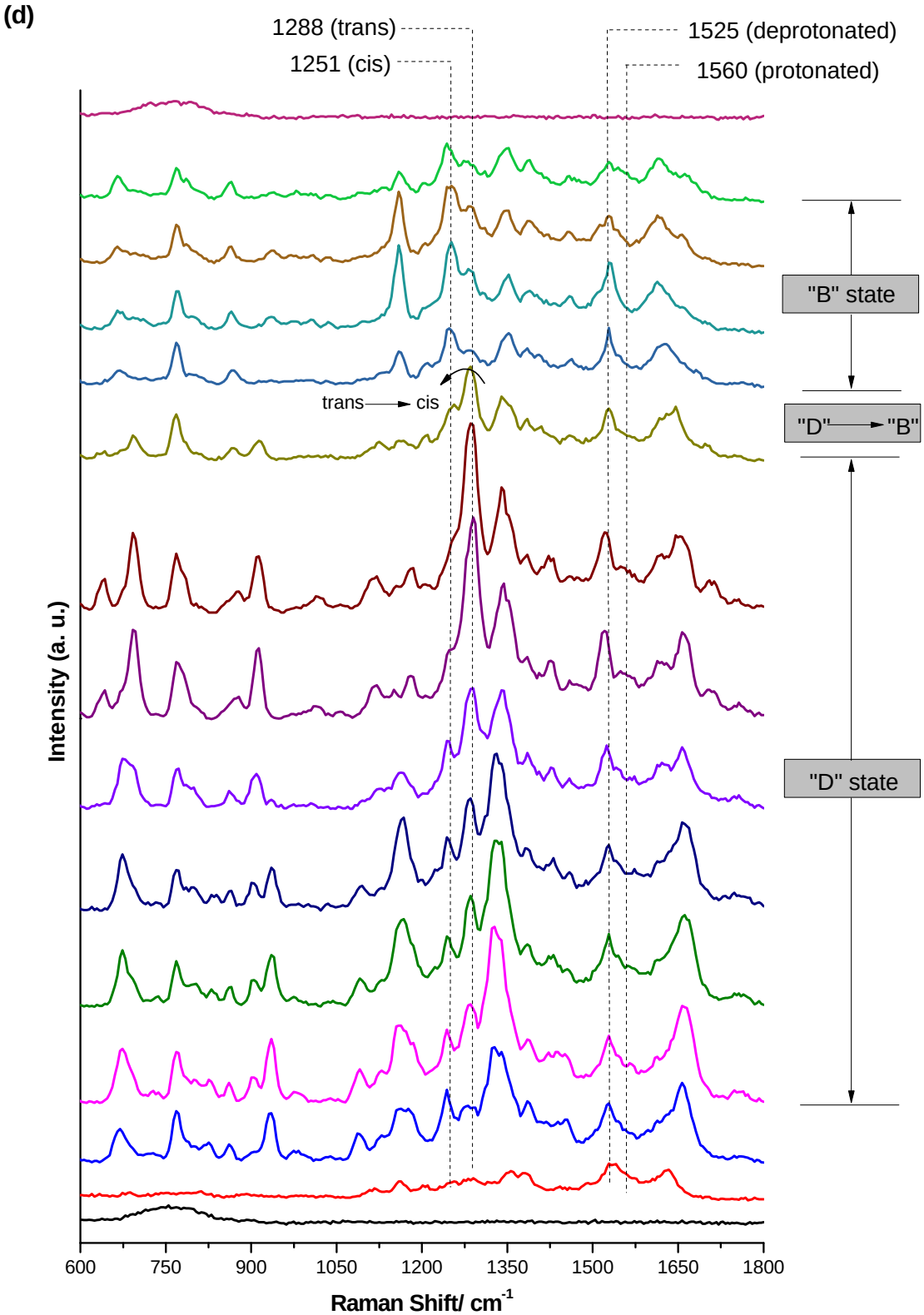

Figure IV.20. Time series SERS spectra illustrating transitions between the states B and D of individual GFP molecules (50 ms integration time, 700 μW laser intensity).

IV.5. Statistical analysis

IV.5.1. Population distribution

As reported so far in the literature, it is well established that wtGFP can stay either in A (cis/protonated) or B (cis/deprotonated) state and conversion between these two states can take place [5, 50, 80, 101]. On the other hand, there is no significant evidence on the trans states of the wtGFP chromophore in the literature. Although in recent years several groups reported on the neutral trans form (C state) of the synthetic GFP chromophores (i.e., HBDI and GFP (Y66)) [91, 99, 100], mystery about the as suggested trans state is still very much unresolved for the wtGFP chromophore. In this present thesis work, for the first time we observed presence of a state with trans/protonated configuration of the wtGFP chromophore at single molecule level which agrees well with the as suggested C state by Nifosi *et al.* for HBDI [91]. Moreover, our SM-SERS data confirms presence of one more state with trans/deprotonated configuration (as termed D state by the authors) of the chromophore, which was not reported earlier.

Histograms of population of the wtGFP chromophore states (A, B, C and D) are shown in the Figure IV.21 for two different laser excitations (100 and 700 μW). More than one thousand single molecule jumps were taken into consideration while plotting these histograms. Here the registered states are those when single GFP molecules are first caught at the hotspots. Interestingly, as can be seen from the Figure IV.21, our data suggests significant presence of all 4 chromophore states. Change in the population of states is observed when the incident laser power is changed from 100 μW to 700 μW. Comparison of the two histograms of the Figure IV.21 indicates that the population of the states B and D is suppressed at high laser excitation, which consequently associates with a significant increase of the population of the C state. Histograms plotted in the Figure IV.22 illustrate the population of the GFP chromophore states at the onset of the hotspot (black) and prior of leaving the hotspot (red) at two different laser powers (100 and

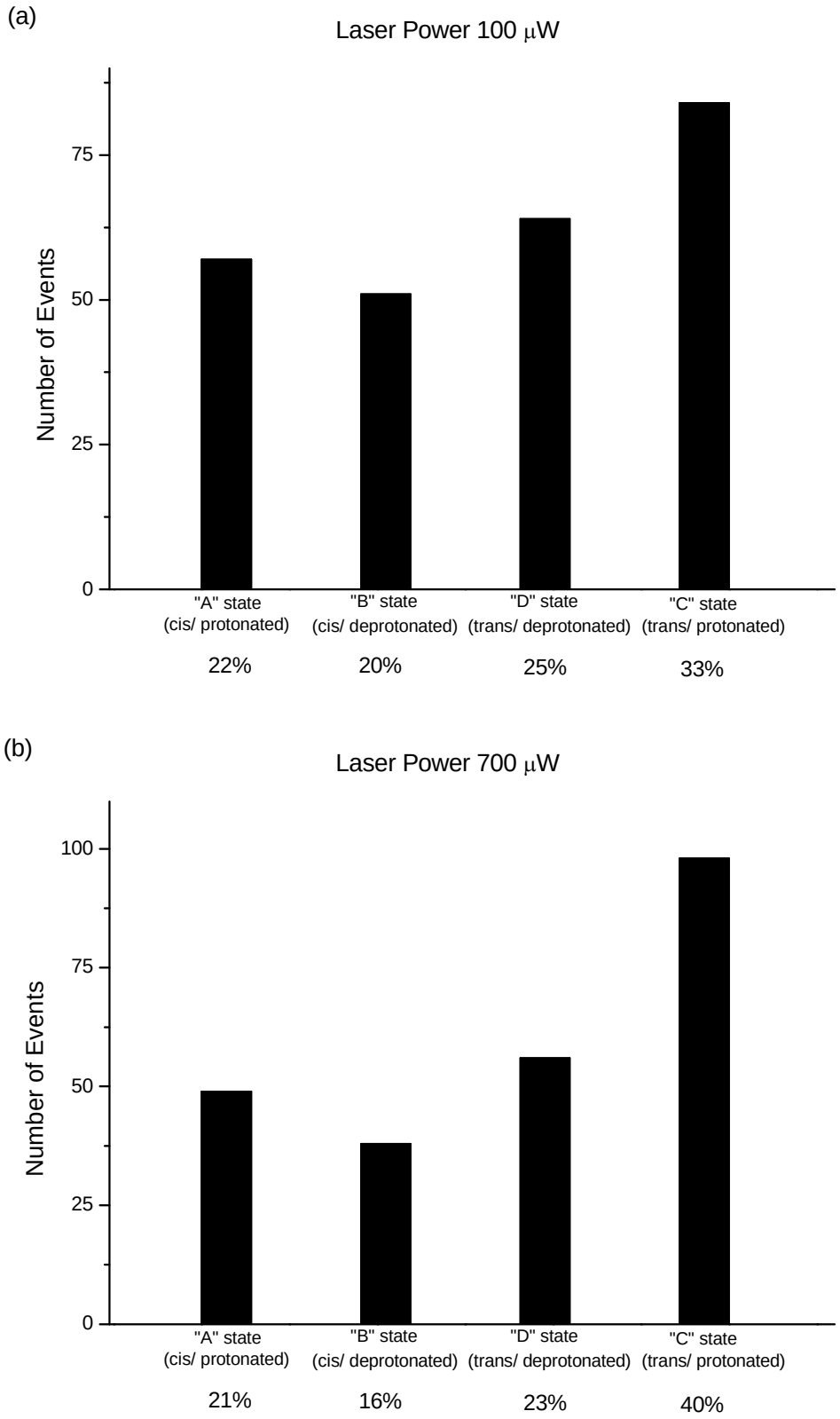

Figure IV.21. Population of 4 conformational states of wtGFP at two different laser intensities: (**a**) 100 μW; (**b**) 700 μW.

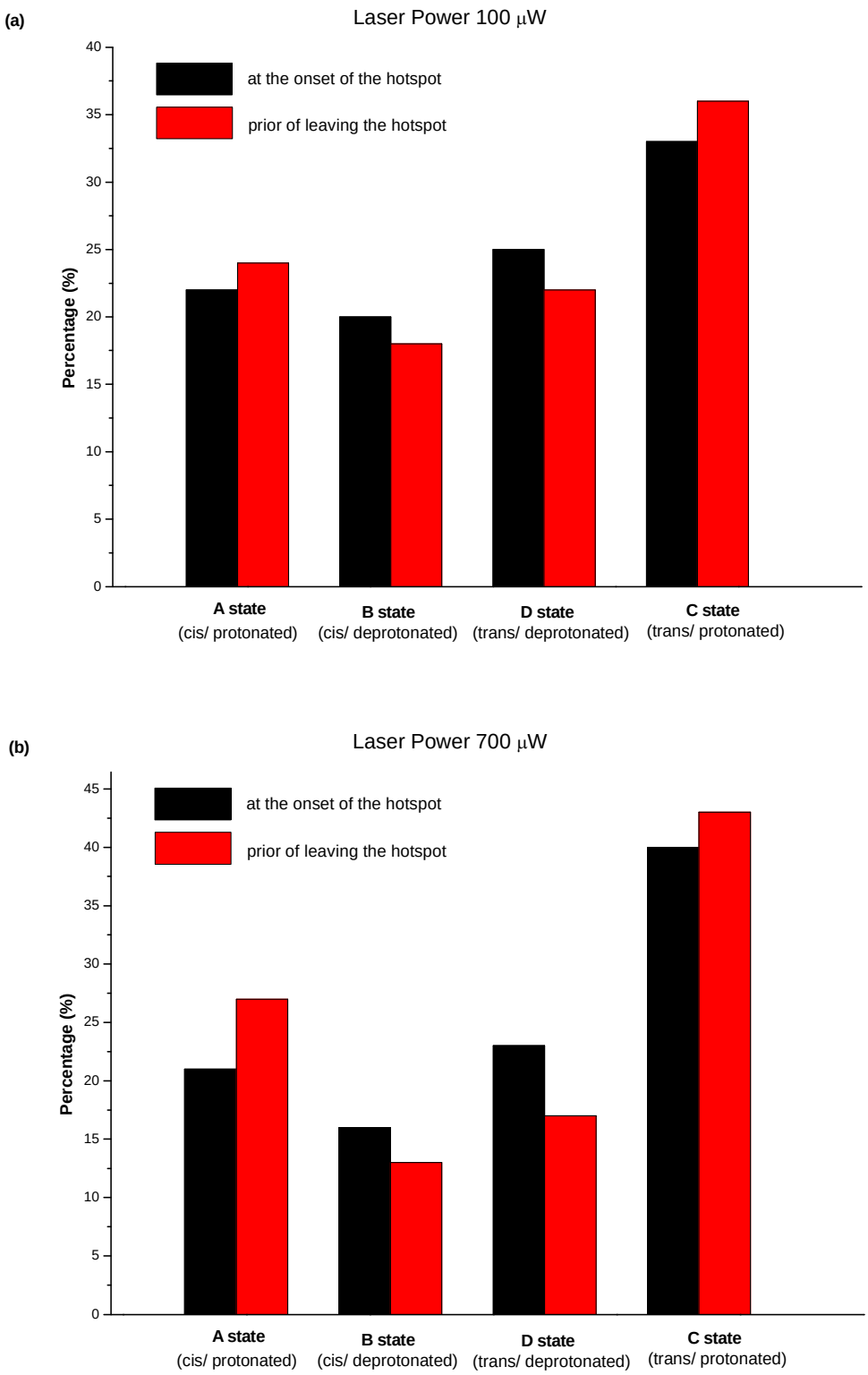

Figure IV.22. Population of 4 conformational states of wtGFP at two different laser intensities: (**a**) 100 μW; (**b**) 700 μW. (black: population at the onset of the hotspot; red: population prior of leaving the hotspot)

700 μW). An immediate observation is the increase in the population of the states A and C while suppressing the population of the states B and D, respectively. For the most part, this increase in the population of the protonated states (A and C) are caused by the transitions of the deprotonated states through B→A and D→C as observed in the Section IV.5 under laser excitation while residing at the hotspots.

IV.5.2. Transition probabilities

Histograms plotted in the Figure IV.23 encapsulate all the transitions captured in the time series SERS scans (exemplified in the Section IV. 4) of single GFP molecules at 100 and 700 μW laser excitations. Histograms also demonstrate probability of transitions between the 4 distinct GFP chromophore states (i.e., A↔B, B↔D, D↔C and C↔D), cis↔trans isomerization and protonation↔deprotonation. Data indicates exceedingly low transition probability between the chromophore states, which is consistent with GFP chromophore's utmost stability inside the β-barrel structure (discussed earlier in the background chapter) [5, 6, 41]. Moreover, excitation of the GFP chromophore at 532 nm is minimal as judged by the author of this thesis work from the weak fluorescence at 508 nm. Nevertheless, transitions are not absolutely prevented as seen in the Section IV. 4.

Comparing all the transition probabilities recorded in the histograms, it reveals higher probability of transitions from the states B and D into the states A and C state, respectively. It indicates higher protonation affinity of the deprotonated states (B and D) of the GFP chromophore under 532 nm excitation rather than the opposite (i.e., protonation→deprotonation). These particular transitions (i.e., B→A and D→C) are found to be more probable at the higher laser excitation (700 μW). On the other hand, states A and C of the GFP chromophore are found to be more stable under 532 nm laser excitation and transformation of these two states are rare.

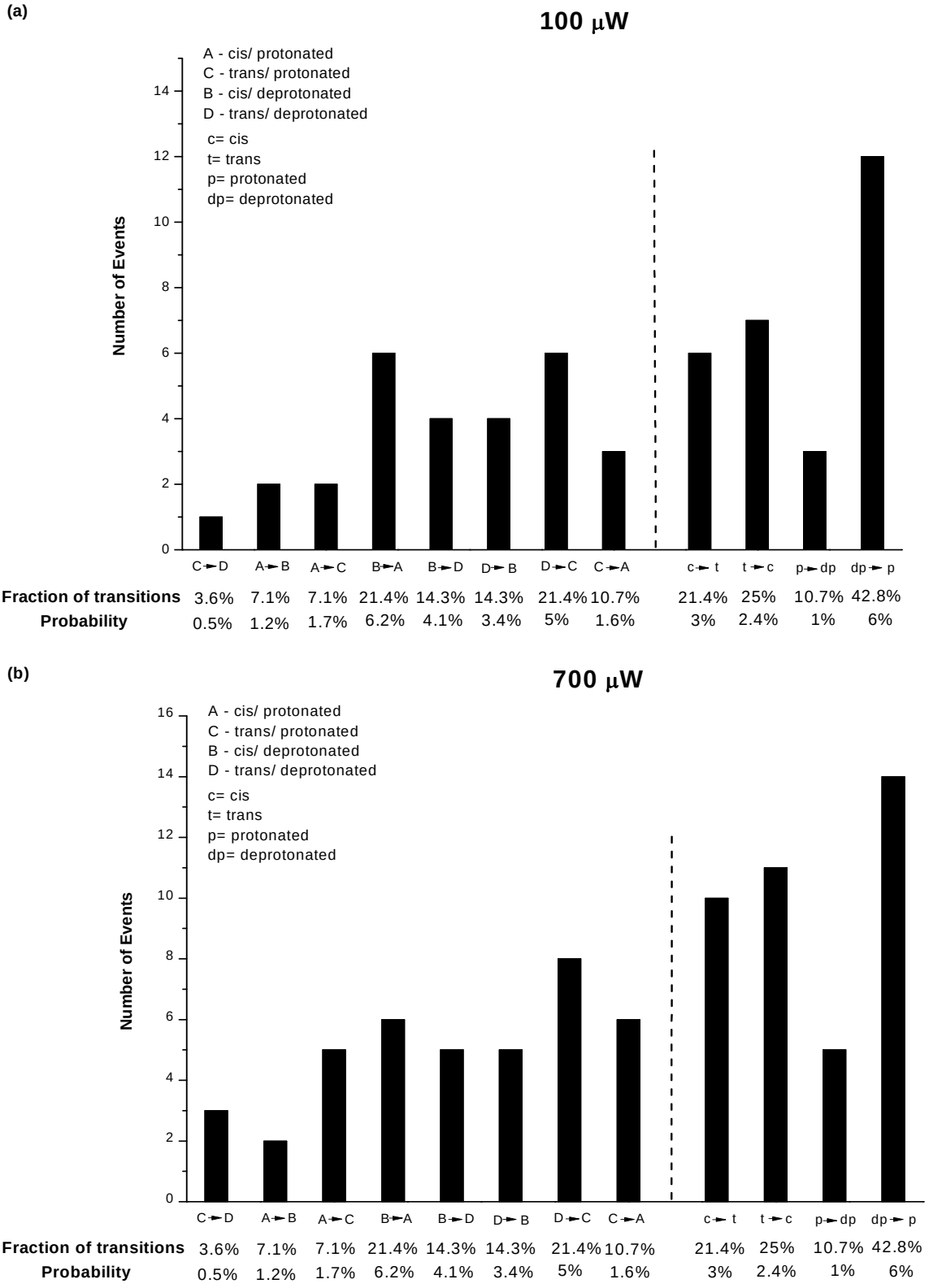

Figure IV.23. Histograms of transitions associated with the GFP chromophore states at two different laser powers: (**a**) 100 μW; (**b**) 700 μW.

Interestingly, histograms also indicate low probability of transitions between the chromophore states, which involves cis⁄trans isomerizations (i.e., A⁄C, B⁄D). This low frequency of cis⁄trans isomerization is consistent with GFP chromophore's rigid stabilization inside the β-barrel structure. Indeed, inhibition of isomerization inside the barrel structure impedes the non-radiative thermalization pathways and makes GFP an efficient fluorophore (discussed earlier in the background chapter).

Change in the probability of transitions between the distinct chromophore states of GFP is observed when the incident laser power is altered from 100 μW to 700 μW. In particular, as depicted in the Figure IV.24, transition probability increases for all observed transitions associated with the GFP chromophore, although signal integration time was reduced from 100 ms to 50 ms. It suggests, even the excitation source was fixed at 532 nm, higher laser power provides higher rate of pumping of the GFP chromophore. Interestingly, specific transitions of the GFP chromophore states such as B→A and D→C were found to be more probable at higher laser excitation, leading to increasing population of the states A and C, respectively. Figure IV.25 illustrates GFP chromophore cycle associated with the probability of transitions at two different laser excitations.

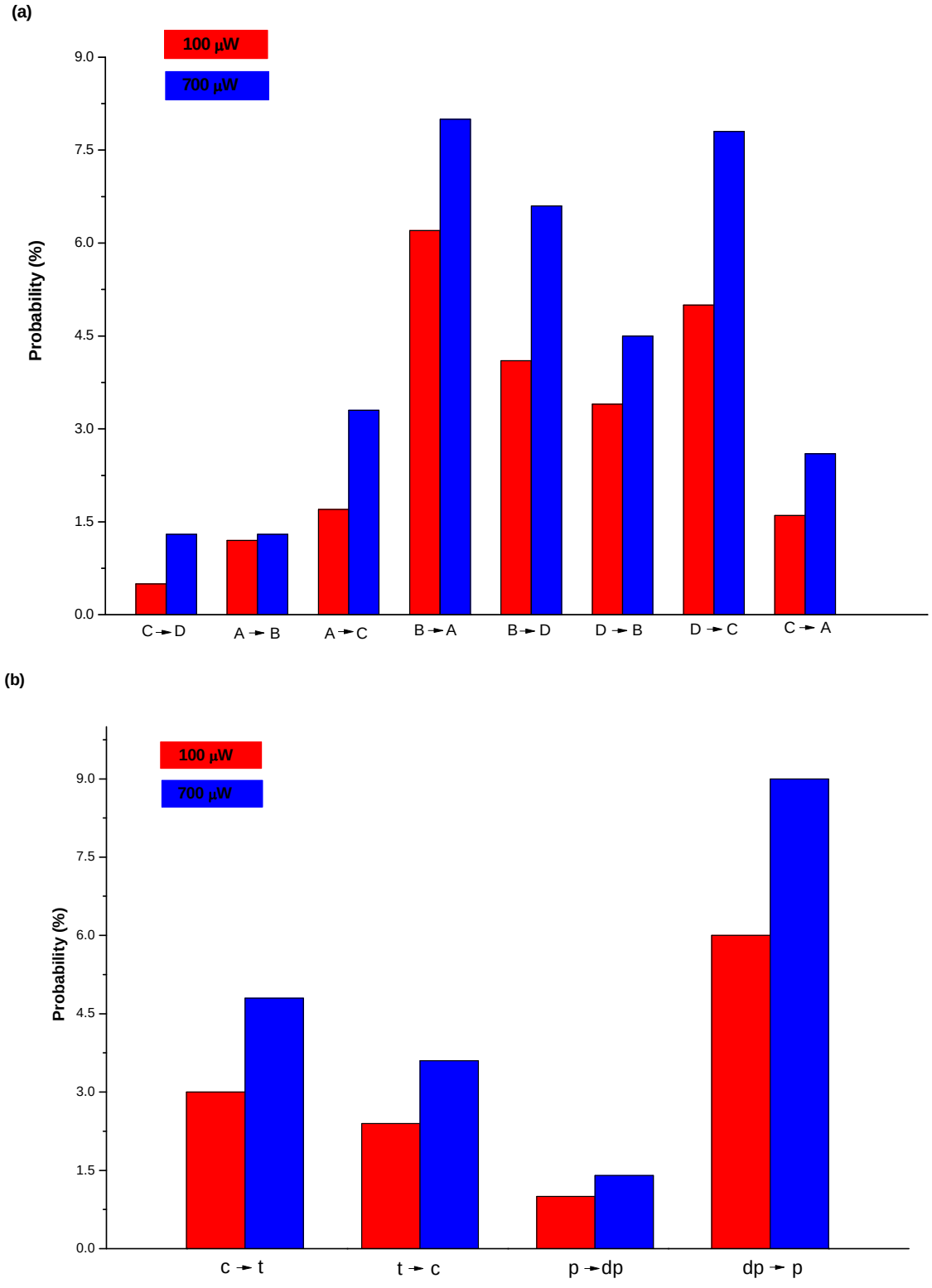

Figure IV.24. Histograms of transitions associated with the GFP chromophore states at two different laser powers (red: 100 μW, blue: 700 μW): (**a**) probability of transitions between the states A, B, C and D; (**b**) probability of cis↔trans isomerization and protonation↔deprotonation.

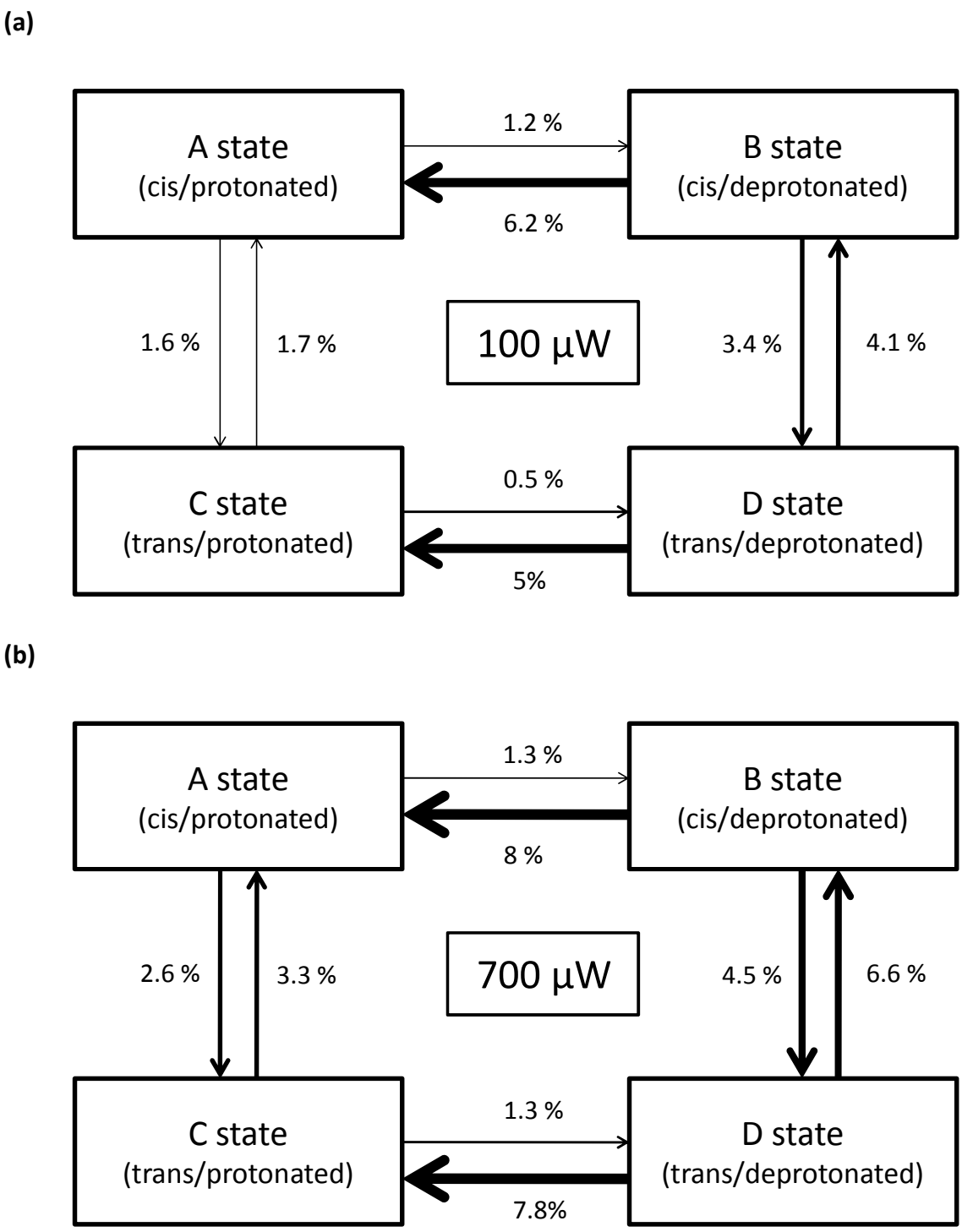

Figure IV.25. GFP chromophore cycle associated with transition probabilities: (**a**) 100 µW and (**b**) 700 µW.

Every single SERS scan was considered as an event during probability calculation. As we registered four different states of GFP in this study, it suggests any single state can stay in its original form or can perform a transition to any of the three remaining states (i.e., state W can convert into X, Y or Z state or stay as it is) during an event. As such we used following expression for probability calculations,

$$\text{Probability}_{W\rightarrow X} = N_{W\rightarrow X} / N(\mathbf{W})$$

Where,

$N_{W\rightarrow X}$ = Number of transitions from "W" to "X"

N (**W**) = Total number of time steps starting with "W" state

$= N_{W\rightarrow W} + N_{W\rightarrow X} + N_{W\rightarrow Y} + N_{W\rightarrow Z}$

($N_{W\rightarrow W}$ refers no transition of the molecule as such molecule stay in its same state. While, $N_{W\rightarrow X}$, $N_{W\rightarrow Y}$ and $N_{W\rightarrow Z}$ refer "number of transitions" of the molecule from W state to X, Y and Z state, respectively.)

CHAPTER V

CONCLUSIONS

Using “nanometal-on-semiconductor” SERS substrates, the present work acquires the vibrational spectra of single wtGFP molecules under 532 nm laser excitation. Once an aliquot of 10^{-9} M wtGFP is spotted on a SERS substrate and a Raman acquisition is started, intense and well-resolved peaks are observed to appear and disappear repeatedly over a weak background. These temporal “spectral jumps” are captured in every half a minute on the average and sustain for 1 s or less. Each jump is associated with a single GFP molecule diffusing into a high SERS enhancement factor site (i.e., a “hotspot”), residing it for 1 s or less, and eventually diffusing out of it. The SERS is acquired in time series at continuous intervals of 50 or 100 ms. Therefore, up to ~20 single molecule spectra can be captured during a spectral jump. The following conclusions are drawn from the results of the present thesis work.

1. The analysis of the time series single molecule spectra shows structural transitions in the chromophore of wtGFP. Typically, these transitions do not occur more than a few times in a second under the Raman acquisition conditions employed in the present work. Therefore, a single GFP molecule can be captured at a single definite conformational state in a 50 or 100 ms time interval. In other words, the “slowness” of the conformational changes in the wtGFP chromophore is a fortunate case, because it

allows the present work to time-resolve the chromophore states and transitions by the Raman spectrophotometer employed. In the time scale of conformational changes in molecules, these structural changes observed for the GFP chromophore are exceptionally slow that is owed to its rigid stabilization inside the β-barrel structure.

2. A minimum of 4 distinct conformational states of the wtGFP chromophore are observed and assigned to cis/protonated (A), cis/deprotonated (B), trans/protonated (C) and trans/deprotonated (D) forms of the chromophore.

3. Statistical analysis of the captured chromophore states reveals substantial presence of all the 4 state populations including the trans (i.e., C and D) states. In contrast, reports on the trans states of the GFP chromophore are rare and also controversial. The shortage of evidence on the trans states in the literature is likely to have led by their nonfluorescent nature (i.e., also called “dark states”). They cannot be probed by fluorescence spectroscopy (time resolved and excitation fluorescence spectroscopy), which has been used extensively to study the photophysics of wtGFP. Rather, the fluorescent spectroscopy reveals only the fluorescent states of the chromophore (i.e., A and B). Second, the past investigations of GFP photophysics also employed optical absorption spectroscopy. Majority of these measurements were conducted at room temperature and revealed the bands peaking at 395 and 475 nm which are ascribed to protonated (A) and deprotonated forms (B), respectively. On the other hand, when analyzed carefully, each band is observed to exhibit a shoulder and be the convolution of two different bands. However, these observations were not reported or discussed elsewhere, let alone the splitting in each band was interpreted as the cis and trans forms.

4. Conformational changes occur in between certain pairs of states that line-up in a cyclic pattern (i.e., A↔B↔D↔C↔A). In other words, only the protonation state or isomerization state of the chromophore changes per transition.
5. Conformational changes of the protonated chromophore states, A and C, are less frequent (i.e., A→B, A→C, C→D and C→A) compared to those of the deprotonated states, B and D. This finding suggests that, the states A and C are more stable than the states B and D under 532 nm excitation. The higher transition probabilities for B and D correlate with the occurrence of optical transitions for these states under 532 nm excitation. Although the optical absorption band peaks at around 475 nm for these states, there is considerable absorption at 532 nm, thanks to the wide absorption tail. In contrast, the 532 nm excitation is off-resonance with the electronic transitions in the A and C states, whose optical absorption bands peak around 395 nm. Consequently, A and C are essentially not excited by 532 nm, whereas B and D are. Comparison of the population of states A, B, C and D at the onset of residing and prior to leaving the hotspots also suggests higher transition probabilities for B and D states, that accounts for population accumulation at the protonated states A and C, respectively. Further, this deduction is confirmed by the calculation of the transition probabilities associated with the chromophore states. As inferred from the transition probability calculations, specific transitions like B→A and D→C through protonation are found to be more probable than A→B and C→D, respectively, under 532 nm laser excitation, leading to an increasing population of the states A and C. This situation is pronounced more at higher laser excitation.
6. Frequency of capturing single GFP molecules during the time series SERS measurements increases when the laser power is increased from 100 to 700 μW. This finding is attributed to optical tweezer effect at the hotspots due to high concentration of the electromagnetic field. Additionally, higher laser intensity is found to increase all the transition probabilities (i.e., A↔B, B↔D, D↔C, C↔A).

7. Transitions between the chromophore states involving cis↔trans isomerization (i.e., A↔C, B↔D) are found to be less frequent compared to transitions involving protonation↔deprotonation (i.e., A↔B, C↔D). This result is consistent with GFP chromophore's rigid stabilization inside the β-barrel structure. Although the transitions A↔B and C↔D also require structural rearrangements, it is believed that the isomerization transitions A↔C and B↔D are impeded to a greater extend inside the β-barrel as they involve rotations. Indeed, inhibition of isomerization inside the barrel structure blocks the non-radiative thermalization pathways and makes GFP an efficient fluorophore.

8. Finally, a valid question is how the transitions are promoted by 532 nm irradiation. It is likely that B↔D occur by photoisomerization, but photoisomerization cannot drive A↔C, because A and C states do not absorb 532 nm photons (i.e., with the exception of two-photon absorption). Further, A↔B, C↔D do not involve photoisomerization. Therefore, the increased transition probabilities with higher laser intensity are explained by increased thermal energy, namely increased amplitude of vibrational modes in the chromophore. The increased amplitude of the vibrations has a higher destabilizing (perturbing) effect for transitions to occur [46]. The increased thermal energy (vibrational energy) of the chromophore under laser excitation occurs due to 3 mechanisms: 1) heat generation in the nanoparticles with subsequent heat (phonon) transfer to the chromophore; 2) non-radiative relaxation of the chromophore excited state where relaxation occurs to vibronic states of the ground state (i.e., generation of phonons or heat). This mechanism requires absorption of the 532 nm radiation; 3) creation of higher vibronic states of the ground state (phonons) by Raman scattering (Stokes shift). This mechanism can be significant in the case of SERS.

These results, thus, provide A framework for future investigation of GFP chromophore's structural dynamics using SM-SERS with high structural sensitivity, and scope for more insight into the biophysics of this Nobel Prize winning protein.

BIBLIOGRAPHY

[1] N. C. Shaner, G. H. Patterson, and M. W. Davidson, “Advances in fluorescent protein technology,” J. Cell Sci. **120**, 4247 (2007).

[2] H. E. Seward and C. R. Bagshaw, “The photochemistry of fluorescent proteins: implications for their biological applications,” Chem. Soc. Rev. **38**, 2842 (2009).

[3] J. K. M. Sanders and S. E. Jackson, “The discovery and development of the green fluorescent protein, GFP” Chem. Soc. Rev. **38**, 2821 (2009).

[4] J. Livet, T. A. Weissman, H. Kang, R. W. Draft, J. Lu, R. A. Bennis, J. R. Sanes and J. W. Lichtman, “Transgenic strategies for combinatorial expression of fluorescent proteins in the nervous system”, Nature. **450**, 56 (2007).

[5] R. Y. Tsien, “The Green Fluorescent Protein”, Annu. Rev. Biochem. **67**, 509 (1998).

[6] M. Zimmer, “Green fluorescent protein (GFP): applications, structure, and related photophysical behavior,” Chem. Rev. **102**, 759 (2002).

[7] M. Ormö, A. B. Cubitt, K. Kallio, L. A. Gross, R. Y. Tsien, and S. J. Remington, "Crystal structure of the Aequorea victoria green fluorescent protein," Science **273**, 1392 (1996).

[8] K. Brejc, T. K. Sixma, P. A. Kitts, S. R. Kain, R. Y. Tsien, M. Ormo, and S. J. Remington, "Structural basis for dual excitation and photoisomerization of the Aequorea victoria green fluorescent protein," Proc. Natl. Acad. Sci. U. S. A. **94**, 2306 (1997).

[9] T. D. Craggs, “Green fluorescent protein: structure, folding and chromophore maturation,” Chem. Soc. Rev. **38**, 2865 (2009).

[10] M. Chattoraj, B. A. King, G. U. Bublitz, and S. G. Boxer, “Ultra-fast excited state dynamics in green fluorescent protein: Multiple states and proton transfer,” Proc. Natl. Acad. Sci. **93**, 8362 (1996).

[11] H. Lossau, A. Kummer, R. Heinecke, P. Pollinger- Dammer, C. Kompa, G. Bieser, T. Jonsson, C. M. Silva, M. M. Yang, D. C. Youvan, M. E. Michel- Beyerle, “Time-resolved spectroscopy of wild-type and mutant green fluorescent proteins reveals excited state deprotonation consistent with fluorophore-protein interactions,” Chem. Phys. **213**, 1 (1996).

[12] J. N. Henderson and S. J. Remington, “The kindling fluorescent protein: a transient photoswitchable marker,” Physiology **21**, 162 (2006).

[13] A. K. Kalkan, and S. J. Fonash, “Laser-activated surface-enhanced Raman scattering substrates capable of single molecule detection,” Appl. Phys. Lett. **89**, 2331031 (2006).

[14] A. K. Kalkan, “Single molecule detection surface-enhanced Raman scattering substrates by electroless synthesis of Ag nanoparticles on nanostructured silicon films,” Electrochem. Soc. Trans. **3**, 9 (2007).

[15] K. Singhal, K. Bhatt, Z. Kang, W. Hoff, A. Xie, and A. K. Kalkan, "Structural dynamics of a single photoreceptor protein molecule monitored with surface-enhanced Raman scattering substrates," Materials Research Society Symposium Proceedings **1077**, L10-04 (2008).

[16] S. Habuchi, M. Cotlet, R. Gronheid, G. Dirix, J. Michiels, J. Vanderleyden, F. C. De Schryver, and J. Hofkens, “Single-molecule surface enhanced resonance Raman spectroscopy of the enhanced green fluorescent protein,” J. Am. Chem. Soc. **125**, 8446 (2003).

[17] K. Singhal and A. K. Kalkan, “Surface-enhanced Raman scattering captures conformational changes of single photoactive yellow protein molecules under photoexcitation,” J. Am. Chem. Soc. **132**, 429 (2010).

[18] A. Otto, “What is observed in single molecule SERS, and why?,” J. Raman Spectrosc. **33**, 593 (2002).

[19] C. L. Haynes, A. D. McFarland, and R. P. Van Duyne, “Surface-enhanced Raman spectroscopy,” Anal. Chem. **77**, 338A (2005).

[20] S. Nie and S. R. Emory, “Probing single molecules and single nanoparticles by surface enhanced Raman scattering,” Science **275**, 1102 (1997).

[21] W. E. Moerner, “A dozen years of single-molecule spectroscopy in physics, chemistry, and biophysics,” J. Phys. Chem. B **106**, 910 (2002)

[22] J. Pietzsch, “The importance of Protein Folding,” Nature (2002)

[23] D. Davenport and J. Nicol, “Luminescence in hyromedusae,” J. A. C. Proc. R. Soc. London, Ser. B **144**, 399 (1955)

[24] O. Shimomura, “The discovery of aequorin and green fluorescent protein,” J. Microsc. **217**, 3 (2005).

[25] O. Shimomura, B. Musicki and Y. Kishi, “Semi-synthetic aequorin- an improved tool for the measurement of calcium-ion concentration,” Biochem. J. **251**, 405 (1988)

[26] O. Shimomura, “A short story of aequorin,” Biol. Bull. **189**, 1 (1995)

[27] O. Shimomura, “Luminescence of aequorin is triggered by the binding of two calcium ions,” Biochem. Biophys. Res. Commun. **211**, 359 (1995)

[28] W. W. Ward, “Energy transfer processes in bioluminescence,” Photochem. Photobiol. Rev. **4**, 1 (1979)

[29] J. G. Morin and J. W. Hastings, “Biochemistry of the bioluminescence of colonial hydroids and other coelenterates,” J. Cell Physiol. **77**, 313 (1971)

[30] O. Shumomura, “Structure of the chromophore of Aequorea green fluorescent protein,” FEBS lett. **104**, 220 (1979)

[31] H. Morise, O. Shimomura, F. H. Johnson and J. Winant, “Intermolecular energy transfer in the bioluminescent systems of Aequorea,” Biochemistry **13**, 2656 (1974)

[32] S. L. Maddalo and M. Zimmer, “The role of the protein matrix in green fluorescent protein fluorescence,” Photochem. and Photobiol. **82**, 367 (2006).

[33] W. Weber, V. Helms, J. A. McCammon, and P. W. Langhoff, "Shedding light on the dark and weakly fluorescent states of green fluorescent proteins," Proc. Natl. Acad. Sci. U. S. A. **96**, 6177 (1999).

[34] S. J. Remington, “Fluorescent proteins: maturation, photochemistry and photophysics,” Curr. Opin. Struct. Biol. **16**, 714 (2006).

[35] S. R. Meech, “Excited state reactions in fluorescent proteins,” Chem. Soc. Rev. **38**, 2922 (2009).

[36] J. J. V. Thor, “Photoreactions and dynamics of the green fluorescent protein,” Chem. Soc. Rev. **38**, 2935 (2009).

[37] M. Zimmer, “Glowing genes: a revolution in biotechnology,” Prometheus Books, Amherst, New York (2005).

[38] M. Zimmer, “GFP: from jellyfish to the Nobel Prize and beyond,” Chem. Soc. Rev. **38**, 2823 (2009).

[39] S. Bonsma, R. Purchase, S. Jezowski, J. Gallus, F. Kcnz, and S. Volker, “Green and red fluorescent proteins: photo-and thermally induced dynamics probed by site-selective spectroscopy and hole burning,” Chem. Phys. Chem. **6**, 838 (2005).

[40] Cotlet, J. Hofkens, M. Maus, T. Gensch, M. V. D. Auweraer, J. Michiels, G. Dirix, M. V. Guyse, J. Vanderleyden, A. J. W. G. Visser and F. C. D. Schryver, “Excited-state dynamics in the enhanced green fluorescent protein mutant probed by picosecond time-resolved single photon counting spectroscopy,” J. Phys. Chem. B **105**, 4999 (2001).

[41] M. Chalfie and S. Kain, “Green fluorescent protein: properties, applications, and protocols,” 2nd Edition, John Wiley & Sons, Hoboken, New Jersey (2006)

[42] T. Misteli and D. L. Spector, “Applications of the green fluorescent protein in cell biology and biotechnology,” Nat. Biotechnol. **15**, 961 (1997).

[43] V. A. Pieribone and D. F. Gruber, “A glow in the dark: the revolutionary science of biofluorescence,” Belknap Press of Harvard University, Cambridge, Massachusetts (2005).

[44] M. Chalfie, Y. Tu, G. Euskirchen, W. W. Ward, and D. C. Prasher, “Green fluorescent protein as a marker of gene expression,” Science **263**, 802 (1994).

[45] H. H. Gerdes and C. Kaether, “Green fluorescent protein: applications in cell biology,” FEBS Lett. **389**, 44 (1996).

[46] C. Fang, R. R. Frontiera, R. Tran and R. A. Mathies, “Mapping GFP structure evolution during proton transfer with femtosecond Raman spectroscopy,” Nature **462**, 200 (2009).

[47] D. S. Ma, A. A. Jaye, P. Matousek, M. Towrie, S. R. Meech, and P. J. Tonge, “Observation of excited-state proton transfer in green fluorescent protein using ultrafast vibrational spectroscopy,” J. Am. Chem. Soc. **127**, 2864 (2005).

[48] M. A. Lill and V. Helms, “Proton shuttle in green fluorescent protein studied by dynamic simulations,” Proc. Natl. Acad. Sci. USA **99**, 2778 (2002).

[49] J. J. V. Thor and J. T. Sage, “Charge transfer in green fluorescent protein,” Photochem. Photobiol. Sci. **5**, 597 (2006).

[50] A. F. Bell, X. He, R. M. Wachter, and P. J. Tonge, “Probing the ground state structure of the green fluorescent protein chromophore using Raman spectroscopy,” Biochem. **39**, 4423 (2000).

[51] C. V. Raman and K. S. Krishran, “A new type of secondary radiation,” Nature **121**, 501 (1928)

[52] A. Smekal, “Zur quantentheorie der dispersion,” Naturwissenschaften **11**, 873 (1923)

[53] E. Smith and G. Dent, “Modern Raman spectroscopy: A practical approach,” John Wiley and Sons, Ltd: West Sussex, England, 210 (2005)

[54] D. J. Gardiner and P. R. Graves, “Practical Raman spectroscopy,” Springer-Verlag: Berlin & New York, 157 (1989)

[55] J. R. Lombardi and R. L. Birke, "A unified approach to surface-enhanced Raman spectroscopy," J. Phys. Chem. C **112**, 5605 (2008).

[56] A. A. Pakhomov and V. I. Martynov, “GFP family: structural insights into spectral tuning,” Chem. and Biol. **15**, 755 (2008).

[57] J. Wiedenmann, S. Ivanchenko, F. Oswald, F. Schmitt, C. Rocker, A. Salih, H. D. Spindler, and G.U. Nienhaus, “EosFP, a fluorescent marker protein with UV-inducible green-to-red fluorescence conversion,” Proc. Natl. Acad. Sci. USA **101**, 15905 (2004).

[58] V. V. Verkhusha and K. A. Lukyanov, “The molecular properties and applications of Anthozoa fluorescent proteins and chromoproteins” Nat. Biotechnol. **22**, 289 (2004).

[59] A. Miyawaki, T. Nagai, and H. Mizuno, “Engineering fluorescent proteins,” Adv. Biochem. Eng. Biotechnol. **95**, 1 (2005).

[60] M. Fleischmann, P. J. Hendra and A. J. McQuillan, “Raman spectra of pyridine adsorbed at a silver electrode,” Chem. Phys. Lett. **26**, 163 (1974)

[61] E. C. L. Ru and P. G. Etchegoin, “Principles of surface-enhanced Raman spectroscopy and related plasmonic effects,” Elsevier, Amsterdam (2009).

[62] G. C. Schatz, M. A. Young, and R. P. Van Duyne, “Electromagnetic mechanism of SERS”, Top. Appl. Phys. **103**, 19 (2006).

[63] K. Kneipp, H. Kneipp, I. Itzkan, R. R. Dasari, and M. S. Feld, “Ultrasensitive chemical analysis by Raman spectroscopy,” Chem. Rev. **99**, 2957 (1999).

[64] Z. Wang, S. Pan, T. D. Krauss, H. Du, and L. J. Rothberg, “The structural basis for giant enhancement enabling single-molecule Raman scattering,” PNAS **100**, 8638 (2003).

[65] D. R. Ward, N. K. Grady, C. S. Levin, N. J. Halas, Y. Wu, P. Norlander, and D. Natelson, “Electromigrated nanoscale gaps for surface-enhanced Raman spectroscopy,” Nano Lett. **7**, 1396 (2007).

[66] C. C. Neacsu, J. Dreyer, N. Behr, and M. B. Raschke, “Scanning-probe Raman spectroscopy with single-molecule sensitivity,” Phys. Rev. B **73**, 193406 (2006).

[67] A. M. Michaels, J. Jiang, and L. Brus, “Ag nanocrystal junctions as the site for surface-enhanced Raman scattering of single rhodamine 6G molecules,” J. Phys. Chem. B **104**, 11965 (2000).

[68] H. Xu, E. J. Bjerneld, M. Käll, and L. Börjesson, “Spectroscopy of single hemoglobin molecules by surface-enhanced Raman scattering,” Phys. Rev. Lett. **83**, 4357 (1999).

[69] D. P. Fromm, A. Sundaramurthy, A. Kinkhabwala, P. J. Schuck, G. S. Kino, and W. E. Moerner, "Exploring the chemical enhancement for surface-enhanced Raman scattering with Au bowtie nanoantennas," J. Chem. Phys. **124**, 061101 (2006).

[70] H. Xu, J. Aizpurua, M. Käll, and P. Apell, "Electromagnetic contributions to single-molecule sensitivity in surface-enhanced Raman scattering," Phys. Rev. E **62**, 4318 (2000).

[71] J. A. Creighton, C. G. Blatchford and M. G. Albrecht, "Plasma resonance enhancement of Raman scattering by pyridine adsorbed on silver or gold sol particles of size comparable to the excitation wavelength," J. Chem. Soc. Faraday **75**, 790 (1979).

[72] A. K. Bosnick, J. Jiang and L. E. Brus, "Fluctuations and local symmetry in single-molecule rhodamine 6G Raman scattering on silver nanocrystal aggregates," J. Phys. Chem. B **106**, 8096 (2002).

[73] H. X. Xu, E. J. Bjerneld, M. Kall and L. Borjesson, "Spectroscopy of single hemoglobin molecules by surface enhanced Raman scattering," Phys. Rev. Lett. **83**, 4357 (1999).

[74] A. R. Bizzarri and S. Cannistraro, "Surface-enhanced resonance Raman spectroscopy signals from single myoglobin molecules," Appl. Spectrosc. **56**, 1531 (2002).

[75] I. Delfino, A. R. Bizzarri and S. Cannistraro, "Single molecule detection of yeast cytochrome c by surface enhanced Raman spectroscopy," Biophys. Chem. **113**, 41 (2005).

[76] A. R. Bizzarri and S. Cannistraro, "Evidence of electron-transfer in the SERS spectra of a single iron-protoporphyrin IX molecule," Chem. Phys. Lett. **395**, 222 (2004).

[77] Z. Wang and L. J. Rothberg, "Origins of blinking in single molecule Raman spectroscopy," J. Phys. Chem. B **109**, 3387 (2005).

[78] H. X. Xu and M. Kall, "Polarization dependent surface-enhanced Raman spectroscopy of isolated silver nanoaggregates," Chem. Phys. Chem. **4**, 1001 (2003).

[79] R. M. Dickson, A. B. Cubitt, R. Y. Tsien and W. E. Moerner, "On/off blinking and switching behavior of single molecules of green fluorescent protein," Nature **388**, 355 (1997).

[80] X. He, A. F. Bell and P. J. Tonge, "Isotopic labeling and normal mode analysis of a model green fluorescent protein chromophore," J. Phys. Chem, B **106**, 6056 (2002).

[81] D. C. Loos, S. Habuchi, C. Flors, J. Hotta, J. Wiedenmann, G. U. Nienhaus, and J. Hofkens, "Photoconversion in the Red Fluorescent Protein from the Sea Anemone Entacmaea quadricolor: Is Cis-Trans Isomerization Involved?," J. Am. Chem. Soc. **128**, 6270 (2006).

[82] K. Nienhaus, H. Nar, R. Heilker, J. Wiedenmann and G. U. Nienhaus, "Trans-cis isomerization is responsible for the red-shifted fluorescence in variants of the red fluorescent protein eqFP611," J. Am. Chem. Soc. **130**, 12578 (2008).

[83] T. Andruniow, "Vibrational analysis of a solvent green fluorescent protein chromophore," J. Mol. Model **13**, 775 (2007).

[84] P. Schellenberg, E. Johnson, A. P. Esposito, P. J. Reid and W. W. Parson, "Resonance Raman scattering by the green fluorescent protein and an analogue of its chromophore," J. Phys. Chem. B **105**, 5326 (2001).

[85] A. P. Esposito, P. Schellenberg, W. W. Parson and P. J. Reid, "Vibrational spectroscopy and mode assignments for an analog of the green fluorescent protein chromophore," J. Mol. Struct. **569**, 25 (2001).

[86] R. Nifosi and V. Tozzini, "Cis-trans photoisomerization of the chromophore in the green fluorescent protein variant E^2GFP: a molecular dynamics study," Chem. Phys. **323**, 358 (2006).

[87] Y. Liu, H. R. Kim and A. A. Heikal, "Structural basis of fluorescence fluctuation dynamics of green fluorescent proteins in acidic environments," J. Phys. Chem. B **110**, 24138 (2006).

[88] X. He, A. F. Bell and P. J. Tonge, "Ground state isomerization of a model green fluorescent protein chromophore," FEBS Lett. **549**, 35 (2003).

[89] T. M. H. Creemers, A. J. Lock, V. Subramaniam , T. M. Jovin and S. Volker, "Three photoconvertible forms of green fluorescent protein identified by spectral hole-burning," Nature **6**, 557 (1999).

[90] J. L. Schwartz and G. H. Patterson, "Development and use of fluorescent protein markers in living cells," Science **300**, 87 (2003).

[91] R. Nifosi, A. Ferrari, C. Arcangeli, V. Tozzini, V. Pellegrini and F. Beltram, "Photoreversible dark state in a tristable green fluorescent protein variant," J. Phys. Chem. B **107**, 1679 (2003).

[92] V. Voliani, R. Bizzarri, R. Nifosi, S. Abbruzzetti, E. Grandi, C. Viappiani and F. Beltram, "Cis-trans photoisomerization of fluorescent protein chromophores," J. Phys. Chem. B **112**, 10714 (2008).

[93] R. A. G. Cinelli, V. Pellegrini, A. Ferrari, P. Faraci, R. Nifosi, M. Tyagi, M. Giacca and F. Beltram, "Green fluorescent proteins as optically controllable elements in bioelectronics," Appl. Phys. Lett. **79**, 3353 (2001).

[94] G. U. Nienhaus, "The green fluorescent protein: a key tool to study chemical processes in living cell," Angew. Chem. Int. Ed. **47**, 8992 (2008).

[95] M. Andresen, A. C. Stiel, S. Trowitzsch, G. Weber, C. Eggeling, M. C. Wahl, S. W. Hell and S. Jakobs, "Structural basis for reversible photoswitching in Dronpa," Proc. Natl. Acad. Sci. 104, 13005 (2007).

[96] S. Habuchi, R. Ando, P. Dedecker, W. Verheijen, H. Mizuno, A. Miyawaki and J. Hofkens, "Reversible single-molecule photoswitching in the GFP-like fluorescent protein Dronpa," Proc. Natl. Acad. Sci. USA **102**, 9511 (2005).

[97] X. Li, L. W. Chung, H. Mizuno, A. Miyawaki and K. Morokuma, "A theoretical study on the nature of on- and off-states of reversibly photoswitching fluorescent protein dronpa: absorption, emission, protonation, and Raman," J. Phys. Chem. B **114**, 1114 (2010).

[98] S. D. Hsu, G. Blaser and S. E. Jackson, "The folding, stability and conformational dynamics of β-barrel fluorescent proteins," Chem. Soc. Rev. **38**, 2951 (2009).

[99] S. Luin, V. Voliani, G. Lanza, R. Bizzarri, R. Nifosi, P. Amat, V. Tozzini, M. Serresi and F. Beltram, "Raman study of chromophore states in photochromic fluorescent proteins," J. Am. Chem. Soc. **131**, 96 (2009).

[100] S. Abbruzzetti, R. Bizzarri, S. Luin, R. Nifosi, B. Storti, C. Viappiani and F. Beltram, "Photoswitching of E222Q GFP mutants: "concerted" mechanism of chromophore isomerization and protonation," Photochem. Photobiol. Sci. **9**, 1307 (2010).

[101] A. F. Bell, D. Stoner-Ma, R. M. Wachter and P. J. Tonge, "Light-driven decarboxylation of wild-type green fluorescent protein," J. Am. Chem. Soc. **125**, 6919 (2003).

[102] P. C. Lee and D. Meisel, "Adsorption and surface-enhanced Raman of dyes on silver and gold sols," J. Phys. Chem. **86**, 3391 (1982).

VITA

Md. Shafayet Khurshid

Candidate for the Degree of

Master of Science

Thesis: CONFORMATIONAL STATES AND TRANSITIONS IN GREEN FLUORESCENT PROTEIN CHROMOPHORE STUDIED BY SINGLE MOLECULE SERS

Major Field: Mechanical and Aerospace Engineering

Personal Data:
Sex: Male
DOB: 06/03/1985
Hometown: Chittagong, Bangladesh

Education:

- Completed the requirements for the Master of Science in Mechanical and Aerospace Engineering at Oklahoma State University, Stillwater, Oklahoma in May, 2011.

- Completed the requirements for the Bachelor of Science in Mechanical Engineering at Bangladesh University of Engineering and Technology, Dhaka, Bangladesh in 2007.

Experience:

- Graduate Research Assistant, MAE, OSU Stillwater (Aug 2008 – Dec 2010)
- Graduate Teaching Assistant, MAE, OSU Stillwater (Aug 2008 – April 2010)

Name: Md. Shafayet Khurshid Date of Degree: May, 2011
Institution: Oklahoma State University Location: Stillwater, Oklahoma

Title of Study: CONFORMATIONAL STATES AND TRANSITIONS IN GREEN FLUORESCENT PROTEIN CHROMOPHORE STUDIED BY SINGLE MOLECULE SERS

Pages in Study: 104 Candidate for the Degree of Master of Science
Major Field: Mechanical and Aerospace Engineering

Green fluorescent protein (GFP) from *Aequorea victoria* won the Nobel Prize in 2008 for its revolutionary impact on bio-imaging. However, conformational states of its chromophore as well as transitions between them are not understood well. Using "nanometal-on-semiconductor" SERS substrates, the present work acquires the vibrational spectra of single GFP molecules under 532 nm laser excitation. Once an aliquot of 10-9 M GFP is spotted on a SERS substrate and a Raman acquisition is started, intense and well-resolved peaks are observed to appear and disappear repeatedly over a weak background. These temporal "spectral jumps" are captured in every half a minute on the average and sustain for 1 s or less. Each jump is associated with a single GFP molecule diffusing into a high SERS enhancement factor site (i.e., a "hotspot"), residing it for 1 s or less, and eventually diffusing out of it. The SERS is acquired in time series at continuous intervals of 50-100 ms. A minimum of 4 conformational states of the GFP chromophore were observed as cis/trans and protonated/deprotonated combinations. Statistical analysis of the GFP populations at different states reveals substantial presence of all 4 states. Among the 4 states, the transitions occur in between certain pairs of states that line-up in a cyclic pattern. Further, as inferred from the calculated transition probabilities, particular transitions become more probable under 532 nm excitation. Consequently, this bias leads to the increased population of certain states that is pronounced more with increasing laser intensity.

ADVISER'S APPROVAL: Dr. Ali Kaan Kalkan